Biochemical characterization of the β-mannanase activity of *Bacillus paralicheniformis* SVD1

Thesis submitted in fulfillment of the requirements for the degree of

Master of Science (Biochemistry)

at

Rhodes University

by

Matthew David Clarke

May 2018

Abstract

Products produced via the enzymatic hydrolysis of lignocellulosic biomass, the most abundant renewable terrestrial source of carbon, can potentially replace a lot of the fuels and chemicals currently produced using non-renewable hydrocarbons. Mannan is a polysaccharide component of lignocellulose that is abundant in softwoods and legume seeds. Enzymatic hydrolysis of mannan by β-mannanases has various industrial applications, including use in biofuel and prebiotic mannooligosaccharide (MOS) production for the improvement of human and animal health. The industrial use of β-mannanases depends on their biochemical characteristics, such as their activity, stability and substrate specificity. Knowledge of their synergistic interactions with other enzymes is also useful for effective hydrolysis. *Bacillus paralicheniformis* SVD1 was used as a source for β-mannanases. The two mannanases of *B. paralicheniformis* SVD1 have not been biochemically characterized apart from minor characterization of crude β-mannanase activity. The protein sequences of the two β-mannanases, of glycosyl hydrolase family 5 and 26, have a 95% - 96% identity to the β-mannanases of *B. licheniformis* DSM13^T (=ATCC14580^T). These small protein sequence differences could lead to quite different biochemical characteristics. These mannanases were characterized as these enzymes may have industrially useful characteristics.

To induce mannanase production, *B. paralicheniformis* SVD1 was cultured in broth containing the mannan substrate locust bean gum. Various growth curve parameters were measured over 72 h. Mannanase activity was the highest after 48 h of growth - this was the time at which mannanase activity was concentrated, using 3 kDa centrifugal filtration devices, for biochemical characterization of the crude activity. Zymography revealed that the crude concentrated mannanase fraction consisted of at least two mannanases with relative molecular weights (MWs) of 29.6 kDa and 33 kDa. This was smaller than expected - based on their theoretical molecular masses. Protease activity, which was detected in the broth, was probably the reason. There were two pH optima, pH 5.0 and pH 7.0, which also indicated the presence of two mannanases. The concentrated mannanase displayed characteristics that were expected of a *B. paralicheniformis* β-mannanase. The temperature optimum was 50°C and the activity loss was less than 7% at 50°C after 24 h. Substrate specificity assays revealed that there was predominantly mannanase activity present. Thin layer chromatography (TLC) analysis of mannan and MOS hydrolysis showed that mainly M2 and M3 MOS were produced; only MOS with a degree of polymerization of 4 or higher were hydrolyzed. Hydrolysis was minimal on mannoligosaccharides with galactose substituents. Activity and MOS production was the highest on soluble, low branched mannan substrates. The highest activity observed was on konjac glucomannan.

Purification of the mannanase activity was then attempted using various methods. Ammonium sulfate precipitation, acetone precipitation, as well as centrifugal filtration device concentration was assessed for concentration of the mannanase activity. Concentration was not very successful due to low activity yields (≤ 20%). Anion exchange chromatography (AEC) and size exclusion chromatography (SEC) was used for purification. AEC gave good activity yield and fold purification, but SDS-PAGE analysis revealed the presence of many different proteins so further purification was necessary. SDS-PAGE analysis showed that there were only a few protein contaminants in the SEC fraction. However, the yield was too low to allow for biochemical characterization. The optimized purification procedure, which partially purified the mannanase activity, used 85% ammonium sulfate precipitation, followed by AEC. The fold purification was high (88.9) and the specific activity was 29.5 $U.mg^{-1}$. A zymogram of the partially purified mannanase showed a mannanase active band with a MW of 40 - 41 kDa. A serine protease inhibitor, phenylmethylsulfonyl fluoride (PMSF), was added during the purification steps. This indicated that the mannanase/s in the crude concentrate, without PMSF added, was hydrolyzed by serine protease activity. Native PAGE zymograms suggested that at least two different isoforms of mannanases were present. Additional purification would be required to determine the true characteristics of the mannanase/s.

The biochemical characteristics of the crude and partially purified mannanases were similar. The pH optima of the partially purified mannanases were different; the pH optima were 6.0 and 9.0. The substrate specificities were similar, except that the partially purified mannanases displayed no cellulase and β-D-galactosidase activity, but showed a small amount of α-L-arabinase activity. The partially purified mannanase and a *Cyamopsis tetragonolobus* GH27 α-galactosidase synergistically hydrolyzed locust bean gum. The M50G50 combination displayed the highest extent of hydrolysis; after 24 h there was a 1.39 fold increase in reducing sugar release and the degree of synergy (DS) was 4.64. TLC analysis indicated that synergy increased the release of small MOS. These MOS could be useful as prebiotics. The synergy between the partially purified mannanase and the commercial cellulase mixture Cellic® CTec2 (Novozymes) on spent coffee grounds (SCG) was also determined. SCG is an abundant industrial waste product that has high mannan content. The SCG was pretreated using NaOH, and the monosaccharide, soluble phenolics and insoluble contents were determined. Glucose and mannose were the dominant monosaccharides in the SCG; the pretreated SCG contained 20.4% (w/w) glucose and 18.5% (w/w) mannose, respectively. The NaOH pretreatment improved mannanase hydrolysis of SCG. It resulted in the opening up and swelling of the SCG particles and removed some of the insoluble solids. The partially purified *B. paralicheniformis* SVD1 mannanase displayed no detectable activity on SCG, but showed synergy with CTec2, in

terms of DS, on untreated and NaOH pretreated SCG. This is the first report of mannanase-cellulase synergy on SCG; other studies found that increased hydrolysis was due to additive effects. The results obtained in this study are only an initial assessment of the biochemical properties of *B. paralicheniformis* SVD1 mannanase activity and its synergy with other enzymes. These results can be used to inform future studies.

Acknowledgements

I would like to thank:

Professor Pletschke for facilitating my research.

My mother, sister, aunt and gran for always encouraging and supporting me. I would not have been able to get this far without all of you.

Members of the Enzyme Synergy Research group for their helpful discussions.

My family and friends for their support and motivation.

The National Research Foundation of South Africa (NRF) and the Ernst and Ethel Eriksen Trust for providing me with the funding that enabled me to complete this study. Any opinions, findings and conclusions or recommendations expressed in this material are those of the author(s) and the NRF or Ernst and Ethel Eriksen Trust does not accept any liability in regard thereto.

List of outputs

Publications

1) Pletschke, B.I., Malgas, S., Bhattacharya, A., Bhattacharya-Shrivastava, A., Clarke, M.D., Mafa, M.S., Morake, S., Thoresen, M. Enzyme synergism: A powerful tool for decreasing enzyme loading for efficient biomass conversion. 24th European Biomass Conference & Exhibition, Amsterdam, The Netherlands, 6 – 9 June 2016. [Paper]. ISBN 978-88-89407-165.

Local conference proceedings

1) Clarke, M.D., Pletschke, B.I. “Biochemical characterization and mannooligosaccharides production by *Bacillus licheniformis* SVD1 β-mannanase”, 25th Congress of the South African Society for Biochemistry and Molecular Biology (SASBMB), East London, South Africa, 10 – 14 July 2016. [Oral presentation].

Table of contents

List of abbreviations

°C	Degree(s) Celsius
µg	Microgram
µL	Microlitre
µM	Micromolar
µmol	Micromole
AEC	Anion exchange chromatography
BCA	Bicinchoninic acid
BSA	Bovine serum albumin
CBM	Carbohydrate binding domain
CMC	Carboxymethyl cellulose
DNS	Dinitrosalicylic acid
DP	Degree of polymerization
DS	Degree of synergy
EC	Enzyme commission number
g	Gram
GH	Glycoside hydrolase
GG	Guar gum
HPLC	High performance liquid chromatography
h	Hour
INM	Ivory nut mannan
kDa	Kilo Daltons
LBG	Locust bean gum
MOS	Mannooligosaccharide
mg	Milligram
min	Minute
ml	Millilitre
mM	Millimolar
MW	Molecular weight
MWCO	Molecular weight cut-off

nm	Nanometer
NREL	National Renewable Energy Laboratory
OD	Optical density
PMSF	Phenylmethylsulfonyl fluoride
*p*NP	*p*-Nitrophenol
R_f	Retention factor
SCG	Spent coffee grounds
SDS	Sodium dodecyl sulphate
SDS-PAGE	Sodium dodecyl sulphate polyacrylamide gel electrophoresis
SEC	Size exclusion chromatography
SEM	Scanning electron microscopy
TLC	Thin layer chromatography
U	Units of enzyme activity

List of Figures

List of tables

Chapter 1 – Introduction

1.1. Products from the enzymatic hydrolysis of lignocellulosic biomass

Non-renewable hydrocarbons supply most of our energy needs and products such as chemicals and plastics (Olsson & Saddler, 2013; Conti et al., 2016). Renewable methods of producing energy and petrochemicals are being pursued due to the depletion of fossil fuel reserves, negative environmental impacts and supply issues. Renewable energy is the fastest growing energy source (Karlen et al., 2015; Conti et al., 2016). Lignocellulose biomass is potentially a good feedstock for replacing a lot of the fuels and chemicals currently produced using non-renewable hydrocarbons. Lignocellulose is the most abundant form of renewable terrestrial carbon and is not used for human consumption, unlike the edible starch and sucrose components from corn and sugar cane, respectively. The main components of lignocellulose are the sugar polymers cellulose and hemicellulose, as well as lignin, which is an aromatic polymer (Youngs & Somerville, 2012). To produce biofuels and various other products, the sugar polymers need to be broken down. One means of doing this is by enzymatic hydrolysis (non-hydrolytic proteins can also assist in depolymerization). Biomass can be broken down thermally or thermo-chemically, but the advantage of enzymatic hydrolysis is that the reaction is more controlled, there is potential for high monosaccharide yield using mild reaction conditions and there are less by-products that could inhibit fermentative organisms that may be used to ferment monosaccharides into biofuels or other products such as organic acids (Hasunuma et al., 2013; Jönsson et al., 2013; Harris et al., 2014; Donohoe & Resch, 2015). A major problem with the enzymatic route is that enzymes are expensive and pretreatment of the biomass is usually required prior to enzymatic hydrolysis, as typically less than 20% of glucan (the most abundant sugar polymer in lignocellulose) in untreated lignocellulose is solubilized by enzymes alone (Zhang & Lynd, 2004). The low hydrolysis efficiency of enzymes on native lignocellulose substrates is due to biomass recalcitrance, which is its resistance to breakdown by microbes and their enzymes. This recalcitrance is due to various structural features such as inter- and intra-sugar chain bonding, but it is mainly thought to be due to the hydrophobic association and covalent bonding between cell-wall polysaccharides and lignin, which forms lignin carbohydrate complexes (Qing et al., 2013; Malgas et al., 2015[b]). Pretreatment is needed to remove or modify lignin, which is the major barrier to efficient enzymatic hydrolysis. There are various types of pretreatment methods including acid, steam and alkaline treatment (Van

Dyk & Pletschke, 2012). The structural and chemical complexity of lignocellulose makes it challenging for use in biofuel production but it also makes it possible to produce various types of co-products such as bioplastics (Karlen et al., 2015; Olsson & Saddler, 2013). The production of co-products adds to the economic viability of biorefineries (Olsson & Saddler, 2013). Lignin, which is normally extracted before polysaccharide hydrolysis, can also be used for the production of co-products such as plastics, fuels and chemicals (Ragauskas et al., 2014). More research, implementation and political backing is still needed for lignocellulosic biofuels to become competitive with fossil fuels (Karlen et al., 2015). Along with fuels and chemicals and polymers, novel materials and pharmaceuticals can also be produced from lignocellulosic biomass (Ragauskas et al., 2014).

1.1.1. The global importance of biofuels and co-products from lignocellulosic biomass.

The major importance of biofuel is that it is currently the only viable replacement for high energy density liquid fossil fuels that are used for aviation, shipping and long distance trucking (Fulton et al., 2015). There are, however, potential problems with the use of lignocellulosic biomass for fuels. Some studies have shown that large scale harvesting of plant biomass can have negative environmental impacts such as the reduction of soil organic carbon and nutrients (Liska et al., 2014). These negative impacts have occurred in specific cases and, given that biomass production, transportation and transformation into products is a complex process with many variables, the impacts will differ based on the processes used. If done correctly, lignocellulosic biofuel and co-product production can have many environmental, social and economic benefits (Dale et al., 2014; Karlen et al., 2015; Lynd et al., 2015).

1.2. The structure of lignocellulose

Plant cell walls, which consist primarily of lignocellulose, make up the majority of terrestrial biomass (Sorek et al., 2014). The main components of lignocellulose, as seen in Figure 1.1, are the sugar polymers cellulose and hemicellulose as well as lignin, which is an aromatic polymer. Cellulose consists of glucose units and hemicelluloses are heteropolysaccharides that are classified based on the major monosaccharide present in the polymer backbone. Hemicelluloses may be linear or branched (Van Zyl et al., 2010; Youngs & Somerville, 2012). The polysaccharide pectin as well as proteins, minerals, ash and salt are also components of lignocellulose (Van Dyk & Pletschke, 2012).

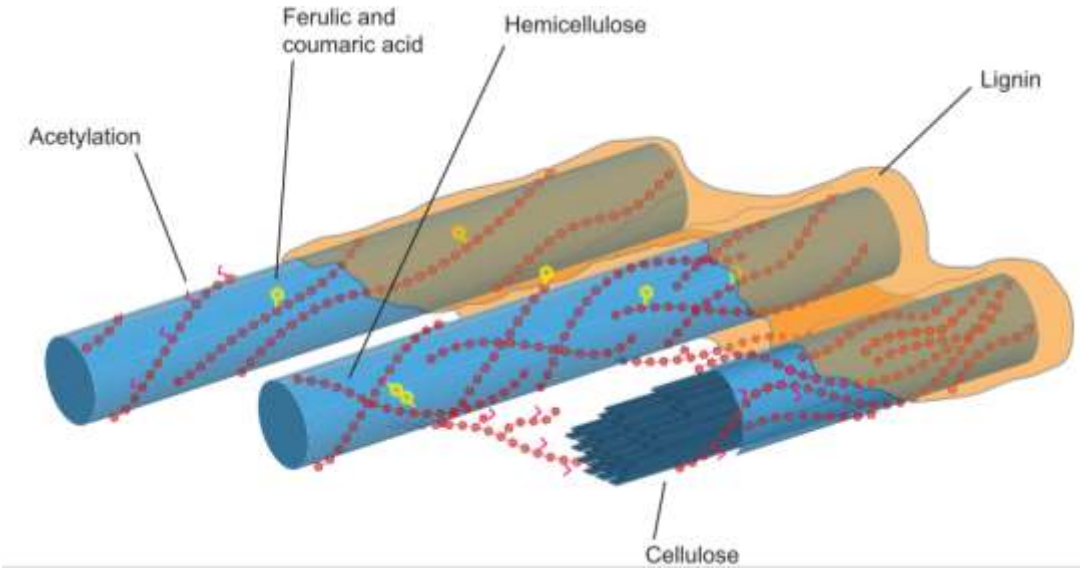

Figure 1.1. The major structural components of lignocellulose (not to scale). [Taken from Sorek et al. (2014)]

1.2.1. Cellulose

Cellulose is an unbranched homopolysaccharide made up of glucose monomers with β-1,4 linkages. Cellulose is believed to be the most abundant bio-polymer on earth. It provides structural strength to the cell wall. Each glucose monomer is β-1, 4 linked and adjacent glucose monomers are rotated 180 degrees relative to one another. The hydroxyl groups form intramolecular hydrogen bonds. These characteristics make the individual cellulose chains straight, flat and quite inflexible. These ordered polymers aggregate with other cellulose polymers through hydrogen bonds and Van der Waals forces to form cellulose microfibrils (Sorek et al., 2014). There are also regions in cellulose fibrils that are less ordered. The cellulose is said to be amorphous in these areas. These regions are thought to be more susceptible to cellulolytic attack (Gourlay et al., 2015). Hydrolysis of cellulose microfibrils is relatively slow compared to the hydrolysis of starch, which is used for biofuel production from corn (Merino & Cherry, 2007; Kalambur, 2012; Wang et al., 2012; Liu et al., 2013).

1.2.2. Hemicellulose

Hemicelluloses make up about 20 – 30% of plant biomass (Yang et al., 2011). They are heteropolysaccharides that are classified based on the major monosaccharide present in the polymer backbone (Van Zyl et al., 2010). The majority of hemicelluloses have a backbone consisting of β-1,4 linked glucose, xylose, mannose or glucose (Sorek et al., 2014). They

may be linear or branched with single or multiple glycosyl residues (Van Zyl et al., 2010; Sorek et al., 2014). These polysaccharides are mostly amorphous and are usually associated with cellulose and are thought to surround cellulose microfibrils; they commonly form hydrogen bonds with cellulose (Yang et al., 2011). The compositional and structural complexity of hemicellulose makes its hydrolysis problematic. The composition varies not only between species but also between different plant tissues and it changes during plant development (Van Dyk & Pletschke, 2012; Sorek et al., 2014). Hemicellulose, like cellulose, provides the cell wall with structural strength. Hemicellulose cross-links, covalently and non-covalently, with cellulose, lignin, cell-wall proteins, pectin and non-structural polysaccharides. In some types of hemicelluloses sugar acid branches or modifications such as phenolic compound branches and acetylation are present. Phenolic compound side chains such as ferulic acid and ρ-coumaric acid can form covalent cross-links between themselves and lignin. This cross-linking increases structural rigidity and makes enzymatic hydrolysis less efficient.

1.2.2.1. Mannan

Mannan is a type of hemicellulose that has a backbone consisting of β-1,4 linked mannose and it may also contain β-1,4 linked glucose. The backbone has varying degrees of galactose and acetyl branching. Mannans are classified based on their composition as linear mannan, glucomannan, galactomannan or galactoglucomannan as seen in Figure 1.2. Mannan, like other hemicelluloses, binds to and intertwines around cellulose microfibrils. This increases the structural strength of the cell wall and provides a physical barrier to cellulolytic attack (Malgas et al., 2015[c]; Srivastava & Kapoor, 2017). Mannans also have other functions: they have a storage function (as a carbohydrate reserve) in the endosperm walls or vacuoles of seeds and vegetative tissues (Srivastava & Kapoor, 2017). They have also been shown to function as signaling molecules during plant growth and development (Liepman et al., 2007). Mannan is the predominant hemicellulose in softwoods, where it has a structural role (Van Zyl et al., 2010). Mannan is also abundant in legume seeds, where it has a structural and storage role (Dhawan & Kaur, 2007).

Linear mannans, as seen in Figure 1.2 A, have a backbone composed of β-1,4 linked D-mannose monomers and contain 5% or less D-galactose branching (Van Zyl et al., 2010). Linear mannan has a structural role in the seeds of many plants including ivory nuts (*Phytelephas* spp.) and green coffee (*Coffea* spp.) (Chauhan et al., 2012). Glucomannans,

as seen in Figure 1.2 B, normally have a backbone consisting of β-1,4 linked D-mannose and D-glucose monomers in a 3:1 ratio (Van Zyl et al., 2010). Glucomannans may also be acetylated. In the wood of conifers up to 50% of the hemicellulose is glucomannan (Van Zyl et al., 2010). Galactomannans, as seen in Figure 1.2 C, have a backbone composed of β-1,4 linked D-mannose monomers and contain greater than 5% D-galactose branching (Van Zyl et al., 2010). The mannose to galactose ratio depends on the source; locust bean gum, guar gum and fenugreek gum have a 4:1, 2:1 and 1:1 ratio, respectively (Moreira & Filho, 2008; Malgas et al., 2015[b]). The distribution of D-galactose side chains on the mannan backbone show an ordered, block-wise or random distribution (Jian et al., 2013). Galactoglucomannans, as seen in Figure 1.2 D, are glucomannans with greater than 5% D-galactose branching. Galactoglucomannans may also be O-acetylated. Acetylated galactoglucomannans are the major hemicellulose in hardwoods (Van Zyl et al., 2010). In all types of mannan where galactose branching occurs, galactose monomers are bonded to mannose residues (Malgas et al., 2015[b]).

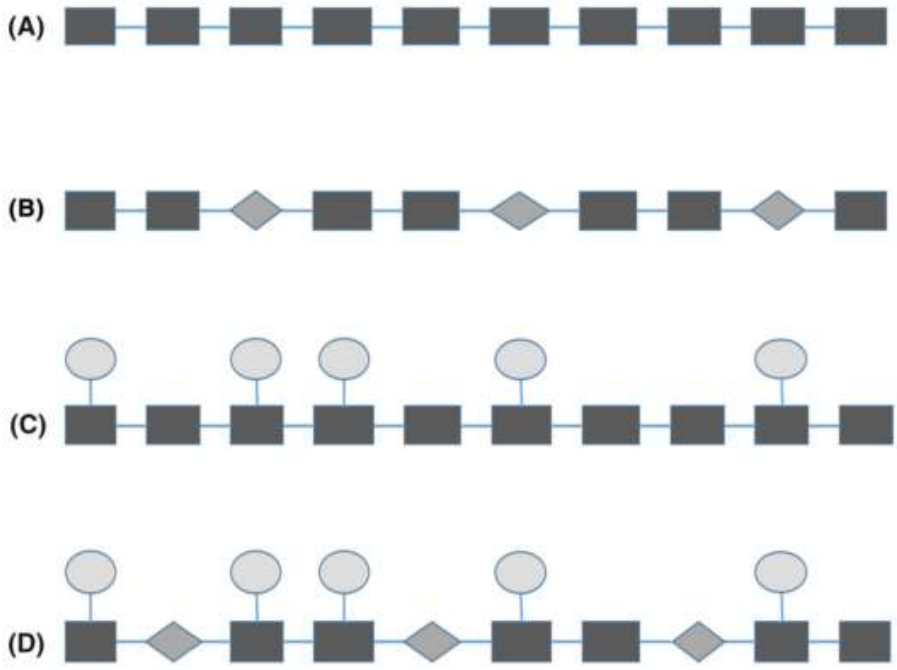

Figure 1.2. Generalized structure of the different types of mannan. A: Linear mannan, B: Glucomannan, C: Galactomannan and D: Galactoglucomannan. The lines represent glycosidic bonds between the sugar monomers, the squares represent mannose, the diamonds represent glucose and the circles represent galactose. [Taken from Malgas et al. (2015[b])]

1.2.3. Lignin

Lignin is an amorphous, irregular aromatic polymer consisting of phenylpropane units. It is found in the cell walls of higher plants (Van Dyk & Pletschke, 2012; Youngs & Somerville, 2012; Sorek et al., 2014). During cell wall formation, phenylpropane monomers are secreted into the cell wall and spread between the polysaccharides. The phenylpropane monomers are randomly polymerized by a free-radical process and the rigid lignin polymer is very resistant to degradation. Lignin gives plant cell walls strength, rigidity and water proofing. Lignin also sterically blocks pathogen cellulase access to the cell walls cellulose and also inhibits cellulase activity by binding to and inactivating cellulases (Sorek et al., 2014). Lignin inhibits other types of lignocellulolytic enzymes, such as mannanases, as well (Malgas et al., 2015[a]). The composition and amount of lignin varies due to many factors such as species and plant growth stage (Van Dyk & Pletschke, 2012; Sorek et al., 2014). The lignin amount and composition affects both enzymatic and pretreatment efficiency. Pretreatment often leads to the formation of by-products such as phenolics and acids. These have been shown to inhibit enzymatic hydrolysis and may also be toxic to fermentative microorganisms (Jönsson et al., 2013). These factors need to be considered when choosing and evaluating a pretreatment method.

1.3. Enzymatic hydrolysis of lignocellulose

1.3.1. Glycoside hydrolases

The major group of enzymes that hydrolyze the glycosidic bonds of polysaccharides and oligosaccharides are the glycoside hydrolases. They are classified with an Enzyme Commission number (EC number) based on the reaction they catalyze (BRENDA enzyme information system: http://www.brenda-enzymes.org/). For example, β-mannanases have an EC number 3.2.1.78. In order for an enzyme to obtain an EC number its function needs to be characterized biochemically. Glycoside hydrolases are also classified based on their sequence, and consequently their structure, into Glycoside hydrolase (GH) families. Enzymes in the same family often have similar substrate specificity (Henrissat, 1991; "Glycoside Hydrolases" in CAZypedia, available at URL http://www.cazypedia.org/). This classification system is very useful as it can be used to identify glycoside hydrolases based on genome and metagenome sequences, which are rapidly growing in number. This is useful for rapid screening of novel enzymes (Payne et al., 2015). Information on GH families can be found in the Carbohydrate Active enzyme Database (Lombard et al., 2014;

http://www.cazy.org/). The glycoside hydrolases relevant to this study are the mannan and cellulose degrading glycoside hydrolases.

1.3.2. Mannan degrading enzymes

Mannan degrading enzymes are produced by several groups of organisms, particularly bacteria and fungi (Van Zyl et al., 2010). Various glycoside hydrolase enzymes are required to hydrolyze mannan into its monomer sugars (Malgas et al., 2015[b]). The main enzymes required are endo-1,4,-β-mannanases (also called β-mannanases) that randomly hydrolyze the β–1,4 D-mannan backbone and β-mannosidases that hydrolyze mannan and mannooligosaccharides (MOS) produced by β-mannanases into mannose (Malgas et al., 2015[b]). Other enzymes may be required such as β-glucosidases, α-galactosidases and acetyl mannan esterases (Moreira & Filho, 2008).

1.3.2.1. β-mannanases

The main group of enzymes involved in mannan hydrolysis are β-mannanases; they are found in GH families 5, 26 and 113 (Lombard et al., 2014; http://www.cazy.org/). These β-mannanases belong to clan GH-A, they have a $(\alpha/\beta)_8$ TIM (triose phosphate isomerase) barrel fold and catalyze hydrolysis of internal β-1,4 mannosidic bonds of a mannan backbone, releasing poly- or oligosaccharides (Chauhan et al., 2012). These endo-acting enzymes have an open active site cleft that allows random binding to multiple sugar residues in a polysaccharide, which leads to random hydrolysis (Davies & Henrissat, 1995). The hydrolysis mechanism is illustrated in Figure 1.3. Two active site carboxylates (glutamates or aspartates) act as general acid/ base catalysts for a double displacement reaction. Firstly, a nucleophilic carboxylate attacks the anomeric carbon of the mannan bond, forming a glycosylated mannanase intermediate. Secondly, the other active site carboxylate catalyzes hydrolysis of the intermediate, which releases a poly- or oligosaccharide (Withers, 2001). The anomeric configuration of the reducing end of the mannan/ MOS is retained. These are therefore retaining glycosidases as opposed to inverting glycosidases.

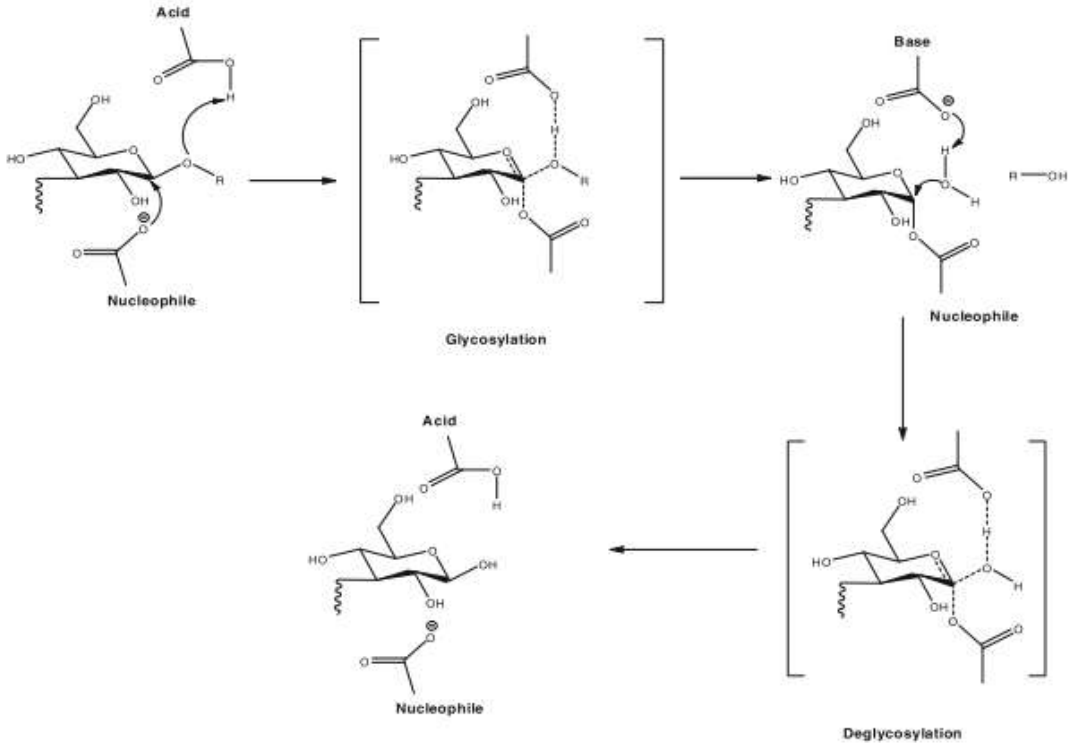

Figure 1.3. Hydrolysis mechanism of β-mannanases. The two active site carboxylates are shown. [Taken from Chauhan et al. (2012)]

β-mannanases require four or more sugar residues for efficient binding and hydrolysis (Tailford et al., 2009; Couturier et al., 2013). The substrate binding surface is classified into subsites (specific monomeric sugar residues) numbered from the non-reducing end (- n) to the reducing end (+ n) of the bound sugar. Hydrolysis occurs between subsites -1 and +1 (Chauhan et al., 2012). Galactose or acetyl group branching can sterically hinder hydrolysis (von Freiesleben et al., 2016). The presence of glucose residues in the backbone, such as in glucomannan, also affects hydrolysis. β-mannanases from different families and even within families show variation in their mannan substrate specificity (Tailford et al., 2009). Tailford et al. (2009) showed that GH5 mannanase from *Bacillus agaradaerens* and GH26 mannanases from *B. subtilis* and *Cellvibrio japonicus* showed differences in their ability to bind glucose residues in their active site. The GH5 β-mannanases bound to mannose or glucose residues in their -1 and +2 subsites. The GH26 β-mannanases could only bind mannose residues. This explained why the GH26 β-mannanases hydrolyzed linear mannan best and the GH5 β-mannanases hydrolyzed glucomannan best. It was proposed that the ecological significance of this is that GH26 β-mannanases are optimized for the hydrolysis of linear seed mannans and GH5 β-mannanases are optimized for the hydrolysis of plant cell wall glucomannans. GH5 β-mannanases often have a carbohydrate binding module (CBM), which also indicates

their role in the hydrolysis of plant cell wall glucomannans. Zhang et al. (2014) found that *C. japonicus* GH26 β-mannanases had a much higher activity on small MOS than the GH5 β-mannanase that had a CBM. Their results indicated that mannan is first hydrolyzed by the GH5 β-mannanases, then the soluble oligomers are hydrolyzed by the GH26 β-mannanases - they probably act co-operatively to hydrolyze mannan. However, the division of function between the two different families is not so clear. Couturier et al. (2013) also found complementary activity between GH5 and GH26 β-mannanases of *Podospora anserina*. However, the GH26 mannanases have a CBM and produce large MOS compared to the GH5 β-mannanases that have no CBM. The GH5 β-mannanases could hydrolyze smaller MOS. Even β-mannanases within the same GH family and organism have been shown to have different biochemical properties (Hogg et al., 2003). Furthermore, von Freiesleben et al. (2016) found that some fungal GH5 and GH26 β-mannanases have different galactomannan degradation patterns due to structural differences that affect galactose accommodation in the active site cleft. The GH26 β-mannanases had a ~4 x higher percent conversion of guar gum (high degree of galactose branching) than the GH5 β-mannanases. The *Aspergillus nidulans* GH26 could accommodate galactose in the -2, -1 and +1 subsites, which is a novel characteristic that expanded the known substrate specificities of β-mannanases. Transglycosylation activity has also been reported in β-mannanases (Yamabhai et al., 2014). This can complicate the measurement of hydrolysis in terms of reducing sugar release, which is a commonly used method, as transglycosylation can lead to a decrease in hydrolysis. This diversity in biochemical properties may be due to the heterogeneous nature of lignocellulose composition and structure (Tailford et al., 2009). Clearly, there is still much to be learnt about the structure-function relationship between and within glycosyl hydrolase families. A better understanding of the structure-function relationships will allow for better selection and engineering of enzymes for more effective biomass hydrolysis.

1.3.2.2. β-mannosidases

These exo-acting enzymes have a pocket shaped active site cleft that allows accommodation of the non-reducing end of mannan, MOS and mannobiose. They hydrolyze the β-1,4 bonds releasing mannose units (Davies & Henrissat, 1995; Dhawan & Kaur, 2007). The β-mannosidases are grouped into GH families 1, 2 and 5 (Lombard et al., 2014; http://www.cazy.org/).

1.3.2.3. β-glucosidases

These exo-acting hydrolytic enzymes release glucose units from the non-reducing ends of oligosaccharides that are produced by β-mannanase hydrolysis of glucomannan and galactoglucomannan (Malgas et al., 2015[b]). The β-glucosidases are grouped into GH families 1, 3 and 5 (Lombard et al., 2014; http://www.cazy.org/).

1.3.2.4. α-galactosidases

These enzymes hydrolyze the α-1,6 bonds of D-galactose side chains of galactomannan and galactoglucomannan (Van Zyl et al., 2010). These enzymes are required to remove galactose substituents that sterically hinder mannan hydrolysis by β-mannanases and β-mannosidases (Malgas et al., 2015[c]). They are grouped into GH families 4, 27 and 36 (Lombard et al., 2014; http://www.cazy.org/). GH36 and GH27 α-galactosidases from *Aspergillus niger* were found to have different substrate specificities (Ademark et al., 2001). The GH27 α-galactosidases had higher activity on galactomannan polymers and galacto-mannoligosaccharides. The GH36 α-galactosidases had no activity on galactomannan and little to no activity on galacto-mannoligosaccharides. They displayed higher activity than the GH27 α-galactosidases on small galactose containing oligosaccharides. However, Wang et al. (2015) found that the two GH27 α-galactosidases produced by *Neosartorya fischeri* P1, Gal27A and Gal27B, showed differences in galactomannan and galacto-mannoligosaccharide hydrolysis. The Gal27A displayed higher galactomannan hydrolysis and lower galacto-mannoligosaccharide hydrolysis than Gal27B. The difference in substrate specificity was due to the 3D structure of their active sites. The Gal27A active site had a larger pocket-shaped structure that probably allowed it to accommodate highly branched galactomannans. Also, contrary to the findings by Ademark et al. (2001), Reddy et al. (2016) found that a GH36 α-galactosidase from *Bacteroides ovatus* efficiently hydrolyzed galactose on galactomannans. A 3D model revealed that the GH36 α-galactosidases had wider active site clefts than other GH36 α-galactosidases, which probably allows them to accommodate a galactomannan polymer. This shows, as with the GH5 and GH26 β-mannanases, that clear division of biochemical properties into GH families is not always possible. The 3D structure needs to be considered to more fully understand the biochemical properties.

1.3.2.5. Acetyl mannan esterases

These enzymes hydrolyze acetyl side chain groups of glucomannan and galactoglucomannan (Van Zyl et al., 2010). They are grouped into GH family CE16 (Lombard et al., 2014; http://www.cazy.org/).

1.3.2.6. Mannobiohydrolases

Mannobiohydrolases are exo-acting enzymes that hydrolyze from the non-reducing ends of mannan and MOS, releasing mannobiose (Araki & Kitamikado, 1988; Cartmell et al., 2008; Tsukagoshi et al., 2014). They have a tunnel-shaped active site that allows the polysaccharide to be passed through the enzyme, allowing product release while the enzyme is still bound to the substrate. This allows for efficient hydrolysis of crystalline mannan (Davies & Henrissat, 1995). Cartmell et al. (2008) reported that the *C. japonicus* mannobiohydrolase CjMan26C was very similar in structure to the endo- acting *C. japonicus* β-mannanase CjMan26A. These authors showed that endo-activity could be introduced by altering residues in a four residue extension of a surface loop that sterically blocks the -2 subsite of the mannanase. This suggests that mannobiohydrolases evolved from β-mannanases and that only minor changes were required for the change in activity (Cartmell et al., 2008; Davies & Henrissat, 1995).

1.3.3 Cellulose degrading enzymes

There are three types of hydrolytic enzymes involved in the complete hydrolysis of cellulose: cellobiohydrolases, endoglucanases and β-glucosidases. Cellobiohydrolases release cellobiose from the ends of cellulose chains, some hydrolyze from the reducing end and others hydrolyze from the non-reducing end (Van Dyk & Pletschke, 2012; Resch et al., 2013). Endoglucanases randomly cleave in the middle of cellulose chains and β-glucosidases release glucose from cellooligomers and cellobiose (Van Dyk & Pletschke, 2012; Hu et al., 2013). Other non-hydrolytic proteins have also been found to be involved in cellulose depolymerization such as lytic polysaccharide monooxygenases, swollenin and carbohydrate binding domains (Harris et al., 2014).

1.4. Synergy between mannanolytic enzymes

Enzyme synergy is the co-operative action of different types of enzymes hydrolyzing a substrate; their hydrolysis in combination is higher than the theoretical sum of individual hydrolysis by each type of enzyme (Van Dyk & Pletschke, 2012). Some reasons for why

synergy occurs include: the action of one enzyme creates more hydrolysis sites for another enzyme, one enzyme removes side chains that sterically hinder another enzyme, one enzyme hydrolyzes another enzyme product leading to a reduction in product inhibition, and the activity of one enzyme may release another enzyme non-productively bound to a substrate (Igarashi et al., 2011; Van Dyk & Pletschke, 2012). Synergy is required for the complete hydrolysis of lignocellulose polysaccharides and optimization of synergy is one of the ways in which lignocellulose hydrolysis can be made more efficient and less costly (Van Dyk & Pletschke, 2012). Synergy can be measured in terms of degree of synergy (DS), which is calculated as follows: the hydrolysis of a substrate by a mix of different enzymes is divided by the theoretical sum of hydrolysis by the individual enzymes. A DS of 1 indicates that no synergy occurred, the enzymes act independent of one another on the substrate, a DS > 1 indicates synergy and a DS of < 1 indicates anti-synergy, which may be due to enzymes competing for the same binding sites on the substrate (Van Dyk & Pletschke, 2012). Anti-synergy may also be due to the products of one type of enzyme inhibiting the hydrolysis of another type of enzyme (Kumar & Wyman, 2014).

Broadly speaking, there are two types of synergy: homeosynergy and heterosynergy. Homeosynergy refers to synergy between main chain cleaving enzymes or between side chain cleaving enzymes - for example, between β-mannanases and β-mannosidases. Heterosynergy refers to the synergy between main chain cleaving enzymes and side chain cleaving enzymes (Malgas et al., 2015[b]) - for example, between β-mannanases and α-galactosidases. The sequence of application of different enzymes can have a large effect on hydrolysis efficiency. There are three enzyme application types: simultaneous, sequential and successive. Simultaneous application is when all the enzymes are added at the same time in the reaction mixture. Sequential application is when one enzyme is added to a substrate and then after some time is allowed for hydrolysis, the enzyme is denatured (for example, by heating the mixture) and then another enzyme is added. Successive synergy is similar to sequential synergy, except that the first added enzyme is not denatured before the second enzyme is added (Van Dyk & Pletschke, 2012; Malgas et al., 2017a).

Various studies have reported heterosynergy and homeosynergy, with simultaneous or sequential application, between mannanolytic enzymes (Malgas et al., 2015[b]). Wang et al. (2015) found that simultaneous application of the α-galactosidase GH27A and the mannanase Man5P1 from *Neosartorya fischeri* on galactomannan led to synergy. An increase in reducing sugar release of up to 11.67 fold was observed. Malgas et al. (2015[c]) found that GH family affiliation of β-mannanases and α-galactosidases affects their

synergistic relationship. They found that GH27 α-galactosidase from *Cyamopsis tetragonolobus* seeds displayed synergy with a *Clostridium cellulovorans* GH5 β-mannanase and an *Aspergillus niger* GH26 β-mannanase on locust bean gum and synergy with the GH5 β-mannanase on guar gum. The *A. niger* GH36 α-galactosidase that was assessed did not display any synergy. Malgas et al. (2015[b]) proposed a model for the efficient hydrolysis of galactomannan (homeosynergy and heterosynergy), as shown in Figure 1.4. First, a GH27 α-galactosidase removes galactose substituents. β-mannanase then cleaves the mannan backbone into small oligomers. β-mannosidase removes mannose from the non-reducing ends of MOS until a galactose substituted mannose impedes further hydrolysis. These galactose substituents are then hydrolyzed by GH36 α-galactosidases.

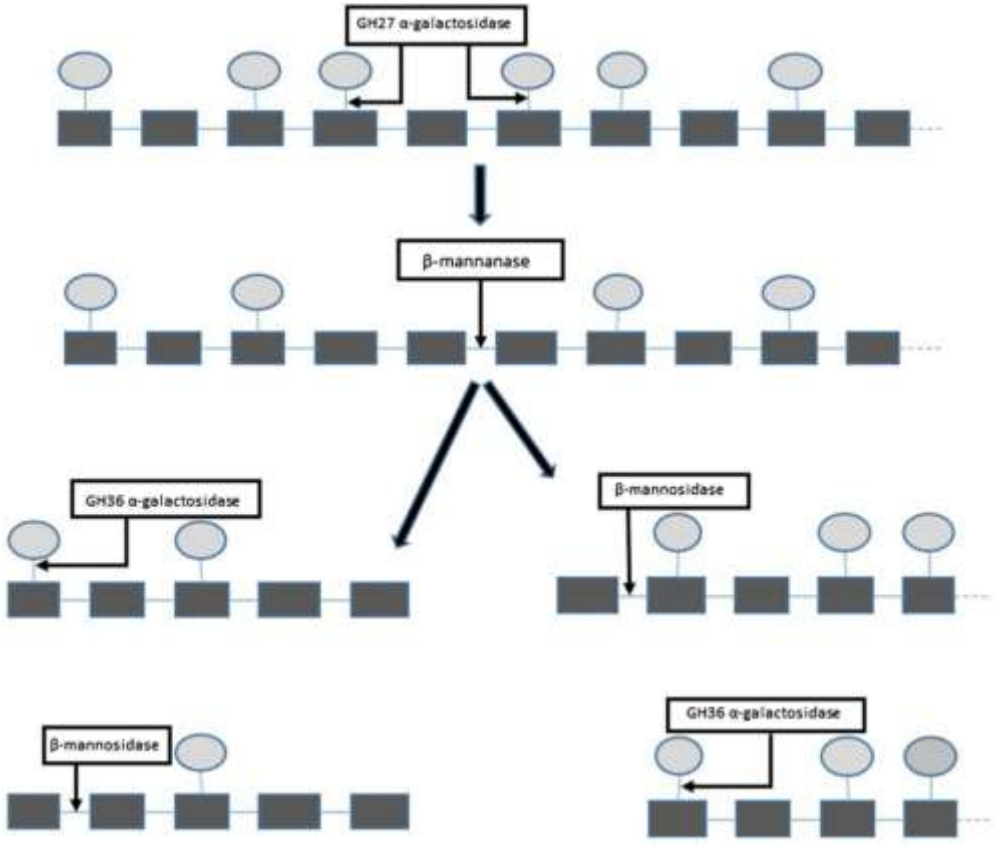

Figure 1.4. Model for synergistic galactomannan hydrolysis. The lines represent glycosidic bonds between the sugar monomers, the squares represent mannose and the circles represent galactose. From Malgas et al. (2015[b]).

Most mannanase synergy studies have been conducted using model substrates such as locust bean gum and guar gum (Malgas et al., 2015[b]). However, a few studies have been conducted on raw, more industrially relevant substrates. These studies showed how hydrolysis of one polysaccharide can improve the hydrolysis of another polysaccharide. This

probably occurs because mannans, along with other hemicelluloses, are interspersed amongst cellulose microfibrils. Hydrolysis of one polysaccharide can increase another polysaccharide's accessibility (Sorek et al., 2014). Synergy between a β-mannanase and xylanase, as well as between a mannanase, xylanase and a galactosidase was observed on softwood paper pulp. The synergy was observed as an increase in pulp bleaching ability as well as an increase in reducing sugar release (Clarke et al., 2000). Jørgensen et al. (2010) showed synergy between a β-mannanase, mannosidase and cellulase on palm kernel press cake. Mannose and glucose release increased. Malgas (2015) observed synergy between mannanase and a cellulase cocktail on de-lignified sugarcane bagasse. An increase in reducing sugar release was observed.

1.5. Applications of β-mannanases

β-mannanases have various industrial applications including use in biofuel production, MOS production and paper bleaching (Yamabhai et al., 2014). MOS have been shown to have prebiotic effects (Walton et al., 2010). β-mannanases have a wide variety of substrate specificities and physico-chemical characteristics and consequently have many potential applications. Suitable application depends on specific characteristics. Thermostable and acid stable β-mannanases are suitable for use in the hydrolysis of lignocellulose for biofuel production, whereas thermostable and alkaline stable β-mannanases are suitable for bio-bleaching of paper pulp and for use in detergents (Van Zyl et al., 2010; Chauhan et al., 2012). The industrial application of lignocellulolytic enzymes determines the level of enzyme purity required (Szakacs et al., 2006). Novozymes®, which is the biggest manufacturer and supplier of industrial enzymes, often makes use of concentrated enzyme solutions with specific activities. Most are produced by genetically modified microorganisms for increased production and purity (Paloheimo et al., 2016; Novozymes®, 2017). Food industry enzymes require high purity, which includes enzymes used for the production of prebiotic oligosaccharides (Qing et al., 2013; Jain et al., 2015). Lignocellulases used as animal feed supplements do not require high purity (Chauhan et al., 2012). Crude enzyme cocktails with multiple activities are used for the hydrolysis of complex agricultural residues for biofuel production. Purified enzymes may also be added to these enzyme cocktails to enhance hydrolysis efficiency (Hu et al., 2015, Malgas et al., 2017b).

1.5.1 Pretreatment severity and biofuel production

Recently less severe pretreatments, such as reduced use of chemicals or lower process temperatures for various types of pretreatments, have been used for the production of lignocellulosic biofuels. This reduces the capital cost of biorefineries and minimizes waste generation. Less severe pretreatments lead to an increase in residual hemicellulose, including mannan, which is the focal substrate in this study (Harris et al., 2014). For this study, a low pressure, low temperature (low severity) NaOH pretreatment was selected as it has been shown to be an effective pretreatment method that does not solubilize most of the hemicelluloses (Gümüşkaya & Usta, 2006; Zhao et al., 2008; Sills & Gossett, 2011; Chen et al., 2013). NaOH pretreatment is discussed further in Chapter 4. Hydrolysis of this hemicellulose can increase the total sugar yield and can also improve cellulose hydrolysis by reducing steric hindrance by hemicellulose (Van Dyk & Pletschke, 2012; Harris et al., 2014). β-mannanases are particularly useful for enzymatic biofuel production from substrates with a high mannan content such as palm kernel press cake, softwoods and spent coffee grounds (SCG) (Van Zyl et al., 2010).

1.5.2 Prebiotic mannooligosaccharide production

The mammalian gastrointestinal tract has a complex community of microbiota. The composition and metabolism of these microbes appears to play important roles in nutrition, physiology and pathology. These microbes can influence or be involved in intestinal conditions such as irritable bowel syndrome and colon cancer (Roberfroid, 2008). A prebiotic is a non-digestible compound that is metabolized by microorganisms in the gut, causing a change in the composition and/or activity of the gut microbiota that leads to beneficial physiological effects for the host (Bindels et al., 2015). MOS have been shown to have prebiotic effects (Walton et al., 2010). Yeast cell wall MOS have been shown to have prebiotic effects in a mouse model of acute colitis. MOS ingestion reduced weight loss, diarrhoea, mucosal damage and sickness related anxiety (Ferenczi et al., 2016).

These oligosaccharides can be produced by thermal, chemical or enzymatic methods. Enzymatic hydrolysis is advantageous over other methods as it is more specific so it does not have undesirable by-products (Jain et al., 2015). The most important enzyme for MOS production is β-mannanase (Yamabhai et al., 2014). Other enzymes may also be involved for more complete hydrolysis of mannan and to produce MOS with a specific structure. The effect of MOS structure on its prebiotic effect is yet to be resolved (Yamabhai et al., 2014). A potentially good source of MOS is SCG. SCG are the unextracted solids remaining after

soluble extraction from coffee. Around 65% (w/w) of green coffee beans remain as residual solids otherwise known as SCG (Murthy & Naidu, 2012). Dried SCG consists of around 45.3% (w/w) polysaccharides. Cellulose and mannan are the dominant polysaccharides present (Simões et al., 2013).

1.5.3 Other uses

Mannanases have various other current and potential applications such as use in animal feed, paper bleaching, detergents, dye removal and pharmaceutical production. Mannanases used as an animal feed supplement have been shown to improve digestion and increase weight gain by assisting in feed digestibility (Van Zyl et al., 2010). Mannanases have been shown to aid in paper pulp bleaching (Clarke et al., 2000) and have been shown to remove various dyes from textiles (Ge et al., 2016). Alkaline stable mannanases are used in some detergents for the removal of mannan stains - mannans are widely used in the food industry as a thickener (Moreira & Filho, 2008). Glucomannan from *Punica granatum* was shown to have antioxidant, immunomodulatory and anticancer effects using *in vitro* and *in vivo* models. Glucomannan oligosaccharides, produced by mannanase hydrolysis of glucomannan, may also have these properties.

1.6. *Bacillus paralicheniformis* SVD1 as a potential source of β-mannanase

Bacillus paralicheniformis is a recently described gram-positive, facultatively anaerobic, endospore forming bacterium that is very closely related to *B. licheniformis* (Dunlap et al., 2015). Dunlap et al. (2015) provided evidence that the two phylogenomic groups that *B. licheniformis* strains can be divided into are sufficiently different to split *B. licheniformis* into two species. The group two strains were given the new species name *B. paralicheniformis*. The species can be distinguished from each other based on various phylogenomic and phenotypic characteristics. One of these differences is that *B. paralicheniformis* has multiple unique carbohydrate-metabolizing enzymes, including arabinofuranohydrolase (Genbank accession no. BaLi_c36440) and xylosidase (Genbank accession no. BaLi_c29190). Both species produce an array of hydrolytic enzymes that allows them to utilize many types of carbohydrate and nitrogen sources and consequently contribute to nutrient cycling in nature. *B. licheniformis* is used industrially for the production of enzymes, antibiotics and other biochemicals (Rey et al., 2004; Veith et al., 2004). *B. paralicheniformis* shows promise for the commercial production of various hydrolases (Akcan, 2011[a]; Akcan, 2011[b]; Akcan,

2012). *B. paralicheniformis* SVD1 was isolated by Van Dyk (2009) from a co-culture with *Clostridium beijerinkii* sLM01 in a biosulfidogenic bioreactor (Mayende, 2006). Studies by Van Dyk and colleagues have shown that this strain is mostly hemicellulolytic and produces a xylanolytic multi-enzyme complex with various other glycosyl hydrolase activities (Van Dyk, 2009; Van Dyk et al., 2009). The genome of *B. paralicheniformis* SVD1 has been partially (~95%) sequenced (Sakka et al., 2012). It was originally identified as *B. licheniformis* SVD1 by Sakka et al. (2012) but re-analysis of the genome showed that it is more similar to the closely related species, *B. paralicheniformis* (Section 2.4.2). *B. paralicheniformis* and *B. licheniformis* produce two different β-mannanases, a GH5 (GenBank accession no. AB643490) and a GH26 β-mannanase (GenBank accession no. AB643507) (Rey et al., 2004; Veith et al., 2004; Sakka et al., 2012; Dunlap et al., 2015). Amongst *the B. licheniformis* strains, the GH26 β-mannanase of *B. licheniformis* DSM13^T (=ATCC14580^T) has been biochemically characterized but the GH5 has not been (Songsiriritthigul et al., 2010). Amongst the *B. paralicheniformis* strains, the crude β-mannanase activity of *B. paralicheniformis* SVD1 has only been partially biochemically characterized (Van Dyk, 2009). The *B. paralicheniformis* SVD1 GH26 β-mannanase has a 95% protein sequence identity to the GH26 β-mannanase of *B. licheniformis* DSM13^T (=ATCC14580^T). The protein sequence of the *B. paralicheniformis* SVD1 GH5 β-mannanase has a 96% sequence identity to the GH5 β-mannanase of *B. licheniformis* DSM13^T (=ATCC14580^T) (Sakka et al., 2012). However, small protein sequence differences can lead to quite different biochemical characteristics (Fenel et al., 2004).

1.7. Problem statement

β-mannanases have various industrial uses. Their use depends on their biochemical characteristics. The β-mannanases of *B. paralicheniformis* SVD1 have not been fully biochemically characterized. Commercial application of currently available β-mannanases is limited by factors such as their activity, stability and knowledge of their synergy with other enzymes.

1.8. Hypothesis

The β-mannanases have industrially useful biochemical characteristics. The β-mannanases, along with α-galactosidases, can be used to synergistically hydrolyze locust bean gum. The β-mannanases, along with a commercial cellulase mixture, can be used to synergistically hydrolyze spent coffee grounds, an industrial waste product. Characterization of β-

mannanases elucidates their function. This, along with follow-up structural studies, can help determine structure-function relationships, leading to an improved understanding of mannanases and how they synergistically hydrolyze mannan. This can aid the industrial production of mannoligosaccharides and development of improved enzyme cocktails for complete lignocellulosic biomass hydrolysis.

1.9. Aims and Objectives

- To grow *B. paralicheniformis* SVD1 on locust bean gum, a galactomannan, to induce mannanase production
- To measure growth curve parameters to determine when mannanase activity is maximal during growth
- To concentrate the crude supernatant containing β-mannanase
- To characterize crude mannanase activity, including mannooligosaccharide production
- To purify the mannanase activity and characterize the purified mannanase, including mannooligosaccharide production
- To determine synergy between the purified mannanase and an α-galactosidase on locust bean gum
- To pretreat and characterize spent coffee ground
- To assess the synergistic hydrolysis of spent coffee ground, an industrial waste product, by the purified mannanase and commercial cellulase mixture.

1.10. Overview of thesis

The growth curve parameters of *B. paralicheniformis* SVD1 in mannan broth were used to optimize β-mannanase production. The concentrated secretome that displayed predominantly β-mannanase activity was then characterized. The β-mannanases released small MOS from various mannan substrates; these oligosaccharides may have useful prebiotic properties. This is described in Chapter 2. Chapter 3 describes the attempted purification of the β-mannanase and biochemical characterization of the partially purified β-mannanase. The purification was not successful as the β-mannanase was only partially

purified. The β-mannanase displayed synergy with an α-galactosidase in terms of reducing sugar release and MOS production. In chapter 4, the partially purified β-mannanase's synergy with a commercial cellulase mixture on an industrial waste product, SCG, was assessed. This chapter describes the first report of synergy between β-mannanase and cellulase on SCG. In chapter 5, the study is discussed in general and suggestions are offered for further studies.

Chapter 2 – Biochemical characterization of *Bacillus paralicheniformis* SVD1 β-mannanase activity when cultured on locust bean gum

2.1. Introduction

Bacillus paralicheniformis produces an array of hydrolytic enzymes that allows it to utilize many types of carbohydrate and nitrogen sources (Ferrero et al., 1996; Veith et al., 2004; Van Dyk, 2009; Sakka et al., 2012; Dunlap et al., 2015). Many of the genes involved in catabolism of these carbon and nitrogen sources require induction and the absence of catabolite repressors, such as glucose, for high levels of expression (Stülke & Hillen, 2000; Voigt et al., 2007). Easily metabolized carbon and nitrogen sources such as glucose and amino acids are preferred. This conserves energy as the required proteins, including the hydrolytic enzymes, are only synthesized when needed (Madigan et al., 2003). Selective induction of hydrolytic enzymes in response to changing environmental conditions allows bacteria to utilize alternative carbon and nitrogen sources, which aids their survival (Voigt et al., 2007). Bacteria have been shown to regulate expression of hydrolases depending on the substrates available (Stülke & Hillen, 2000; Van Dyk, 2009). Multiple hydrolytic enzymes may be induced by a single substrate due to induction of an operon that encodes multiple hydrolases (Lynd et al., 2002). Genomic analysis has shown that *B. paralicheniformis* ATCC9945A as well as the closely related *B. licheniformis* DSM13^T (=ATCC14580^T) have gene clusters involved in holocellulose hydrolysis and utilization (Rey et al., 2004; Rachinger et al., 2013).

Bacteria require carbon, nitrogen and oxygen sources as well as various other nutrients and minerals for metabolic processes and growth (Madigan et al., 2003). To optimize growth conditions for hydrolase production there must be a balance between optimizing for cell growth and optimizing for enzyme production. Subramaniyan et al. (2001) concluded that the optimal nitrogen source (yeast extract and peptone) for xylanase production by a *Bacillus* sp. was a balance between sufficient nitrogen for growth and enzyme production. High nitrogen source loadings potentially induce a high level of protease production or suppress hydrolytic enzyme production due to easily metabolized nitrogen and carbon sources. Proteases can hydrolyze lignocellulolytic enzymes. Ferrero et al. (1996) found that the nitrogen source, as well as the carbon source, affected the production of proteases in *B. licheniformis* MIR 29.

Growth media composition can be altered to minimize protease expression and protease inhibitors can be added to extracts and purified fractions of the protein of interest (Deutscher, 2009). The time allowed for growth is an important consideration for maximal enzyme production. Changes in nutrient supply in the late exponential growth phase and stationary phase induce protease and glycosyl hydrolase production in *B. licheniformis* (Ferrero et al., 1996; Bose & Das, 1996). However, Voigt et al. (2007) found that in *B. licheniformis* DSM13^T (=ATCC14580^T) only a few glycosyl hydrolase and protease genes were induced by glucose starvation. Most of these enzymes probably require an inducer and the absence of easily metabolized carbon sources (Stülke & Hillen, 2000).

B. paralicheniformis SVD1 produces β-mannanase activity when grown in locust bean gum broth (Van Dyk, 2009). It does not have β-mannosidase activity as it does not have β-mannosidase genes (Sakka et al., 2012). Purification of the β-mannanases was attempted (Chapter 3) in order to characterize the individual β-mannanase activities. The crude β-mannanase fraction could contain two types of β-mannanases. *Bacillus licheniformis* SVD1 has two β-mannanase genes from different glycosyl hydrolase (GH) families, a GH5 and a GH26 β-mannanase (Rey et al., 2004; Sakka et al., 2012). The *B. paralicheniformis* SVD1 GH5 β-mannanase protein sequence has 96% sequence similarity to the *B. licheniformis* DSM13^T (=ATCC14580^T) GH5 β-mannanase. The *B. paralicheniformis* SVD1 GH26 β-mannanase protein sequence has 95% sequence similarity to the *B. licheniformis* DSM13^T (=ATCC14580^T) GH26 β-mannanase. This indicates that the mannanases of the two strains are very similar. However, small protein sequence differences can lead to quite different biochemical characteristics. For example, a T2C:T28C mutation of the *Trichoderma reesei* endoxylanase XYNII increased thermostability of the enzyme by about 15°C without altering the kinetic properties (Fenel et al., 2004). Mannanase production by *B. paralicheniformis* SVD1 and characterization of the crude β-mannanase has been assessed briefly by Van Dyk (2009) and Van Dyk et al. (2010). Mannanase production was induced by growth in locust bean gum broth. The crude mannanase displayed two pH optima (pH 7.0 and 9.0) and two activity bands were seen on a locust bean gum zymogram (23 kDa and 33 kDa).

In order to assess an enzyme's fitness for industry, it needs to be characterized. Characterization is important to determine the industrial applications and the optimal reaction conditions for an enzyme. It also helps in the development of a purification protocol for an enzyme (Ghosh et al., 2013; Chauhan et al., 2014). The aims of this chapter were to

measure the growth curve parameters of *B. paralicheniformis* SVD1, when grown in locust bean gum broth, and then further characterize the crude mannanolytic activity of *B. paralicheniformis* SVD1 to assess its potential industrial use.

2.2. Objectives

- To induce mannanase production in *B. paralicheniformis* SVD1 by growth in mannan containing liquid media,
- To determine growth curve parameters
- To determine when to concentrate β-mannanase for characterization and purification by using the growth curve parameters
- To concentrate β-mannanase from a broth culture
- To determine the temperature optimum, pH optimum and temperature stability of β-mannanase activity
- To determine the glycosyl hydrolase activities present
- To assess the secretome and the size of mannanases using SDS-PAGE and zymography
- To determine mannooligosaccharide production over time from crude mannanase hydrolysis of mannan-rich substrates

2.3. Materials and Methods

2.3.1. Revival of a *Bacillus paralicheniformis* SVD1 glycerol stock

Van Dyk (2009) isolated *B. paralicheniformis* SVD1 from a co-culture with *Clostridium beijerinkii* sLM01 in a biosulfidogenic bioreactor (Mayende, 2006). It was stored as glycerol stocks at -20°C. This stock was revived by thawing the stock on ice. The stock was then mixed well and 50 µl was pipetted, using a standard aseptic technique, and spread onto agar plates. The agar plates were composed of 0.5% (w/v) locust bean gum, 0.5% (w/v) yeast extract, 0.4% (w/v) tryptone, 0.02% (w/v) $MgSO_4$ and 1.2% (w/v) agar in 0.05 M pH 7.0 potassium phosphate buffer (Choudhury et al., 2006). The suppliers of the reagents are provided in Appendix 1. The plates were incubated at 37°C overnight until growth was observed. Colonies were visually assessed for contamination. To assess if the agar cultures were producing mannanases, a single agar plate colony of *B. paralicheniformis* SVD1 was streaked onto a fresh agar plate and incubated at 37°C overnight until growth was observed.

The plate was then incubated with 10 ml of 0.3% (w/v) Congo Red solution for 15 min to stain the carbohydrates. The plate was then destained by incubating the plate with 15 ml of 1 M NaCl; this was repeated two times. Destained areas indicate mannanase activity (Teather & Wood, 1982).

2.3.2. Confirmation of identity by 16S rRNA sequencing

Agar plate cultures were sent to Inqaba Biotechnical Industries Pty. Ltd., South Africa for gDNA isolation and 16S rRNA sequencing. The ZR Fungal/ Bacterial DNA Kit (Zymo Research) was used for DNA isolation. The 16S rRNA was amplified using DreamTaq DNA polymerase (Thermo Scientific) and the following primers: 16S-27F (5' – AGAGTTTGATMTGGCTCAG - 3') and 16S-1492R (5' - CGGTTACCTTGTTACGACTT - 3'). PCR products were gel extracted (Zymo Research, Zymoclean Gel DNA Recovery Kit), and sequenced in the forward and reverse directions using an ABI PRISM 3500xl Genetic Analyser. Purified sequencing products (Zymo Research, ZR-96 DNA Sequencing Clean-up Kit) were analysed using CLC Main Workbench 7. BLAST (Altschul et al., 1990; http://blast.ncbi.nlm.nih.gov/BlastAlign.cgi) was used for a multiple sequence alignment of the sense strand of the sequenced 16S rRNA and the 16S rRNA sequence of *B. paralicheniformis* SVD1 (GenBank accession no. EU 770587; Van Dyk, 2009).

2.3.3. Culture maintenance

Fresh glycerol stocks were made from the revived glycerol stock (Section 2.3.1.). They were prepared as follows: The glycerol stock was plated and incubated until colonies formed as in section 2.3.1. and then a single colony was used to inoculate 40 ml of liquid media. This was done in triplicate. The liquid media had the same composition as the plate (section 2.3.1.) except it did not contain agar. The cultures were incubated at 37°C with shaking at 150 rpm under aerobic conditions. The optical density at 600 nm (OD 600) was measured to determine whole cell density so that the bacterial growth rate could be monitored. This was done by taking 1 ml aliquots at different time intervals. The aliquots were centrifuged at 16 060 *x g*) for 15 min, the pellet was re-suspended in 1 ml of 0.05 M potassium phosphate buffer (pH 7.0) and then the absorbance at 600 nm of three 300 µl aliquots was measured using a Powerwave X microplate reader from Bio-Tek Instruments using KC Junior software. Samples were gently shaken in the microplate reader for 10 seconds prior to absorbance readings being taken. Exponential phase cultures (0.5 ml) were added to 0.5 ml of

autoclaved 40% (v/v) or 80% (v/v) glycerol in deionized water to make 20% and 40% glycerol stocks. The stocks were mixed and then stored at -20°C.

2.3.4. Growth curve

2.3.4.1. Culturing, cell growth and pH

Glycerol stocks (1 ml) were thawed on ice. The stock was mixed well and then pipetted, using standard aseptic technique, into seed broth cultures (40 ml) that were prepared as in section 2.3.3. The cultures were incubated at 37°C with shaking at 150 rpm under aerobic conditions. Production broth (400 ml) was inoculated with 1% (v/v) log-phase seed culture and was incubated at 37°C with shaking at 150 rpm under aerobic conditions. Aliquots of 5 ml were taken from the production broth every ~6 h for 72 h and were centrifuged at 16 060 *x g* for 15 min to pellet the cells. Various parameters were measured as described in sections 2.3.4.1. – 2.3.4.4. The cell growth was measured using OD 600 as described in Section 2.3.3. The pH was measured using a PHS-3BW microprocessor pH/mV/temperature meter (BANTE Instruments).

2.3.4.2. β-mannanase activity

Enzyme activity of the cell-free supernatant was measured as the amount of reducing sugars released using a modified dinitrosalicylic acid (DNS) assay (Miller, 1959). The hydrolysis reaction was performed by mixing 100 µl crude supernatant with 300 µl locust bean gum in 0.05 M pH 7.0 potassium phosphate buffer. The final concentration of locust bean gum in the reaction mixture was 0.5% (w/v). The protein load was 3.34 mg protein.g^{-1} locust bean gum. The hydrolysis reaction was conducted for 3 h at 50°C in an AccuBlock digital dry bath heater (Labnet). The reaction mixtures were then centrifuged at 16 060 *x g* for 5 min to remove any insoluble substrate. The DNS assay was performed by adding 150 µl of hydrolyzate supernatant to 300 µl DNS reagent. DNS reagent was prepared as described in Appendix 2. The assay mixtures were then heated at 100°C for 5 min and then cooled on ice for 5 min. An aliquot (250 µl) was then pipetted into a 96-well microtiter plate and the absorbance readings were then taken at 540 nm using a Powerwave X microplate reader (BioTek Instruments) and KC Junior software. The reducing sugar concentration was determined using a mannose standard curve (Appendix 2 – Figure A.1). Two negative controls were used: an enzyme control and a substrate control. The enzyme control contained the enzyme solution and buffer. The substrate control contained the substrate and buffer. A solution with a known concentration of mannose was used as a positive control.

The assays were performed in triplicate. One unit of enzyme activity (U) was defined as the amount of enzyme that released 1 µmol of reducing sugar per min under the assay conditions used.

2.3.4.3. Protein concentration

Bradford's protein assay (Bradford, 1976) was used to determine protein concentration using Bradford's reagent (Sigma). Bovine serum albumin (BSA) in 0.05 M potassium phosphate buffer (pH 7.0) was used as a standard to construct standard curves (Appendix 3). Two types of Bradford's protein assays were conducted depending on the protein content of the sample: a high concentration range assay and a low concentration range assay. For the high concentration range assay, 230 µl of Bradford's reagent was added to 25 µl of suitably diluted protein solution in a 96-well microtiter plate. For the low concentration range assay, 150 µl of Bradford's reagent was added to 150 µl of suitably diluted protein solution in a 96-well microtiter plate. The plates were then gently mixed for 5 min at room temperature. Absorbance was then measured at 595 nm with a Powerwave X microplate reader (Bio-Tek Instruments) using KC Junior software. Samples were gently shaken in the microplate reader for 10 seconds prior to absorbance readings being taken. A solution with a known concentration of BSA was used as a positive control. The assays were performed in triplicate.

2.3.4.4. Protease activity

Sigma's universal protease assay, using casein and the Folin-Ciolcalteu phenol reagent, was used to determine protease activity (Folin & Ciocalteau, 1927; Anson, 1938; http://www.sigmaaldrich.com/life-science/learning-center/life-science-video/universal-protease, Date of access: 14/ 02/ 2016). L-tyrosine was used to generate a standard curve. The assays were performed in triplicate.

2.3.5. *In silico* characterization of *Bacillus paralicheniformis* SVD1 β-mannanases

The Genbank accession numbers of the *B. paralicheniformis* SVD1 β-mannanase gene sequences (GH 26 β-mannanase - AB643507; GH5 β-mannanase - AB643490) were obtained from the partially determined genome sequence of *B. paralicheniformis* SVD1 (Sakka et al., 2012). The sequences were accessed on the NCBI website (www.ncbi.nlm.nih.gov) and translated into their amino acid sequences. Some physico-

chemical properties of the mannanases were determined *in silico* using the ProtParam tool in the ExPasy Bioinformatics Resource Portal (https://www.expasy.org; Gasteiger et al., 2005) as well as UniProt (http://www.uniprot.org/). The putative signal sequences were removed prior to *in silico* determination of their physico-chemical properties..BLAST (Altschul et al., 1990; http://blast.ncbi.nlm.nih.gov/BlastAlign.cgi) was used to find homologous mannanases.

2.3.6. Concentration of β-mannanase

Locust bean gum broth cultures (400 ml) were grown for 48 h as described in Section 2.3.4.1. The culture was centrifuged at 13 250 *x g* for 15 minutes using an Avanti centrifuge. The cell-free supernatant was concentrated using 3 kDa Amicon® Ultra-15 centrifugal filter devices using the protocol provided by the manufacturer. Glycerol (20% (v/v)) and 0.03% (w/v) sodium azide was added to the concentrate and an aliquot of the cell-free supernatant.

2.3.7. β-mannanase activity and protein concentration determination

Enzyme activity of the cell-free supernatant and 3 kDa concentrate was determined using a modified DNS assay for determining reducing sugars as described in section 2.3.4.2., except that the assay was conducted for 30 min and not 3 h. The protein load of the cell-free supernatant was 5.46 mg protein.g^{-1} locust bean gum. The protein load of the 3 kDa concentrate was 2.93 mg protein.g^{-1} locust bean gum. The Bradford assay was used to determine protein concentration as described in section 2.3.4.3.

2.3.8. Time study

Enzyme activity was measured using the enzyme activity assay as described in Section 2.3.4.2., except that different hydrolysis times (5 min - 90 min) were used.

2.3.9. Temperature optimum and stability

The temperature optimum was determined using the standard enzyme activity assay (Section 2.3.7.) at different temperatures (25°C, 37°C, 45°C, 50°C, 55°C, 60°C, 65°C, 70°C, 75°C). The temperature stability was determined by incubating the appropriately diluted mannanase solution at 37°C or 50°C for 0 h to 24 h and then measuring the residual activity.

The activity was represented as % relative activity, compared to activity at the temperature optimum or compared to activity at time = 0.

2.3.10. pH optimum

The pH optimum was determined using the standard enzyme activity assay (Section 2.3.7.) with different pH buffers in a pH range from 3.0 – 11.0. The buffers used were: 0.05 M sodium citrate (pH 3.0 – 5.0), 0.05 M potassium phosphate (pH 6.0 – 8.0) and 0.05 M glycine (pH 9.0 – 11.0). The activity was represented as % relative activity, compared to activity at the pH optimum.

2.3.11. Substrate specificity

The activities of the enzymes were assessed on different substrates. For polymeric substrates, the standard assay was used (Section 2.3.7.). The polymeric substrates assessed were: locust bean gum, guar gum, ivory nut mannan, konjac glucomannan, carboxymethyl cellulose and Avicel®. The activity on konjac glucomannan was too high (using the standard assay) so the protein load was reduced by a half to 1.47 mg protein.g^{-1} substrate. Activity on *p*-nitrophenyl (*p*NP) substrates was also assessed. The substrates assessed were: *p*NP α-L-arabinofuranoside, *p*NP β-D-mannopyranoside, *p*NP β-D-galactopyranoside, *p*NP α-D-galactopyranoside, *p*NP β-D-glucopyranoside and *p*NP β-D-cellobioside. Activity on *p*NP based substrates was conducted as follows: concentrated mannanase (100 µl) was added to 300 µl of 2.67 mM *p*NP substrate in 0.05 M potassium phosphate buffer (pH 7.0) in eppendorf tubes. The tubes were incubated at 50°C for 30 min in an AccuBlock digital dry bath heater (Labnet). The reactions were terminated by the addition of 400 µl of 2 M Na_2CO_3 in diH_2O. Aliquots (250 µl) were then pipetted into a 96-well microtiter plate and the absorbance readings were then taken at 405 nm using a Powerwave X microplate reader (BioTek Instruments) and KC Junior software. The concentration of *p*NP released was determined using a *p*NP standard curve (Appendix 4 – Figure A.8). One unit of enzyme activity was defined as the amount of enzyme that released 1 µmol of *p*NP per min under the assay conditions specified.

2.3.12. SDS-PAGE and zymography

Sodium dodecyl sulphate polyacrylamide gel electrophoresis (SDS-PAGE) was conducted using the method developed by Laemmli (1970) and modified according to Bollag et al. (1996), except that the SDS-PAGE gels were silver stained using a Piece® Silver stain kit according to the supplier's instructions. A broad range pre-stained MW marker was used (New England BioLabs). Zymograms were used to determine the MWs of the mannanase/s. Polyacrylamide gels were prepared as for SDS-PAGE except for a few changes. In the stacking and separating gel solutions, diH_2O replaced the 10% (w/v) sodium dodecyl sulphate **(**SDS) solution. The separating gel had mannan substrate added to it. The mannan substrates used were konjac glucomannan, locust bean gum, ivory nut mannan or guar gum. Prior to polymerization all of the separating gel solution components were added except the acrylamide/ bis-acrylamide solution. Then a mannan substrate was added to a concentration of 0.1% (w/v) and the solution was mixed with a magnetic stirrer for 30 min prior to the addition of the acrylamide/ bis-acrylamide solution. For sample preparation, the concentrated β-mannanase and SDS-sample buffer mixture was boiled for 45 s instead of 5 min (Van Dyk, 2009).

After electrophoresis the MW marker lane and a lane with the concentrated β-mannanase was excised for silver staining. The remaining lanes with the concentrated β-mannanase were renatured by removing SDS. The gels were washed then incubated with 100 ml of 2.5% (v/v) Triton X-100 in either 0.05 M sodium citrate buffer (pH 5.0) or 0.05 M potassium phosphate buffer (pH 7.0) for 1 h at room temperature with occasional shaking. The Triton X-100 solution was then removed and the gels were washed with buffer. Buffer was then added and the gels were incubated for 30 min at room temperature with occasional shaking. The gels were rinsed again, buffer was added and then the gels were incubated at 37°C for 48 h. The gels were stained by incubation in 0.3% (w/v) Congo Red (25 ml) for 30 min to detect hydrolysis of the incorporated mannan substrates (Carroll & Van Dyk, 1952). The gels were destained by incubation in 25 ml of 1 M NaCl for 15 min. Destaining was repeated until bands appeared. The silver stained and Congo Red stained gels were then aligned and imaged using a BioRad ChemiDoc XRS+ with Image Lab^{TM} software.

2.3.13. TLC analysis of mannan hydrolysis

Products of mannan and MOS hydrolysis were analysed using thin layer chromatography (TLC). The reaction mixtures consisted of 75 µl of 0.5% (w/v) mannan substrate in 0.05 M potassium phosphate buffer (pH 7.0) and 25 µl of concentrated β-mannanase in eppendorf tubes. The enzyme load was 146.6 mg protein.g^{-1} substrate (0.30 U). The reaction mixtures were incubated in a dry heating bath at 50°C for 30 min to 24 h. Samples were then boiled for 5 minutes at 100°C and centrifuged at 16 060 *x g* for 5 minutes. The supernatant was used for TLC. Identical volumes (5 µl) of the supernatant were applied to Silica Gel HPTLC plates (Merck). Monosaccharide and MOS standards (0.5% (w/v)) were also applied. Plates were developed twice with n-butanol: acetic acid: water (2:1:1, v/v). To detect carbohydrates, plates were air dried then briefly (a few seconds) submerged in methanol containing 5% (v/v) sulfuric acid and 0.3% (w/v) α-naphthol. Plates were then air dried and heated at 120°C for 10 minutes for colour development.

2.4. Results

2.4.1. Revival of *Bacillus paralicheniformis* SVD1 glycerol stocks

The plated glycerol stock formed multiple colonies overnight and produced mannanases as seen by the clearance zone around the colonies of the Congo Red stained agar plate (Figure 2.1). This was expected as *B. paralicheniformis* SVD1 produces mannanases when grown on locust bean gum.

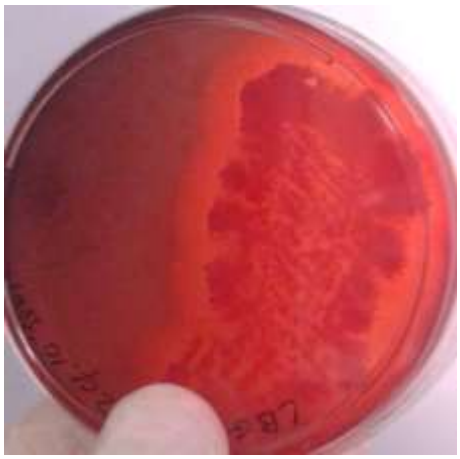

Figure 2.1. A typical photo of an overnight locust bean gum agar plate culture of *B. paralicheniformis* SVD1. The plate was stained with Congo Red then destained with NaCl. The clearance zone around the colonies indicates β-mannanase activity.

2.4.2. Confirmation of identity by 16S rRNA sequencing

To confirm the identity of the revived *B. paralicheniformis* SVD1 glycerol stock, its 16S rRNA sequence was determined. It had a 99.75% 16S rRNA sequence identity to *B. paralicheniformis* SVD1 (Appendix 5). Mismatches were due to base pairs identified as only pyrimidine or purine (Van Dyk, 2009; GenBank accession no. EU 770587). This indicated that the revived glycerol stock was not contaminated. However, the 16S rRNA sequence had 99.92% sequence identity (one nucleotide was only identified as a purine, preventing 100% sequence identity) with that of *B. licheniformis, B. paralicheniformis, B. sonorensis, B. mojavensis, B. aerius, and B. freudenreichii.* When the identity of the bacterium was first determined several years ago using 16S rRNA sequence analysis, it was identified as *B. licheniformis* and was given the strain name SVD1 (Van Dyk, 2009). The partially determined genome of *B. licheniformis* SVD1 (Sakka et al., 2012) was used to further determine the identity of the bacterium. Sakka et al. (2012) sequenced approximately 95% of the genome. Re-evaluation of the *B. licheniformis* SVD1 genes using BLAST (https://blast.ncbi.nlm.nih.gov) provides evidence that *B. licheniformis* SVD1 should be re-named *B. paralicheniformis* SVD1.

2.4.3. Growth curve

Various growth curve parameters were measured in order to determine when mannanase activity was highest during growth and to determine some of the factors that could affect β-mannanase activity. The various growth curve parameters are shown in Figure 2.2. The pH increased by 1.12 units over the 72 h period (Figure 2.2. A), from ~40 h onwards the rate of increase was slightly higher. Protease activity was detected in the broth. The increase in pH was possibly due to protease activity. The decrease in protein concentration between 12 h - 24 h and 40 h - 56 h indicated protease activity. Amino acids released by protease activity would be utilized by *B. paralicheniformis* SVD1, releasing ammonia in the process.

The cell growth, measured as OD 600, peaked after ~24 h then peaked again at ~62 h (Figure 2.2. A and C). The first peak was probably due to utilization of readily available sugars and amino acids from the yeast extract and tryptone media components. Peptides were present in the media from the yeast extract and tryptone (Figure 2.2. B). The Bradford assay does not detect free amino acids or small peptides, only peptides with a molecular

weight (MW) of about 3 kDa and larger (Anon., 2010). A decrease in protein concentration over the first 24 hours corresponded with an increase in cell growth (Figure 2.2. A). Depletion of these readily available carbon and nitrogen sources probably induced mannanase and protease activity. The second peak may have been due to utilization of amino acids and sugars released by protease and mannanase hydrolysis. Proteases would have hydrolyzed peptides from yeast extract and tryptone. Arabinose released by α-galactosidase activity may have been used as an energy or carbon source for growth. Some mannose may have also been released by β-mannanase activity. The increase in protein concentration between 24 h and 36 h was probably due to the secretion of proteins by *B. paralicheniformis* SVD1, including β-mannanases. β-mannanase activity was quantifiable from 24 h (late log phase) onwards and peaked around 48 h (stationary phase/2nd exponential phase), then decreased (Figure 2.2. C). Therefore, the best time to concentrate the β-mannanase activity for further characterization was at 48 h. The reduction in activity after ~48 h was possibly due to a combination of product inhibition, temperature denaturation, catabolite repression and protease activity. The protein concentration profile over time (Figure 2.2. B) is probably due to a combination of protease hydrolysis and protein secretion. Reducing sugars in the media increased up to 40 h then plateaued (Figure 2.2. D). The reducing sugars were probably mannan fragments and MOS. They were probably not consumed to a large degree as *B. paralicheniformis* SVD1 has β-mannanases but does not have a β-mannosidase. This may explain why reducing sugars accumulated over time. This also indicates that the crude secretome could potentially be used to generate MOS without first purifying the β-mannanase.

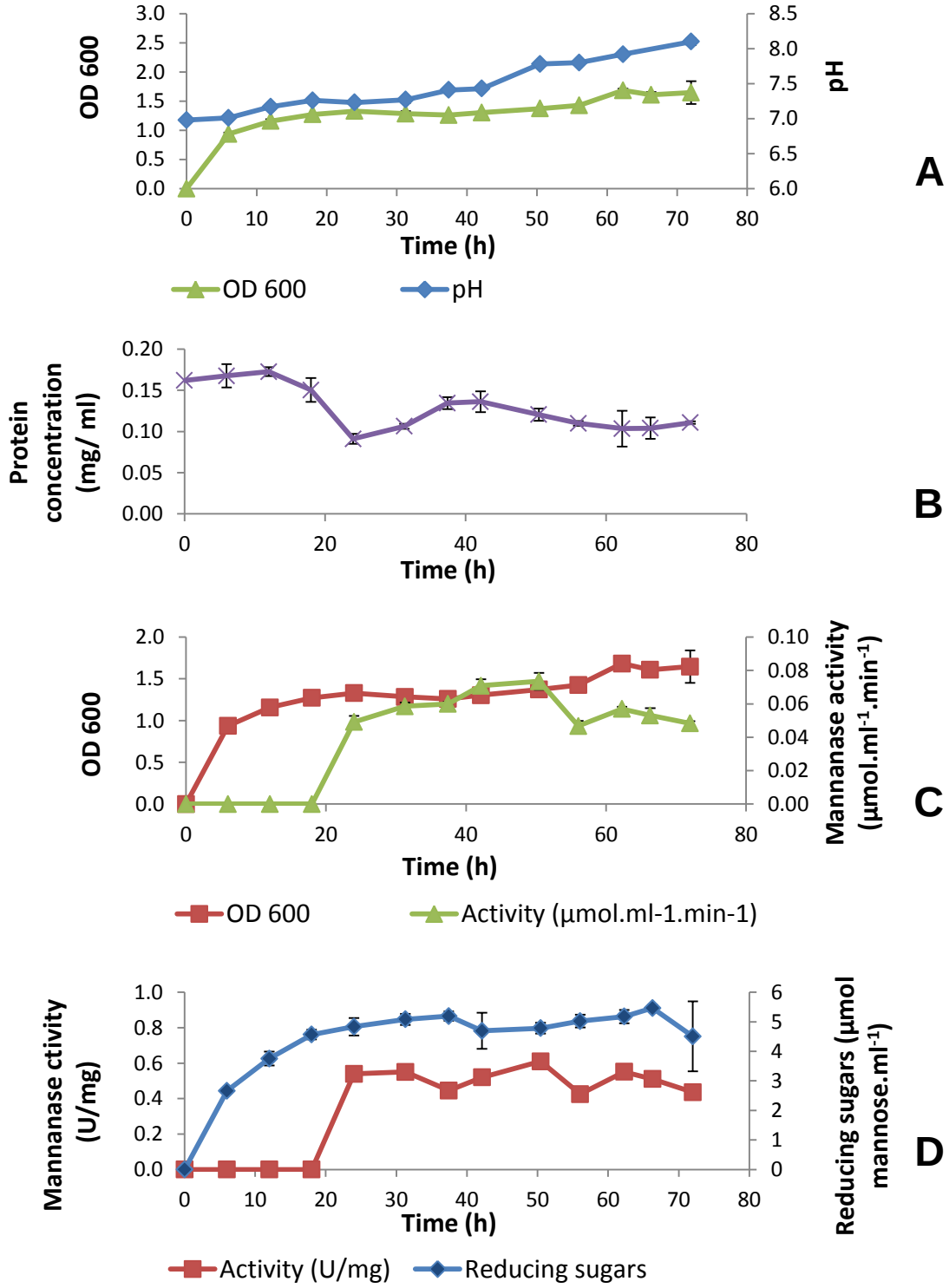

Figure 2.2. Growth curve of a 400 ml *B. paralicheniformis* SVD1 culture in locust bean gum broth at 37°C, with shaking at 150 rpm under aerobic conditions. The culture was grown over 3 days and 5 ml samples were taken every ~6 h to measure various

growth curve parameters. Pelleted cells were resuspended in phosphate buffer, pH 7.0, and absorbance at 600 nm was measured to determine whole cell density. The pH, protein concentration, reducing sugars concentration and β-mannanase activity of the cell-free supernatants were also measured. Plots of these parameters and their relationships are shown in A, B, C and D. Values, excluding pH (n = 1), are represented as mean values ± standard deviations, n = 3.

2.4.4. *In silico* characterization of *Bacillus paralicheniformis* SVD1 β-mannanases

Sequence analysis using UniProt confirmed that the GH5 and GH26 were classified into the correct GH families. According to the Carbohydrate-Active enzymes (CAZY) database (Lombard et al., 2014; http://www.cazy.org) GH family 5 and 26 enzymes have a retaining catalytic mechanism, a $(\beta/\alpha)_8$ protein fold, glutamate as the nucleophile/ base as well as catalytic proton donor. Both families have enzymes with various substrate specificities. The families differ in their amino acid sequence similarities and GH5 has a higher diversity of substrate specificities. A BLAST search revealed that two *B. paralicheniformis* translated gene sequences, from different strains, were identical to the *B. paralicheniformis* SVD1 GH 26 β-mannanase translated gene sequence (Genbank accession no. AJO16961.1 and CP023168). The *B. paralicheniformis* SVD1 translated gene sequence was 99.98% identical to the translated gene sequence of *B. paralicheniformis* 14DA11 (Genbank accession no. CP023168). For both β-mannanases there were various *B. paralicheniformis* and *B. licheniformis* genes mannanases with sequence identity greater than 95%. The *B. licheniformis* DSM13^T (=ATCC14580^T) GH26 and GH5 β-mannanase had 95% and 96% sequence identity, respectively. *In silico* characterization of some physical and biochemical properties of the β-mannanases was conducted using the translated DNA sequences, without signal sequences, of the β-mannanases. The characterization results are shown in Table 2.1. The MW and pI of the two β-mannanases are very similar.

Table 2.1. *In silico* characteristics of *B. paralicheniformis* SVD1 β-mannanases obtained using ProtParam, UniProt and PROSITE.

GH family	GH5	GH26
GenBank accession number	AB643490	AB643507
UniProt ID	H1AD13	H1AD30
Sequence length (without signal peptide sequence)	364	336
Signal peptide length	31	24
Predicted molecular weight (kDa) (without signal peptide)	42.1	37.9
pI	5.38	5.1

2.4.5. Concentration of β-mannanase

β-mannanase activity was concentrated for further characterization, using Amicon centrifugal filtration devices with a 3 kDa MWCO, from the cell-free supernatant of a locust bean gum culture that was grown for 48 h. This was found to be the time point in growth where mannanase activity was maximal. The protein yield after concentration was high (89.5%) and the activity yield was close to 100% as seen in Table 2.2.

Table 2.2. Protein purification table of *B. paralicheniformis* SVD1 β-mannanase concentration using a centrifugal filtration device with a 3 kDa molecular weight cut-off membrane, n = 3.

Fraction	Vol. (ml)	Protein conc. (mg /ml)	Total protein (mg)	Act. (U/ml)	Total act. (U)	Specific act. (U/mg)	Purific. factor	Act. yield (%)
supernatant	432	0.22 ± 0.0028	94.4 ± 1.22	1.13 ± 0.056	487 ± 24.3	5.05 ± 0.34	1	100
3 kDa concentrate	28.8	2.93 ± 0.11	84.5 ± 3.26	17.8 ± 0.83	513 ± 24.0	8.00 ± 0.19	1.58	105

2.4.6. Time study

In order to determine if the locust bean gum substrate used to determine β-mannanase activity became limiting during the 30 minute hydrolysis reaction, the reducing sugars released over time (1.5 h) was determined (Figure 2.3). The substrate hydrolysis rate increased linearly up to around 60 min and then the substrate started to become limiting to the hydrolysis rate. Therefore, the substrate is not rate limiting in the standard enzyme activity assay (30 min hydrolysis) that was used (Section 2.3.7.).

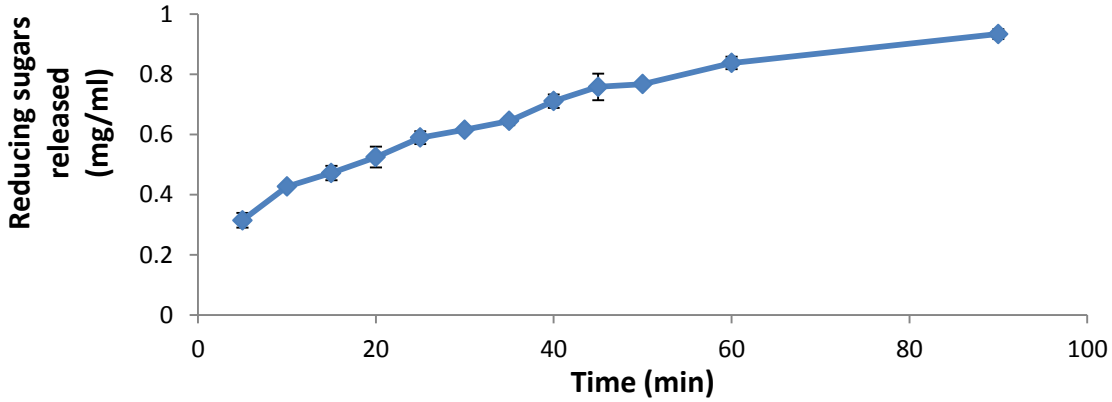

Figure 2.3. Crude β-mannanase activity on locust bean gum over 1.5 h. Values are represented as means ± standard deviations, n = 3.

2.4.7. Temperature optimum and stability

The temperature optimum and stability was assessed in order to determine the appropriate assay conditions for further studies. The temperature optimum of the crude, concentrated mannanase was 50°C (Figure 2.4. A). Between 45°C and 60°C activity was greater than 80% of the maximum. The mannanase retained close to 100% of its activity after 24 h of incubation at 50°C (Figure 2.4. B). Enzyme activity was detectable but not quantifiable at 70°C and 75°C. As 50 °C was used in the standard 30 min assay (Section 2.3.7.), the mannanase/s were not subject to temperature denaturation during the standard assay. The temperature stability assay at 37°C unexpectedly showed an increase in activity between 30 min and 2 h of incubation, which then decreased after 6 h (Figure 2.4. B).

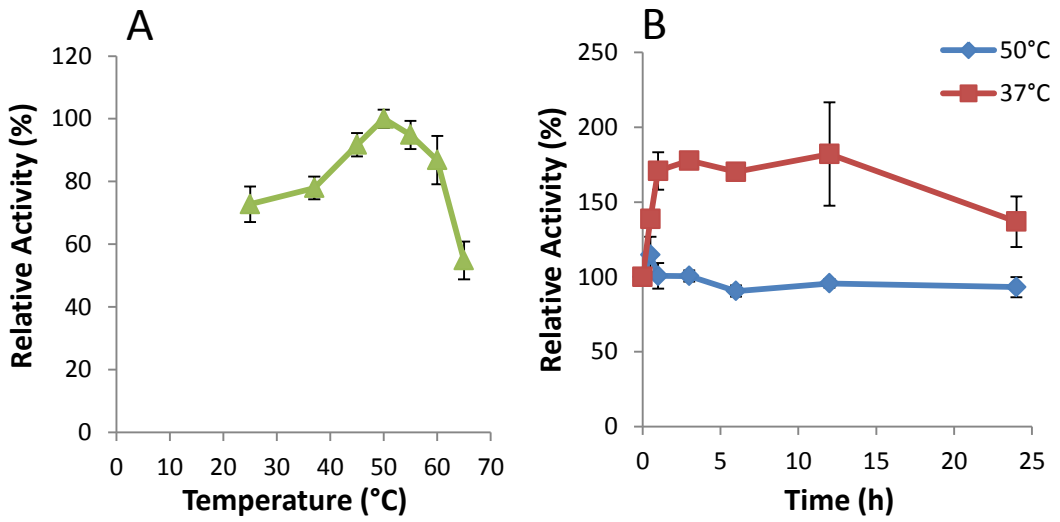

Figure 2.4. A: Temperature optimum of crude mannanase activity. B: Temperature stability of crude β-mannanase activity over 24 h at 37°C and 50°C. Values are represented as mean values ± standard deviations, n = 3.

2.4.8. pH optimum

To further assess the optimal assay conditions for the crude concentrated mannanase/s, the pH optima was determined. The pH optimum was pH 7.0 (Figure 2.5). There was also a peak observed at pH 5.0. Between pH 5.0 and pH 7.0, activity was greater than 80% of the maximum at pH 7.0.

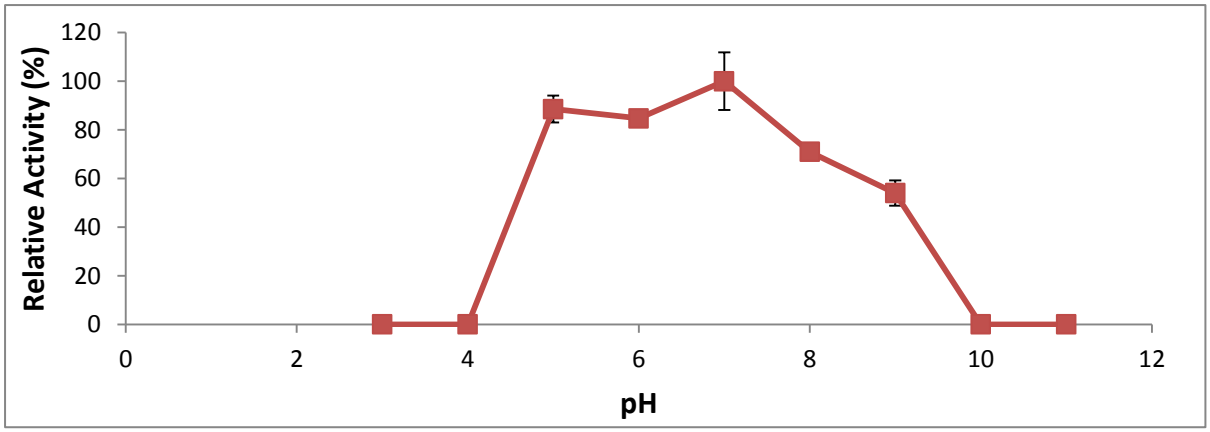

Figure 2.5. pH optimum of crude β-mannanase activity. Values are represented as means ± standard deviations, n = 3.

2.4.9. Substrate specificity

Substrate specificity of the crude concentrated mannanase was determined to assess which mannan substrate was preferred and which other glycosyl hydrolase activities were present in the crude concentrate. Activity was the highest on soluble mannan substrates and galactose branching inhibited hydrolysis. The highest specific activity was on konjac glucomannan (Figure 2.6.). Activity on guar gum galactomannan and carboxymethyl cellulose was detectable but not quantifiable with the DNS assay. Activity on the *p*NP substrates *p*NP β-D-galactopyranoside and *p*NP β-D-cellobioside indicated the presence of a β-1,4-D-galactosidase and β-1,4-D-cellobiohydrolase. However, these activities were relatively low. There was no activity detected on Avicel®, arabinogalactan, *p*NP β-D-mannopyranoside, *p*NP β-D-glucopyranoside, *p*NP α-D-galactopyranoside and *p*NP α–L-arabinofuranoside. These results indicate that there was predominantly β-mannanase activity present in the crude concentrate. The low cellulase activity and lack of α-galactosidase and β-mannosidase activity indicated that the hydrolysis of the mannan substrates was mostly due to hydrolysis of internal β-1,4-glycosidic bonds by β-mannanase/s.

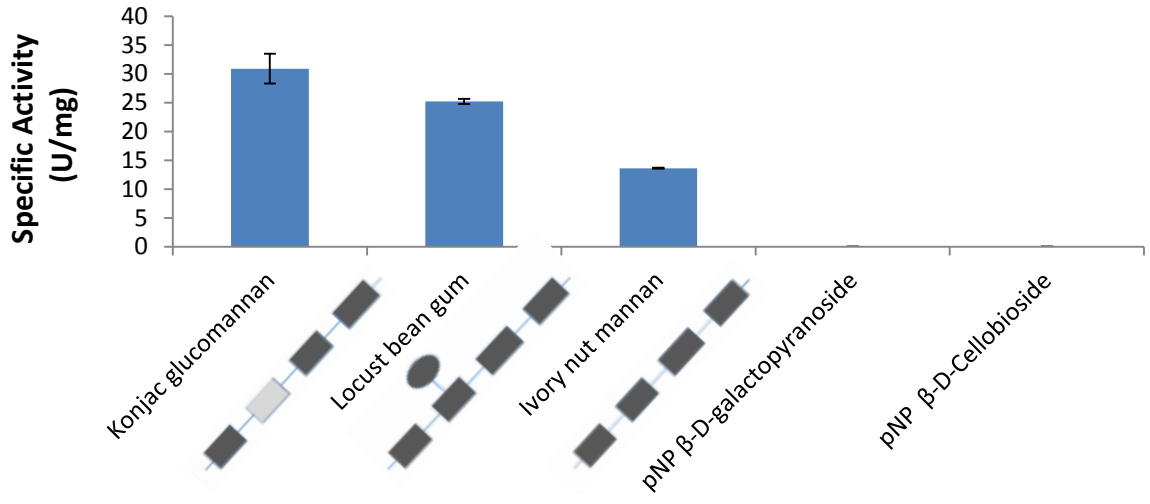

Figure 2.6. Glycosyl hydrolase activities on defined substrates that showed quantifiable activity under the assay conditions used. A diagram of each mannan rich substrate is shown. The dark grey blocks represent mannose, the light grey blocks represent glucose and the circle represents galactose. Values are represented as means ± standard deviations, n = 3.

2.4.10. SDS-PAGE and zymography

SDS-PAGE was performed to assess the protein profile of the crude concentrated β-mannanase. Zymograms were performed with different mannan substrates at pH 5.0 or pH 7.0 to determine the size of the β-mannanases. These pH values were chosen as these were the pH optima (Figure 2.5). Only the locust bean gum and konjac glucomannan zymograms at pH 5.0 showed activity bands (Figure 2.7). The locust bean gum zymogram displayed a single activity band at 33 kDa. The konjac glucomannan zymogram displayed two activity bands at 29.6 kDa and 33 kDa. The sizes of the β-mannanases were smaller than expected, as the *B. paralicheniformis* SVD1 β-mannanases have MWs of 42.1 kDa and 37.9 kDa based on their gene sequences (Table 2.1). The smaller than expected sizes may have been due to proteolytic cleavage of the mannanases (protease activity was detected in the growth media and the protease activity was possibly higher in the concentrated β-mannanase solution). The higher intensity of the activity bands on the konjac glucomannan zymogram compared to the locust bean gum zymogram was expected. Mannanase activity was highest on konjac glucomannan (Figure 2.6). If the locust bean gum zymogram was incubated for longer or if the protein load was increased there may also have been two activity bands. The protein profiles (Figure 2.7 lanes 2 and 5) showed a range of proteins, most were about 60 kDa or less. The SDS-PAGE done concurrently with the locust bean gum zymogram was over-developed during silver staining (Figure 2.7 lane 2).

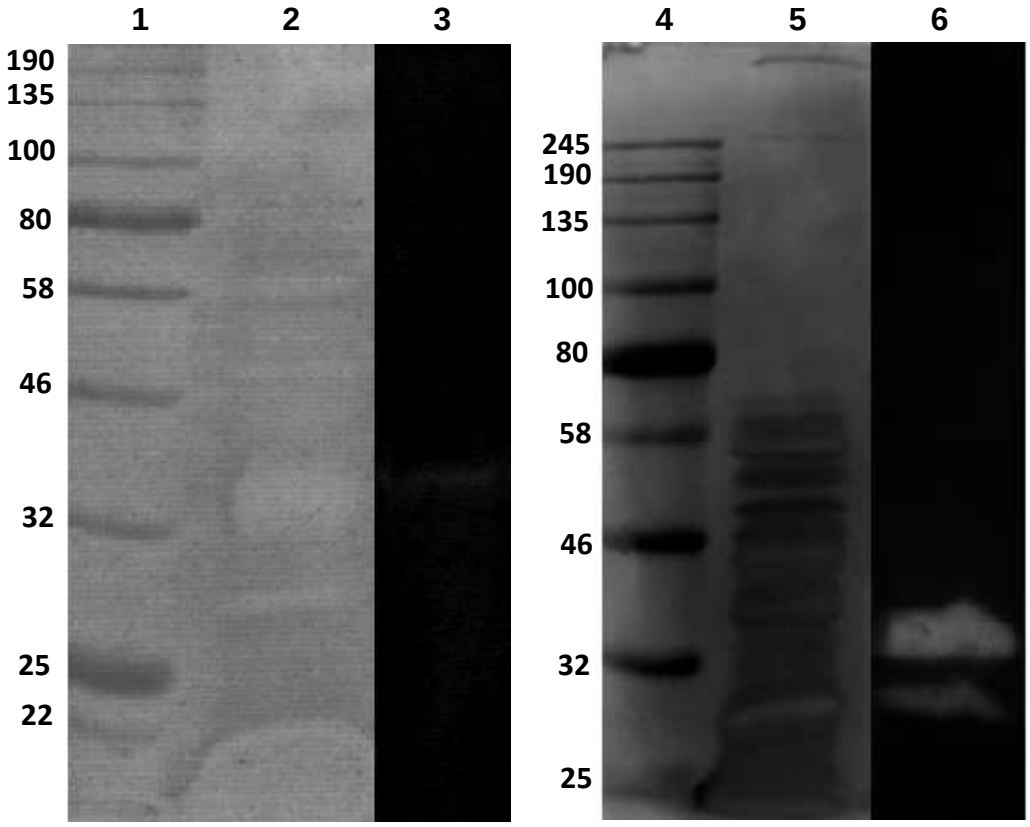

Figure 2.7. SDS-PAGE and zymograms of the crude concentrated β-mannanases from a locust bean gum culture. Lanes 2 and 5 represent proteins of the crude concentrated β-mannanase preparation on a 12% SDS-PAGE gel stained with a Pierce® Silver Stain Kit. Lane 3: Zymogram with 0.1% (w/v) locust bean gum at pH 5.0; Lane 6: Zymogram with 0.1% (w/v) konjac glucomannan at pH 5.0. Lanes 2, 3, 5 and 6 were loaded with 10 µg of protein.

2.4.11. TLC analysis of mannan hydrolysis

Products formed from the hydrolysis of mannans over 24 h, by the concentrated β-mannanases, were qualitatively determined using TLC. This was done in order to assess the production of MOS for potential use as a prebiotic as well as for use in biomass saccharification for biofuel production. The enzyme control, where only the crude concentrated protein was loaded, showed some oligosaccharides with a degree of polymerization (DP) of 5 or more - this could not be clearly seen in the photos of the TLC plates (not shown). The substrate controls, where only substrate was loaded, did not show

any MOS (not shown). As expected, activity on konjac glucomannan was highest based on the number and intensity of the oligosaccharide spots formed (Figure 2.8). Most of the resolved MOS products displayed retention factor (R_f) values between those of mannobiose and mannotetraose. The dominant product had an R_f value between mannobiose and mannotriose. High performance liquid chromatrography (HPLC) and mass spectrometry could also be used to identify the different oligosaccharides. Some glucose was also formed over time. There was lower activity on locust bean gum and also fewer degradation products. The main resolved products were mannobiose, mannotriose, mannopentose and mannohexose. It appears as though galactose was also released, which indicated the presence of an α-galactosidase. Activity was lower on ivory nut mannan and the hydrolysis profile was similar to locust bean gum except there was no visible monosaccharide release. Increased branching and insolubility decreased activity as was seen with the substrate specificity assays (Figure 2.6). The degree of branching impacted on hydrolysis as could be seen with locust bean gum hydrolysis versus guar gum hydrolysis. The hydrolysis profiles did not change much over time, indicating that most of the hydrolysis occurred within the first 30 min. Given that the concentrated mannanase fraction consisted of many proteins, of which at least two had mannanase activity on konjac glucomannan (Figure 2.7), and that *B. paralicheniformis* SVD1 has genes for a GH5 and a GH26 β-mannanase it is not possible to assign the hydrolysis patterns observed to a single enzyme.

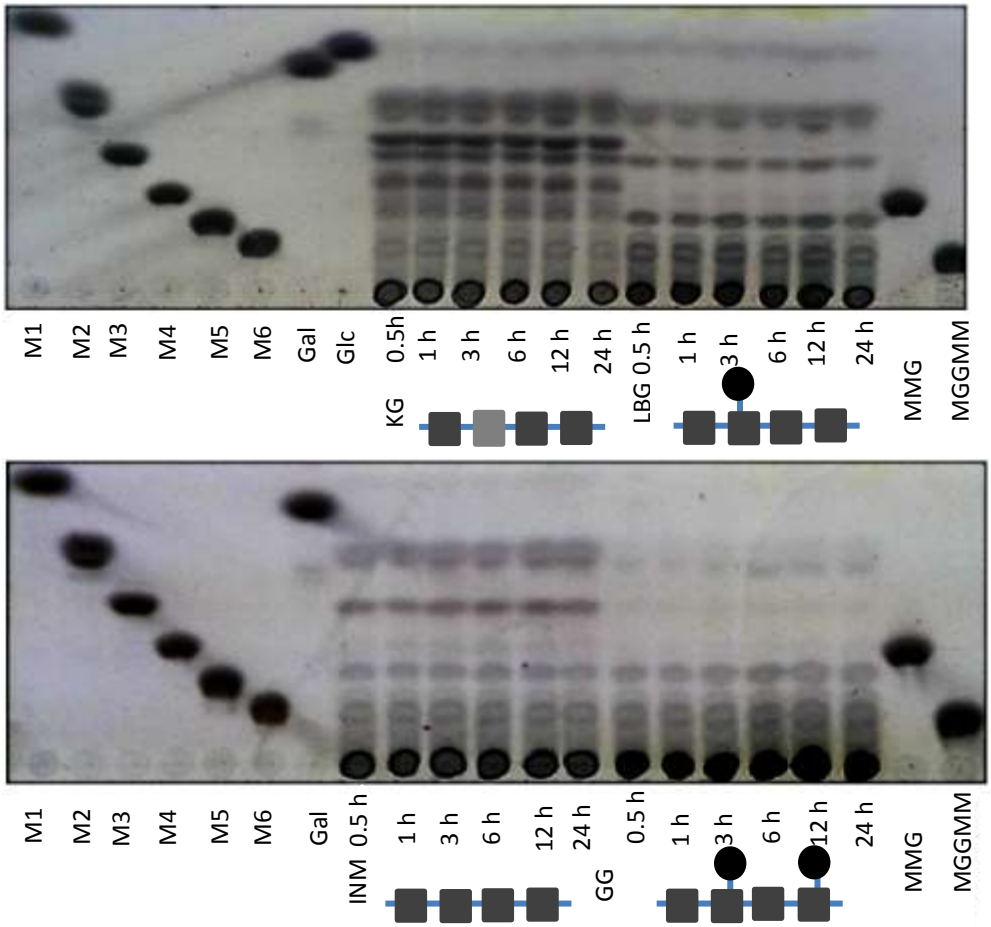

Figure 2.8. Thin layer chromatography of the products formed by hydrolysis of mannan substrates over 24 h. M1 – M6 = mannose to mannohexose. Gal = galactose. Glc = glucose. MMG = mannotriose with a galactose substituent on the reducing end. MGGMM = mannopentose with two galactose substituents. KG = konjac glucomannan. LBG = locust bean gum. INM = ivory nut mannan. GG = guar gum. 0.5 h – 24 h represents the hydrolysis reaction times. A diagram of each mannan rich substrate is shown. The dark grey blocks represent mannose, the light grey blocks represent glucose and the circles represent galactose.

Products formed by the hydrolysis of MOS over 24 h by the crude concentrated β-mannanase were also qualitatively determined. Mannobiose and mannotriose were not hydrolyzed. Mannotetraose was hydrolyzed to mannobiose as well as mannotriose and mannose (Figure 2.9). The stain detected mannotriose better than mannose, which indicates that the stain is more sensitive to larger oligomers**.** Mannopentose was predominantly hydrolyzed to mannnotriose and mannobiose. Hydrolysis to mannotetraose and mannose also occurred. Over time the mannotetraose was hydrolyzed to mannobiose, mannotriose and mannose. Mannohexose was hydrolyzed the most rapidly; most of it was hydrolyzed within 30 minutes to mannotetraose and mannobiose as well as mannotriose. Mannotetraose was then hydrolyzed to mannobioses as well as mannotriose and mannose. There was no hydrolysis of mannotriose with a galactose branch and mannopentose with two galactose branches (Figure 2.9). There were some background oligosaccharides that were present in the substrate and enzyme controls (data not shown). The concentrated mannanase hydrolyzed MOS with a DP > 3 and the main products were mannobiose and mannotriose. Mannanase activity increased with increasing MOS DP, and galactose branching inhibited hydrolysis.

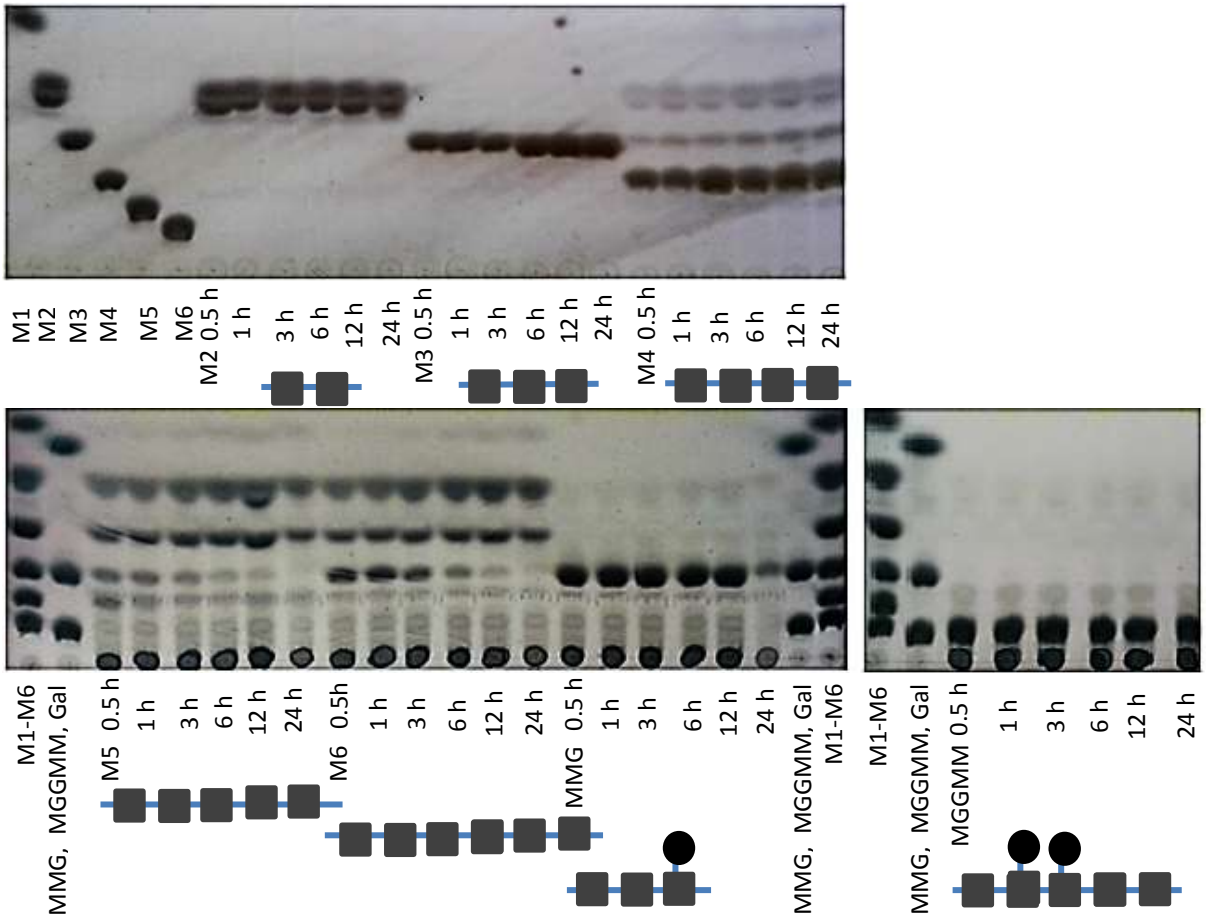

Figure 2.9. Thin layer chromatography of the products formed by hydrolysis of MOS over 24 h. M1 – M6 = mannose to mannohexose. Gal = galactose. Glc = glucose. MMG = mannotriose with a galactose substituent on the reducing end. MGGMM = mannopentose with two galactose substituents. 1 h – 24 h represents the hydrolysis reaction times. A diagram of each MOS is shown. The dark grey blocks represent mannose and the circles represent galactose.

2.5. Discussion

Analysis of the partially determined genome sequence of *B. licheniformis* SVD1 suggested that *B. licheniformis* SVD1 is more closely related to *B. paralicheniformis* than *B. licheniformis*. *Bacillus licheniformis* SVD1 was consequently referred to as *B. paralicheniformis* SVD1 in this thesis. The increase in available sequence data since the Sakka et al. (2012) paper led to this alternative species designation. *B. paralicheniformis* is a recently described species (Dunlap et al., 2015). Dunlap et al (2015), as well as previous

studies, found that *B. licheniformis* can be divided into group 1 and group 2 strains based on phylogenomic and phenotypic differences. Dunlap et al (2015) provided evidence that the differences between the 2 groups are sufficient to classify group 2 *B. licheniformis* strains as a new species: *B. paralicheniformis*.

Sakka et al. (2012) found that 117 of the 118 carbohydrate active genes (glycosyl hydrolases, glycosyl transferases, polysaccharide lyases and polysaccharide esterases) of *B. licheniformis* DSM13^T (=ATCC14580^T) were found in *B. licheniformis* SVD1. The family-6 carbohydrate esterase of *B. licheniformis* DSM13^T (=ATCC14580^T) (BLi02801) was not found in *B. licheniformis* SVD1. *B. paralicheniformis* BL-09, like *B. licheniformis* SVD1, had all 118 carbohydrate active genes (glycosyl hydrolases, glycosyl transferases, polysaccharide lyases and polysaccharide esterases) of *B. licheniformis* DSM13^T (=ATCC14580^T), excluding the family-6 carbohydrate esterase of *B. licheniformis* DSM13^T (=ATCC14580^T) (BLi02801). All 56 glycoside hydrolase genes identified in *B. licheniformis* DSM13^T (=ATCC14580^T) were conserved in *B. licheniformis* SVD1. The DNA sequence identities of the glycoside hydrolases were around 95% for most of the homologs. All of the homologs, except GH32C/BLi02827 had the same or similar number of amino acids. GH32C of *B. licheniformis* SVD1 was smaller than BLi02827 of *B. licheniformis* DSM13^T (=ATCC14580^T) due to a frameshift mutation, yielding a truncated protein. The DNA sequence identities of most *B. licheniformis* SVD1 glycoside hydrolases were around 99% for most of its homologs in *B. paralicheniformis* BL-09. However, *B. paralicheniformis* BL-09 did not have a truncated GH32C homolog like *B. licheniformis* SVD1. This truncation was unique to the *B. licheniformis* SVD1 strain. *B. licheniformis* SVD1 had a family-30 (xyn30A) and family-43 glycoside hydrolase (axh43A) that were not present in the *B. licheniformis* DSM13^T (=ATCC14580^T) genome. This arabinoxylanase gene (axh43A) is one of the genes that are found in *B. paralicheniformis* and not in *B. licheniformis* (Dunlap et al., 2015). Sakka et al. (2012) found that the xyn30A axh43A were part of a 6.86 kb genome region along with a ywqJ-like gene. *B. paralicheniformis* BL-09 has a similar 7.00 kB region with homologous genes, identical gene arrangement and transcription direction. Sakka et al. (2012) found this tandem organization of xyn30A and axh43A homologs, with 86% - 90% sequence identities, in the genomes of some bacilli. The flanking regions of xyn30A and axh43A were not homologous with the corresponding regions of the homologs. The xyn30A and axh43A homologs of *B. paralicheniformis* BL-09 had 100% sequence identity with xyn30A and axh43A, respectively. The ywqJ-like gene and flanking regions sequences were not provided

by Sakka et al. (2012) so they could not be compared to the corresponding regions in *B. paralicheniformis* BL-09.

Various growth curve parameters of *B. paralicheniformis* SVD1 were measured to assess when to concentrate β-mannanase activity for characterization and purification. The increase in pH over time during growth was probably due to ammonia release as a result of the use of amino acids from the media components and protease activity. Sarkar et al. (1993) found that, during *Bacillus* sp. fermentation of soy beans, the pH displayed the same trend (it increased) over 48 h as ammonia was produced. They assumed that the ammonia release was from the bacteria utilizing amino acids released by proteolytic hydrolysis of soy bean proteins. Ammonia is released when bacteria utilize amino acids as a carbon and energy source (Allagheny et al., 1996).

Protease activity was not desirable as it could potentially hydrolyze β-mannanase, which would affect characterization and purification. Altering the nitrogen and carbon sources could minimize protease production but it would also alter β-mannanase production. Subramaniyan et al. (2001) assessed the effect of different nitrogen sources on xylanase production in a *Bacillus* species; they found that a mixture of 0.25% (w/v) yeast extract and 0.25% (w/v) peptone gave the highest xylanase production with low protease activity. They found that at higher yeast extract and peptone concentrations, protease activity increased and xylanase activity decreased. This could have been due to the presence of easily metabolized glucose in the yeast extract that caused catabolite repression (Hahn-Hägerdal et al., 2005). Lower peptone and yeast extract concentrations decreased xylanase activity. The medium used for this work was similar that used by Subramaniyan et al. (2001), except that tryptone was used instead of peptone, a higher pH was used and locust bean gum was used instead of oatspelt xylan so that mannanase production was induced. The media composition was the same used by Van Dyk (2009), which was a modified media of Choudhury et al. (2006). The optimum yeast extract and peptone concentrations used by Subramaniyan et al. (2001) gave the highest xylanase activity and lowest protease activity, although 0.5% (w/v) gave results near the optimum. A problem with their optimized media composition for reducing protease production is that they did not consider product inhibition. Proteases can be inhibited by their hydrolysis products (Leung et al., 2000). Ferrero et al. (1996) found that partially purified alkaline serine proteases from *B. licheniformis* MIR 29 were inhibited by more than 80% by small molecules in the culture supernatant. These could

be removed using an ultrafiltration membrane filtration device with a 10 kDa molecular weight cut-off (MWCO). Protease activity would increase if the protein is concentrated, so the optimized media of Subramaniyan et al. (2001) is probably not ideal for concentration or purification of β-mannanase activity unless protease inhibitors are included in each concentration/ purification step (Beynon & Oliver, 2004). Another potential problem with the media composition is that yeast extract induces extracellular polysaccharide production (Muñoz-Gutiérrez et al., 2009; Van Dyk et al., 2012). This is not ideal for protein concentration and purification (Chapter 3). A preliminary assessment of concentration of the supernatant with centrifugal filtration devices showed that centrifugation took much longer than expected (data not shown). The devices sometimes clogged as well. This problem can be overcome by using concentration procedures that can separate protein from the polysaccharide. Ammonium sulfate precipitation is a suitable method (Walker, 2010b). The accumulation of reducing sugars in the media was assumed to be MOS formed by β-mannanase activity. However, it may have also been due to extracellular polysaccharide production.

Even though β-mannanases are endo-acting enzymes and release MOS from mannan substrates (Moreira & Filho, 2008), some mannose may be produced that may have been utilized as a carbon and energy source. Songsiriritthigul et al. (2010) found that purified GH26 β-mannanase from *B. licheniformis* DSM13^T (=ATCC14580^T) hydrolyzed locust bean gum into various MOS and mannose. A BLAST search showed that there was 95% sequence identity between the GH26 β-mannanase of *B. licheniformis* DSM13^T (=ATCC14580^T) and *B. paralicheniformis* SVD1 so they may have similar hydrolysis characteristics. The structure of proteins is better conserved than their sequence and structure is highly conserved within a GH family (Bourne & Henrissat, 2001). However, the characteristics would need to be tested as minor sequence differences can have a large impact on glycosyl hydrolase activity (Cartmell et al., 2008). The genome also contains an α-galactosidase so the galactose branches of locust bean gum could have been hydrolyzed to release galactose for utilization. Locust bean gum probably induces expression of genes involved in galactomannan catabolism (Voigt et al., 2007; Sakka et al., 2012). *B. paralicheniformis* SVD1 has been shown to utilize mannose and galactose as a carbon source (Van Dyk, 2009). In order to test if there was α-galactosidase activity, the artificial substrate 4-nitrophenyl α-D-galactopyranoside could have been used.

β-mannanase activity (0.0735 U/ml) was relatively low compared to the β-mannanase activity obtained by Feng et al. (2003). They optimized β-mannanase production from *B. licheniformis* NK-27 and obtained an activity of 198.2 U/ml. Other studies also obtained much higher β-mannanase production from *B. licheniformis* (Zhang et al., 2000; Ge et al., 2016). However there were differences in culture conditions and the enzyme activity assays. Hydrolysis was conducted for 3 h (Section 2.3.4.2.) versus 10 min for the other studies. Longer assay times are more suitable for determining an enzyme's true industrial potential as they more closely resemble real reaction conditions (Liu et al., 2013). An alternative β-mannanase production protocol was attempted to try to increase β-mannanase production, using similar media composition and growth conditions to Feng et al. (2003). Their optimal physical conditions for β-mannanase production from *B. licheniformis* NK-27 were 600 rpm on a shaker at 30°C, and growth for 48 h. They found that 37°C had the lowest dissolved oxygen content (DOC) compared to 33.5°C and 30°C. This lower DOC correlated with a larger initial increase in the pH of the medium as well as lower cell growth and β-mannanase activity. The lower DOC could be due to lower oxygen solubility at higher temperatures (Schurmann & Steffensen, 1992). This may have led to a change in metabolism leading to more proteases being produced, which led to ammonia release. Ammonia release may have caused the pH to increase (Sarkar et al., 1993). The pH increase Feng et al. (2003) observed was 2 units, which is similar to the pH increase that was observed in the *B. paralicheniformis* SVD1 culture (1.12 pH units) in our study. Feng et al. (2003) also used different media: konjac glucomannan (3% (w/v)), meat peptone, corn steep liquor, $CaCl_2$ and $FeSO_4$. Corn steep liquor and shakers that could operate above 250 rpm were not available. There was an improvement in activity using the modified optimized growth conditions; 0.469 U/ml of activity was observed compared to 0.0735 U/ml of activity previously. However, there was a higher level of background reducing sugar, 4.891 mg/ml reducing sugar was produced compared to 1.231 mg/ml background reducing sugar previously. The increased reducing sugars would have been due to the higher mannan substrate concentrations used, leading to increased reducing sugar formation from hydrolysis of the konjac glucomannan and also possibly extracellular polysaccharide production. The high background sugar concentration was problematic for concentration of the β-mannanases as the centrifugal filtration devices became clogged and activity yield was low after concentration (8.29%), so these growth conditions were not used, even though the activity (U/ml) observed was higher. These growth conditions may have been more successful if growth was continued for longer and if

the media was filtered with a cheese cloth and a 0.45 µm filter prior to centrifugal filtration. Ammonium sulfate precipitation would have probably been a better concentration method.

The β-mannanase activity was concentrated and characterized as an initial assessment of its potential industrial use in biofuel and prebiotic MOS production. Concentration of the β-mannanase was successful as the activity yield was around 100% (105% ± 4.92). The (hydrolysis) time study indicated that substrate limitation started to occur after 60 min. After centrifugation of the hydrolyzates it was noted that there were still large pellets of substrate remaining, indicating that much of the substrate was unhydrolyzed. The main reason for the decrease in hydrolysis was possibly the decrease in easily hydrolyzable LBG. Temperature denaturation was not the cause for the decrease in hydrolysis rate, as the enzyme retained most of its activity after 24 h at 50°C. von Freiesleben et al. (2016) found that the maximal conversion of locust bean gum by various fungal β-mannanases was 40% and that the maximal conversion was less on guar gum. They concluded that these substrates consisted of regions that were readily hydrolyzable and regions that were inaccessible and not easily hydrolysable. The inaccessibility was likely due to galactose substituents. This shows the importance of the addition of α-galactosidase, not only for maximal monosaccharide release for biofuel production, but also for the production of MOS. In an industrial setting, the use of additional enzymes would need to be considered based on the galactose content of the mannan feedstock, the presence of other polysaccharides and the desired hydrolysis products. The decrease in the rate of hydrolysis may have also been due to non-productive binding, however this was not assessed. The temperature optimum (50°C) of the concentrated β-mannanase agreed with the temperature optimum (50 - 60°C) of a heterologously expressed and purified GH26 β-mannanase from the closely related *B. licheniformis* DSM13^T (=ATCC14580^T) (Songsiriritthigul et al., 2010). Songsiriritthigul et al. (2010) also reported that the *B. licheniformis* DSM13^T (=ATCC14580^T) GH26 β-mannanase had a $T_{1/2}$ of 80 h at 50°C, pH 6.0 and a pH optima of 6.0 – 7.0. The pH optima of the crude concentrated *B. paralicheniformis* SVD1 β-mannanase was 5.0 and 7.0, the $T_{1/2}$ was not calculated but was greater than 24 h. The β-mannanase would not be suitable as a detergent additive or for bio-bleaching of paper pulp as it is not very active at high pH values and is does not seem to be very thermostable. However, it shows good thermostability at 50°C for at least 24 h. Industrial hydrolysis of lignocellulose is typically conducted for 24 h – 72 h (Liu et al., 2013; Malgas et al., 2017b). It may be suitable as an enzyme cocktail supplement for biofuel production (where acidic pretreatment is not used) or for animal feed

MOS production. Purified *B. paralicheniformis* SVD1 β-mannanase could be used for MOS production suitable for human consumption. The two pH optima indicated the presence of two β-mannanases. Van Dyk (2009) reported that concentrated *B. paralicheniformis* SVD1 β-mannanase activity from a birchwood xylan broth culture displayed two pH optima (pH 6.0 – 7.0 and pH 9.0). The difference in pH optima reported by Van Dyk (2009) and this thesis may be due to the different concentrations and ratios of different crude enzyme solution components such as proteins. This may alter the pH and temperature stability as well as temperature and pH optima of the β-mannanases (Deutscher, 2009). The enzyme assays, growth media (excluding carbohydrate source) and conditions used were nearly identical. The carbohydrate source may influence the production of different β-mannanase isoforms or the expression of proteases that may alter the β-mannanase structure. Further studies would need to be performed to assess this. Further studies could include protein sequencing of the β-mannanases and the effect of protease inhibition on the protein sequences of the β-mannanases.

SDS-PAGE gels were run to assess the protein profile of the crude, concentrated β-mannanase. The SDS-PAGE gels were initially stained with Coomassie stain (results not shown) but fewer bands were visible than expected based on work performed by Van Dyk (2009). Silver staining was used to improve sensitivity. Zymograms revealed two activity bands, two on the konjac glucomannan zymogram and one on the locust bean gum zymogram. This indicates that there were at least two mannanase active proteins. This was expected based on the pH optima results - as there were two pH optima. There may have been other mannanase active bands that were not renatured. A native PAGE would need to be performed in order to assess this. The intensity of the bands was greater on the konjac glucomannan zymogram, which had two mannanase active bands (29.6 kDa and 33 kDa). Unexpectedly, the zymogram activity gels detected mannanase activity at pH 5.0 but not at pH 7.0. This was not expected, as the β-mannanase activity was the highest at pH 7.0. However, given that the predicted pI of the β-mannanases is between 5.1 and 5.38 (Table 2.1), the charge of the β-mannanases would have been positive in the pH 5.0 zymogram and negative in the pH 7.0 zymogram. The positively charged β-mannanases may have interacted differently with the PAGE gel matrix compared to the negatively charged β-mannanases. Surface and residual charges on a matrix and the charge of an interacting enzyme may lead to a change in the environment around an enzyme molecule, which may alter the optimum pH of the enzyme and consequently effect activity at a given pH

(Mosbach, 1971). Using zymogram analysis with locust bean gum as a substrate, Van Dyk (2009) found that concentrated *B. paralicheniformis* SVD1 β-mannanase activity from a Birchwood xylan broth also displayed two mannanase active bands (26.8 kDa and 41.5 kDa). Heterologously expressed *B. licheniformis* DSM13^T (=ATCC14580^T) GH26 mannanase had a theoretical MW of 41 kDa and a MW of 45 kDa determined using SDS-PAGE (Songsiriritthigul et al., 2010). Both the study reported in this thesis and the study performed by Van Dyk (2009) found protease activity in the broth but did not use protease inhibitors. The smaller than expected mannanases were possibly catalytically active truncated products of protease hydrolysis. The proteases did not seem to affect β-mannanase activity as the activity yield after concentration was 100% even after 2 months in storage at 4°C. SDS-PAGE gels showed a decrease in the average MW of the proteins when stored in the fridge over time (data not shown). Proteolytic cleavage could be assessed by determining the amino acid sequences of the β-mannanase active bands with tryptic mapping using MALDI-TOF mass spectrometry. These protein sequences could be compared to the expected protein sequences based on their gene sequences. This would also allow identification of the β-mannanases expressed (GH5 and/ or GH26) and the type of protease activity (e.g. serine protease) present.

Assessment of the concentration of reducing sugars released by the β-mannanase revealed that activity was the highest on soluble, low branched mannan substrates, especially glucomannan. These results were similar to that reported by Songsiriritthigul et al. (2010) for the GH26 β-mannanase of *B. licheniformis* DSM13^T (=ATCC14580^T). Galactose branching probably inhibited hydrolysis because the active site is unable to accommodate galactose residues or can only accommodate a single galactose residue. To confirm this, computational ligand docking could be done as was performed for various fungal β-mannanases by von Freiesleben et al. (2016) to assess the effect of galactose substituents on active site binding. The structures of the GH5 and GH26 *B. paralicheniformis* SVD1 mannanases have not been solved, but there are homologous β-mannanases sequences available with solved structures. These could be used as templates for homology modelling. The concentrated *B. paralicheniformis* SVD1 β-mannanase also displayed other glycosyl hydrolase activities. There was endoglucanase, β-galactosidase and cellobiohydrolase activity present. However, these activities were low compared to β-mannanase activity. A study by Van Dyk (2009) found that *B. paralicheniformis* SVD1 grown in a locust bean gum broth also produced various holocellulolytic enzymes. Mannanase activity was the highest

followed by xylanase, pectinase then cellulase activity. In this current study, activity on xylan and pectin was not assessed but these activities may have been present. Microbes that produce holocellulases are thought to constitutively express low levels of holocellulases. When a substrate becomes available it is hydrolyzed to small sugars that induce expression of specific holocellulases as well as other proteins involved in hydrolysis and sugar uptake (Lynd et al., 2002). The inducers produced by locust bean gum hydrolysis, such as mannobiose, may have increased expression of multiple genes and carbohydrate utilization loci. The glucomannan utilization operon of *B. subtilis*, a closely related species (Rey et al., 2004), contains genes for various proteins including a β-mannanase and a β-glucosidase. The operon has been shown to be strongly induced by mannobiose and cellobiose (Sadaie et al., 2008). Van Dyk (2009) found that locust bean gum induced β-mannanase expression in *B. paralicheniformis* SVD1 but cellobiose did not. Therefore it is likely that mannobiose, a MOS, a galactomannan oligosaccharide or a combination of these saccharides induce β-mannanase expression in *B. paralicheniformis* SVD1.

The TLC hydrolysis profile of the crude, concentrated β-mannanase on various mannan substrates was possibly due to activity by β-mannanase and other mannanolytic enzymes. This means that the substrate hydrolysis profile of individual enzymes could not be determined. There was β-glucosidase and α-galactosidase present (based on the TLC profile). These activities were not detected in the substrate specificity assays, which was probably due to the shorter hydrolysis time and lower protein load. The substrate specificity assays generally agree with the TLC results. The oligosaccharides produced could potentially be used as prebiotics. Further studies would need to be performed to assess the oligosaccharides for their prebiotic potential.

2.6. Conclusion

The glycerol stock was confirmed to be *B. licheniformis* SVD1 by its 16S rRNA sequence. However, analysis of the partially determined genome provided evidence that *B. licheniformis* SVD1 should be reclassified as *B. paralicheniformis* SVD1 and was therefore named as such throughout the thesis. β-mannanase activity was induced by locust bean gum and was at its highest after 48 h under the growth conditions employed. The amount of β-mannanase activity produced was less than that reported by other authors, although the differences in activity assays used made direct comparison difficult. The optimal time point

for concentrating and purifying the β-mannanase activity was 48 h. The concentration of the β-mannanase activity was successful as there was no loss in activity yield. The concentrated β-mannanase displayed biochemical characteristics similar to *B. licheniformis* DSM13^T (=ATCC14580^T) GH26 β-mannanase. The predominant activity was β-mannanase activity. The β-mannanases had smaller than expected sizes; this may have been due to protease activity, which was detected. Protease inhibitors were used in further experiments (Chapter 3). These biochemical characteristics are important to know for optimal hydrolysis and synergy with other glycosyl hydrolases (Chapter 3 and Chapter 4). The following chapter describes the attempted purification of the β-mannanases and subsequent biochemical characterization. Purification is required in order to determine the true characteristics of an enzyme and would be required for the production of MOS suitable for human consumption.

Chapter 3 – Partial purification and biochemical characterization of *Bacillus paralicheniformis* SVD1 β-mannanase

3.1. Introduction

Purification of enzymes is an essential first step for characterization. Various methods can be employed, but they can broadly be divided into traditional purification techniques and recombinant protein expression and purification (Walsh, 2002). In this chapter, β-mannanase purification was attempted using traditional purification methods. *B. paralicheniformis* SVD1 was cultured in locust bean gum broth to induce β-mannanase production. The β-mannanase was then concentrated and purified using anion exchange (AEC) and size exclusion chromatography (SEC). The methods that were tested for concentration of the protein exploited differences in the size (centrifugal filtration), hydrophobicity and hydrophilicity (ammonium sulfate precipitation) and solubility (acetone precipitation). AEC separates proteins by exploiting the differential charge of proteins at a given pH. Knowledge of a protein's pI is important to know its charge at a given pH (Anon, 2016a). The pI of a protein can be determined experimentally or *in silico* using its gene sequence. The pI values of the *B. paralicheniformis* SVD1 β-mannanases were determined *in silico* (Chapter 2). SEC was used as a final polishing step (Anon, 2016b). The MWs of the *B. paralicheniformis* SVD1 mannanases were calculated based on their gene sequences (Sakka et al., 2012). The purification of the *B. paralicheniformis* SVD1 β-mannanases could be problematic if they are both expressed under the growth conditions used. They may be difficult to separate from one another as their pI values and sizes are very similar (Chapter 3 – Table 2.1). Five published studies reported the purification of β-mannanases from various *B. licheniformis* strains. Three of the studies used traditional protein purification methods (Wenbo et al., 1995; Zhang et al., 2000; Ge et al., 2016) and two recombinantly expressed β-mannanase in *Escherichia coli* (Kanjanavas et al., 2009; Songsiriritthigul et al., 2010). For the studies where traditional methods were used, concentration and initial purification was performed using acetone precipitation or centrifugal filtration devices. AEC alone, or in combination with SEC, was used as a final purification step.

The partially purified β-mannanase was characterized in order to determine its characteristics and to compare them to what was found for the crude concentrated β-

mannanase (Chapter 2). β-mannanases from *B. paralicheniformis* have not been characterized but β-mannanases from closely related *B. licheniformis* strains have been characterized (Zhang et al., 2000; Kanjanavas et al., 2009; Songsiriritthigul et al., 2010; Ge et al., 2016). The β-mannanases from these various strains seem to be moderately thermostable, with temperature optima of between 40°C - 60°C and most retained >80% activity for 6 h to ≥ 24 h at 50°C. Their pH optima were between 5 and 9. Songsiriritthigul et al. (2010) reported that the recombinantly expressed and purified GH26 β-mannanase of *B. licheniformis* DSM13^{T} (=ATCC14580^{T}) preferred soluble, low branched substrates. This was also found for the crude concentrated *B. paralicheniformis* SVD1 mannanase (Chapter 2). Galactose branching was shown to inhibit hydrolysis of mannans and MOS by the crude concentrated *B. paralicheniformis* SVD1 β-mannanase.

In this chapter, purification of the *B. paralicheniformis* SVD1 β-mannanases was attempted and the partially purified β-mannanase was biochemically characterized Synergy between the partially purified β-mannanase and α-galactosidase was also assessed. A commercial GH27 α-L galactosidase from *Cyamopsis tetragonolobus* seeds (Megazyme) was selected as Malgas et al. (2015^{c}) found that GH27 α-galactosidase displayed synergy with a GH5 β-mannanase and a GH26 β-mannanase on locust bean gum. Malgas et al. (2015^{c}) suggested that GH27 α-galactosidases are more suitable for galactomannan hydrolysis than GH36 α-galactosidases. Biochemical characterization was performed as an initial assessment of the β-mannanases potential industrial use in prebiotic MOS production and biofuel production.

3.2. Objectives

- To culture *B. paralicheniformis* SVD1 in mannan broth to induce β-mannanase production
- To concentrate β-mannanase activity
- To purify β-mannanase activity using anion exchange chromatography and size exclusion chromatography
- To assess protein purification using a protein purification table, SDS-PAGE, native PAGE and zymography
- To determine the temperature optimum, pH optimum and temperature stability of the partially purified β-mannanase.
- To determine the glycosyl hydrolase activities present.

- To determine synergy between the partially purified β-mannanase and a commercial α-galactosidase on locust bean gum in terms of reducing sugar release and mannooligosaccharide production over time.

3.3. Materials and Methods

3.3.1. Culturing

B. paralicheniformis SVD1 was cultured in locust bean gum broth (400 ml) as described in section 2.3.4.1. Cultures were grown for 48 h before concentration of the β-mannanase, as this was the time where activity was highest during growth (Section 2.4.3.).

3.3.2. Protein purification

3.3.2.1. Concentration

3.3.2.1.1. Centrifugal filtration device

Two-step centrifugal filtration was assessed for concentrating and partially purifying mannanase activity. Cell-free supernatant was run through 50 kDa Amicon® Ultra-15 centrifugal devices. The filtrate was then run through 10 kDa PES low protein binding Microsep^{TM} Advance centrifugal filtration devices (Pall Life Sciences). For centrifugal filtration, a Heraeus® Megafuge centrifuge with a swing bucket rotor was used at 4000 *x g*, 4°C. Concentration was conducted using the protocols provided by the manufacturers.

3.3.2.1.2. Ammonium sulfate precipitation

Fractional ammonium sulfate precipitation was assessed as a potential initial purification step. This was tested with 20 ml of cell-free supernatant from a locust bean gum broth (Section 3.3.1) using the method described by Doonan (2004). The ammonium sulfate percent saturation ranges used were: 0% - 20%, 20% - 30%, 30% - 40%, 40% - 50%, 50% - 60%, 60% - 70% and 70% - 80%. A beaker containing cell-free broth was kept on ice and each addition of ammonium sulfate was added slowly over several minutes with gentle mixing by a magnetic stirrer. The solution was left for 10 minutes to allow for further protein precipitation and then centrifuged at 10 000 *x g* for 15 min with an Avanti centrifuge to pellet the precipitated protein. The pellet was then set aside and more ammonium sulfate was added to the supernatant to increase the ammonium sulfate concentration. This was repeated until the solution was 80% saturated with ammonium sulfate. Each pellet was

suspended in a minimum volume of 0.05 M phosphate buffer, pH 7.0, and was then dialyzed against two changes of 0.05 M phosphate buffer, pH 7.0. Dialysis was conducted at 4°C on a shaker at 80 rpm for 6 h for the first round of dialysis and then overnight for the second round of dialysis. The fractions were assessed for protein concentration and mannanase activity.

Concentration using 85% ammonium sulfate saturation was was also assessed. The precipitation was performed for 24 h at 4°C. The pellet was resuspended in a minimal volume of 0.05 M Bis-Tris buffer (pH 6.38) and then dialyzed against two changes of 0.05 M Bis-Tris buffer, pH 6.38.

3.3.2.1.3. Acetone precipitation

Acetone precipitation was tested using small volumes (1 ml) of 0.45 µm filtered cell-free supernatant. Excess acetone (-20°C) was added to protein sample in a 1.4:1 or 4:1 ratio. The solution was then mixed and incubated at -20°C for 1 h or 2 h. The solutions were then centrifuged at 16 060 *x g* for 5 min in a Heraeus bench top centrifuge. The acetone was then evaporated off the pellets at room temperature for 30 min and resuspended in a minimal volume of 0.05 M Bis-Tris buffer, pH 6.38, or the pellets were resuspended in a minimal volume of 0.05 M Bis-Tris buffer, pH 6.38, and then dialyzed. To minimize protease activity in each fraction, phenylmethylsulfonyl fluoride (PMSF) was added to a concentration of 1 mM. Once the best conditions for activity recovery were determined, two fresh locust bean gum cultures were grown as in section 2.3.4.1. The cell-free supernatant was filtered using a 0.45 µm Millex® PVDF syringe filtration membrane (Merck-Millipore) prior to acetone precipitation.

3.3.2.2. Purification

3.3.2.2.1. Anion exchange chromatography

The β-mannanase activity was further purified using AEC. A Toyopearl® DEAE-650M resin (bed volume = 10 ml) was used with 0.05 M Bis-Tris buffer, pH 6.38. All buffers and the protein sample had 0.02% (w/v) NaN_3 added and were filtered using a 0.45 µm Millex® PVDF syringe filtration membrane (Merck-Millipore). The column was equilibrated with 5 column volumes of buffer. The protein sample was then loaded at 26% of the column's total protein binding capacity. The column was washed with 5 column volumes of buffer. Step-wise elution was then performed using a 100 mM – 500 mM NaCl gradient - 2 column

volumes of each NaCl concentration was used. Fractions of 1.07 ml were collected and the absorbance at 280 nm was measured to estimate protein concentration. Fractions with the highest absorbance at 280 nm were assessed for β-mannanase activity. The fractions around the absorbance peaks at 280 nm with β-mannanase activity were then pooled.

3.3.2.2.2. Size exclusion chromatography

SEC was used for the final purification step. The pooled AEC mannanase fractions were concentrated for SEC (Bollag et al., 1996) using a 10 kDa Microsep™ Advance centrifugal device with a PES low protein binding membrane (Pall Life Sciences). A Sephadex® G-75, medium bead size, SEC resin (Sigma) was used with 0.05 M phosphate buffer (pH 7.0, 100 mM NaCl). The buffer was filtered through a 0.45 µm Millex® PVDF syringe filtration membrane (Merck-Millipore) and 0.02% (w/v) NaN_3 was added. The column bed height (cm) and volume (ml) was 17.58 and the volume of sample applied was 0.67% (v/v) of the bed volume. Fractions of 0.22 ml were collected and the protein concentrations of the fractions were estimated by measuring the absorbance at 280 nm. The A280 nm peaks were pooled and their β-mannanase activity was measured. In order to improve resolution, SEC with Sephadex® G-75, superfine bead size resin (Sigma) and Superdex™ 75 prep grade resin (GE Healthcare) was attempted.

3.3.3. Protein concentration determination

The bicinchoninic acid (BCA) assay was used instead of the Bradford assay (Section 2.3.7.) as precipitates formed when the Bradford's reagent was added to the dialyzed ammonium sulfate concentrates (Section 3.3.2.1.2). Dilution of the samples did not eliminate precipitation. The BCA assay was conducted using a BCA protein assay kit (Sigma-Aldrich) according to the supplier's instructions. The 96-well plate assay was used and the plates were incubated at 37°C for 30 min for colour development. The absorbance at 562 nm was measured. BSA was used as a standard to construct standard curves (Appendix 3). A solution with a known concentration of BSA was used as a positive control. The assays were performed in triplicate. Protein concentrations of the fractional ammonium sulfate precipitation, AEC and SEC fractions were determined by measuring the absorbance at 280 nm.

3.3.4. β-mannanase activity

β-mannanase activity was determined using a modified DNS assay for the determination of reducing sugars as described in Section 2.3.7. The protein load used was the required amount that released around 0.5 mg/ml of mannose reducing sugar equivalents (absorbance at 540 nm = ~1).

3.3.5. SDS-PAGE

SDS-PAGE was conducted using the method developed by Laemmli (1970) and modified according to Bollag et al. (1996). The crude cell-free supernatant and ammonium sulfate precipitation fractions were concentrated using acetone precipitation prior to electrophoresis. Four parts ice cold acetone (-20°C) were added to one part of β-mannanase solution. The mixture was vortexed, incubated at -20°C for 1-2 h and then centrifuged for 5 min at 16 060 *x g* using a benchtop centrifuge. The supernatant was then decanted and the pellet air dried at room temperature for 30 min. A minimal volume of 0.05 M phosphate buffer, pH 7.0 was then added to resuspend the pellet (Anon, 2009).

3.3.6. Zymography

Zymograms were used to determine the MW of the purified β-mannanase/s. Zymograms were conducted as in section 2.3.12. The substrates used were locust bean gum or konjac glucomannan.

3.3.7. Native PAGE and native zymogram

The purified fraction was also analysed using native PAGE. Native PAGE was conducted as SDS-PAGE (Section 3.3.5) with the following differences: the running buffer, gels and sample buffer contained no SDS. The samples were concentrated using 10 kDa PES low protein binding Microsep^{TM} Advance centrifugal filtration devices (Pall Life Sciences), and the sample buffer and sample mixture were not heated. Electrophoresis was performed at 100 V on ice. Native zymograms were conducted by running the samples on Native PAGE gels with 0.1% (w/v) konjac glucomannan or locust bean gum added. After electrophoresis, excised lanes containing β-mannanase were incubated in 0.05 M phosphate buffer, pH 7.0 for 3 h and then stained, destained and imaged as in Section 2.3.12.

3.3.8. Enzyme activity and protein concentration determination

Enzyme activity was determined using locust bean gum as a substrate and the DNS assay for determination of reducing sugars as described in Section 2.3.7., except that the substrate hydrolysis time was 1 h and the protein load was 0.560 mg protein.g^{-1} substrate. The protein load and assay time was reduced as the activity (U.ml^{-1}) of the partially purified β-mannanase was much higher than the activity of the crude β-mannanase. Protein concentration was determined using the BCA assay as described in Section 3.3.3.

3.3.9. Time study

Enzyme activity was measured as described in Section 3.3.8. using different times for the hydrolysis assay (5 min – 3 h).

3.3.10. Temperature optimum and stability

The temperature optimum was determined using the standard enzyme activity assay (Section 3.3.8.) at different temperatures (35°C, 40°C, 45°C, 50°C, 55°C, 60°C, 70°C, 80°C, 90°C). The temperature stability was determined by incubating an appropriately diluted β-mannanase solution at 37°C or 50°C for 0 min to 24 h and then measuring the residual activity using the standard enzyme activity assay (Section 3.3.8.).

3.3.11. pH optimum

The pH optimum was determined using the standard enzyme activity assay (Section 3.3.8.) with different pH buffers in a pH range from 3.0 – 11.0. The buffers used were: 0.05 M sodium citrate (pH 3.0 – 5.0), 0.05 M potassium phosphate (pH 6.0 – 8.0) and 0.05 M glycine (pH 9.0 – 11.0).

3.3.12. Substrate specificity

The specific activities of the enzymes were assessed on different substrates. For polymeric substrates, the standard activity assay was used (Section 3.3.8.). The polymeric substrates assessed were: konjac glucomannan, locust bean gum, ivory nut mannan, guar gum, carboxymethyl cellulose, Avicel®, arabinogalactan, beechwood xylan, wheat arabinoxylan, xyloglucan and pectin from apple. Activity on *p*NP based substrates was conducted as

follows: appropriately diluted β-mannanase (100 µl) was added to 300 µl of 2.67 mM *p*NP substrate in 0.05 M potassium phosphate buffer (pH 7.0) in eppendorf tubes. The *p*NP substrates assessed were: *p*NP α-L-arabinofuranoside, *p*NP β-D-mannopyranoside, *p*NP α-D-mannopyranoside, *p*NP β-D-galactopyranoside, *p*NP α-D-galactopyranoside, *p*NP β-D-glucopyranoside, *p*NP α-D-glucopyranoside, *p*NP β-D-cellobioside, *p*NP β-D-xylopyranoside, *p*NP β-D-glucuronide and *p*NP β-D-fucopyranoside. The tubes were incubated at 50°C for 30 min in an AccuBlock digital dry bath heater (Labnet). The reactions were terminated by the addition of 400 µl of 2 M Na_2CO_3 in diH_2O. Aliquots (250 µl) were then pipetted into a 96-well microtiter plate and the absorbance readings were then taken at 405 nm using a Powerwave X microplate reader (BioTek Instruments) and KC Junior software. The concentration of *p*NP released was determined using a *p*NP standard curve (Appendix 4 – Figure A.8). One unit of enzyme activity was defined as the amount of enzyme that released 1 µmol of *p*NP per min under the assay conditions.

3.3.13. Synergy between the partially purified β-mannanase and an α-galactosidase

3.3.13.1. Synergy on locust bean gum

The hydrolysis of locust bean gum by various combinations of the partially purified *B. paralicheniformis* SVD1 β-mannanase and a commercial GH27 α-galactosidase from *Cyamopsis tetragonolobus* seeds (Megazyme) was assessed using the hydrolysis assay and DNS assay for reducing sugar determination as described in Section 3.3.8, except that the assay was conducted at 37°C, pH 5.0 with mixing at 20 rpm because the GH27 α-galactosidase was not stable above 40°C (pH 5.5) according to the supplier's information sheet. Hydrolysis over 24 h was assessed (3 h, 6 h, 12 h, 24 h). The total protein load used was 0.560 mg protein.g^{-1} locust bean gum. Bovine serum albumin was added to a final concentration of 0.5 mg/ ml in the reaction mixture to minimize non-productive adsorption of the enzymes and to increase protein stability. The reactions were terminated by boiling for 5 min followed by centrifugation at 16 060 *x g* for 5 min. The supernatant was assessed for reducing sugars using the DNS assay. The enzymes were added alone or in the following binary combinations: 75% β-mannanase: 25% α-galactosidase (M75G25), 50% β-mannanase: 50% α-galactosidase or 25% β-mannanase:75% α-galactosidase. The DS was calculated by dividing the actual activity of the combination of enzymes by the theoretical sum of the individual enzyme activities (Van Dyk & Pletschke, 2012). The assays were

performed in duplicate. One way analysis of variance (ANOVA), using the Data analysis feature in Microsoft Excel 2010, was used to compare the activity of the different enzyme combinations. The enzyme combinations were assessed for significant ($p < 0.05$) differences in reducing sugar release compared to that released by 100% β-mannanase.

3.3.13.2. TLC analysis of mannan hydrolysis

An aliquot of the hydrolyzate (Section 3.3.13.1.) was used for TLC. The same method was used as in Chapter 2, Section 2.3.13. for spotting, running and developing the plate, except that 20 µl of sample, instead of 5 µl, was applied to the TLC plate to increase detection sensitivity.

3.4. Results

3.4.1. Culturing and centrifugal filtration

Concentration of a locust bean gum culture by ultrafiltration through 50 kDa Amicon® Ultra-15 centrifugal devices (then concentration of the filtrate using 10 kDa PES Macrosep™ Advance centrifugal devices) was attempted. The cell-free culture supernatant was filtered through 0.45 µm Millex® PVDF syringe filtration membranes prior to centrifugal filtration and 100 mM NaCl was added to the cell-free supernatant to minimize protein binding to the membranes. During centrifugation, the concentrates were mixed every few minutes to prevent steep concentration gradients forming that could result in protein precipitation. However, activity yield was low (8%). Partial retention of the β-mannanase on the membranes occurred. Concentration using only the 10 kDa membranes was the most effective.

3.4.2. Acetone precipitation

Acetone precipitation was attempted using different methods that varied the acetone to cell-free supernatant ratio, precipitation time and method of acetone removal after precipitation. A procedure that used 2 h acetone precipitation with a 1.4:1 acetone to protein ratio followed by dialysis gave the best result. Activity yields above 50% were achieved, which were higher than those yields that were obtained, when centrifugal filtration devices were used for concentration. Acetone precipitation of a larger (800 ml) volume using the optimized conditions gave a lower than expected activity yield (12.4%) and fold purification

(3.59). The acetone precipitate was brown, viscous and quite insoluble, possibly due to co-precipitation of locust bean gum and protein. Recovery of the precipitate was difficult as the pellet adhered to the centrifuge tubes. The dialyzed concentrate was applied onto a Toyopearl® DEAE-650M resin AEC column. The concentrated and dialyzed protein had a high concentration of background reducing sugars. These sugars were probably > 10 kDa as they did not pass through the dialysis membrane. The AEC flow through also had a high concentration of reducing sugars (2.64 $mg.ml^{-1}$). The AEC fractions that were tested did not display β-mannanase activity. The high reducing sugar content possibly blocked β-mannanase binding to the AEC column, as 51% of the β-mannanase activity was recovered in the AEC wash. As acetone precipitatation did not work well, ammonium sulfate precipitation was subsequently used for protein concentration.

3.4.3. Purification procedure using ammonium sulfate precipitation

Fractional ammonium sulfate precipitation was attempted in order to concentrate and partially purify the crude β-mannanase. The first trial showed no visible protein precipitation when the ammonium sulfate saturation was below 40%. Most of the mannanase activity (14.1% activity yield) was present in the 70% - 80% fraction. The second trial, which assessed activity yield using a different ammonium sulfate saturation range, gave better activity yields. As with the first trial, the activity yield increased as the ammonium sulfate saturation range increased. The β-mannanase and most of the proteins only precipitated at a high ammonium sulfate concentration, indicating that they are hydrophilic. This is expected for secreted proteins. The fold purification was low (1.24 or less) so ammonium sulfate fractionation was not an effective method for purifying the β-mannanases. Activity yield using ammonium sulfate precipitation can be 80% or more, so the yields were much lower than expected. One possible reason for the low yield may be that the trial volumes used (20 ml) and the relatively low level of β-mannanase production made sample handling difficult as there was not a lot of precipitate that formed. Ammonium sulfate also contains trace amounts of metal ions that may have inhibited the mannanase activity.

Given that the β-mannanase precipitated over a wide range of ammonium sulfate concentrations and that the fold purification and yield was low, concentration using 85% saturated ammonium sulfate solution was attempted. The remainder of the cell-free supernatant (309 ml) was used. Ammonium sulfate precipitation and dialysis was conducted as in Section 3.3.2.1.2, except that only 85% ammonium sulfate saturation was used,

precipitation was performed for 24 h at 4°C and the pellet was resuspended in a minimal volume of 0.05 M Bis-Tris buffer, pH 6.38. This was then dialyzed against two changes of 0.05 M Bis-Tris buffer, pH 6.38. The fractions were assessed for protein concentration and β-mannanase activity. The activity yield was 18.5%, which was lower than expected, given that the second fractional precipitation trial gave higher yield (29.9%). It was noted that much of the protein precipitate did not completely pellet after centrifugation, it remained suspended as flakes in the supernatant. The suspended precipitate was partially recovered by filtering the supernatant through Whatman filter paper. Even though the activity yield was low the concentrate was used for the next purification step, AEC. Ammonium sulfate precipitation can separate protein from polysaccharides that could potentially be problematic for subsequent chromatography. Ammonium sulphate precipitation is also less tedious than centrifugal filtration when large volumes were used.

AEC using a Toyopearl® DEAE-650M resin was conducted to further purify the β-mannanase activity. The column equilibration and efficiency was assessed by determining the theoretical plate count and asymmetry factor using acetone. The AEC chromatogram displayed five distinct large peaks and a smaller peak based on absorbance at 280 nm (Figure 3.1). β-mannanase activity was measured in the fraction of each peak where the absorbance at 280 nm was the highest. Only peak 2 contained mannanase activity (data not shown). The fractions in peak 2 were pooled and used for further experiments. Given that the peak displayed tailing, which indicated more than one protein, it was not expected that the peak consisted of only β-mannanase. Further purification would therefore be necessary.

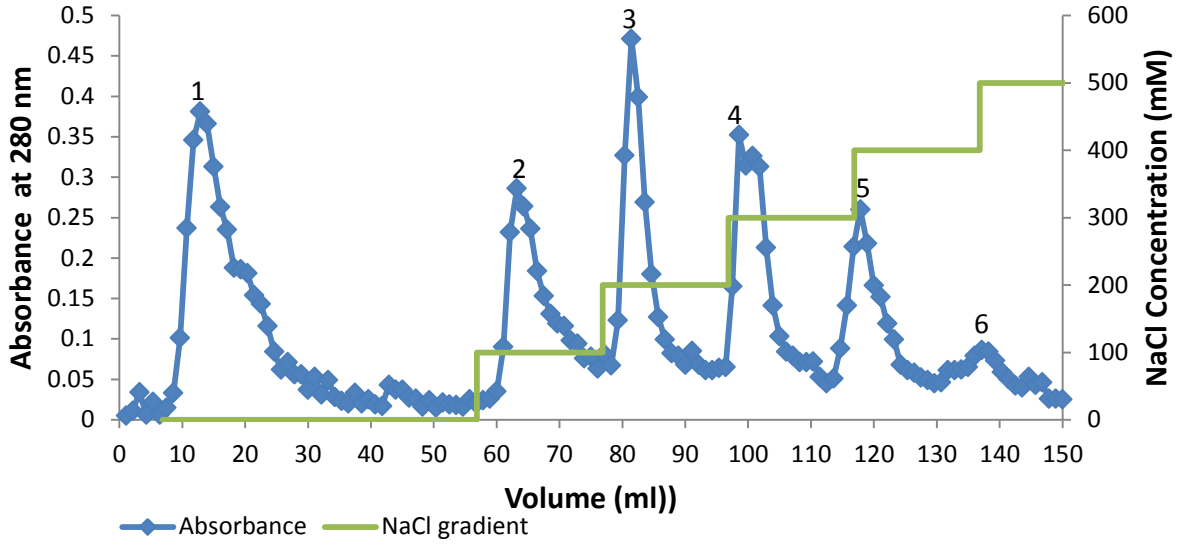

Figure 3.1. Chromatogram of anion exchange step of purification. Toyopearl DEAE 650M anion exchange resin was employed with 50 mM Bis-Tris buffer at pH 6.38. Elution was performed with a stepwise gradient of NaCl (Column 2.5 cm x 2.5 cm, flow rate 1.91 ml.min^{-1}). The peaks in absorbance at 280 nm are labelled 1-6.

SEC using Sephadex® G-75 was conducted to further purify the pooled β-mannanase active fractions from AEC. The SEC chromatogram (Figure 3.2) showed two prominent peaks. The most prominent peak eluted just after the void volume, most likely representing the proteins around 75 kDa. The second (smaller peak) overlapped with the larger peak as well as smaller peaks. The fractions around the two peaks were pooled and tested for β-mannanase activity. Only the second prominent peak contained β-mannanase activity. Given that the second peak with β-mannanase activity had a lower absorbance than the first peak, mannanase was probably not a very abundant protein in the secretome. SEC using Sephadex® G-75 superfine resin and Superdex^{TM} 75 prep grade resin was also attempted but they did not work as gravity-flow filtration was used and the flow rates were extremely slow.

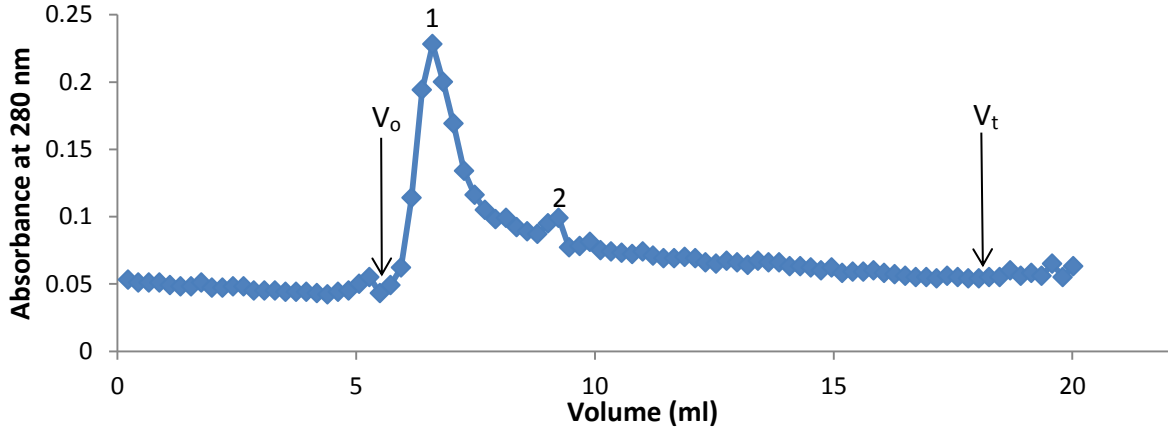

Figure 3.2. Chromatogram of size exclusion step of purification. Sephadex® G-75 resin was used with 50 mM phosphate buffer at pH 7.0 containing 100 mM NaCl. (Column dimensions 17.58 cm x 1 cm, flow rate 0.67 ml.min^{-1}). V_o = void volume, V_t = total column volume. The main peaks are labelled 1-2.

Peak 2 (containing β-mannanase activity) displayed tailing, which indicates more than one protein. Therefore, the purification procedure was repeated but with the following alterations: to increase the activity yield, the ammonium sulfate precipitation time was increased from 10 min to 24 h as some proteins require several hours to completely precipitate (Bollag et al., 1996). To improve the degree of precipitation, centrifugation speed and time was increased to 14 000 *x g*, 30 min. These alterations only improved activity yield by ~1.5%. The pH of the 0.05 M Bis-Tris buffer used for AEC was increased from 6.38 to 6.58 to increase the net negative charge of the β-mannanases and therefore increase binding to the AEC column. A 20 mM to 150 mM (20 mM, 40 mM, 60 mM, 80 mM, 100 mM, 150 mM) step-wise NaCl gradient was used for elution. A final 3 x column volume 1 M NaCl wash was then performed. The 20 - 40 mM NaCl fractions displayed β-mannanase activity. In the following experiments, elution of the β-mannanase was performed using 3 column volumes of 40 mM NaCl. The pooled AEC fractions containing β-mannanase activity were concentrated using 10 kDa PES Microsep^{TM} centrifugal filtration devices prior to SEC. To improve SEC resolution, the column length was increased and the flow rate was reduced. The SEC chromatogram (not shown) showed that there was a low amount of protein that was eluted and the absorbance peaks were not as distinct as in the previous SEC chromatogram (Figure 3.2). The total amount of β-mannanase activity eluted from the SEC column was 2.09 U and the protein concentration was too low to quantify using the BCA

assay. The amount of sample eluted was only enough to assess the β-mannanase activity, protein concentration (A280 nm) and a single run on a SDS-PAGE gel.

A β-mannanase purification table was constructed to assess the success of the purification protocol (Table 3.1). There was loss in activity after each purification step: 80% after ammonium sulfate precipitation, 58% after AEC and 39% after 10 kDa concentration. The fold purification after AEC was high (88.9), however the activity yield was low (5.09%). The SEC results were not included as the protein concentration was too low to be detected using the BCA assay. Estimation of the protein concentration using absorbance at 280 nm, which gave higher protein concentration values than the BCA and Bradfords assay (data not shown), gave a specific activity of 108 $U.mg^{-1}$ and a fold purification of 153 for one of the fractions.

Table 3.1. β-mannanase purification table.

Fraction	Vol. (ml)	Protein conc. (mg/ml)	Total protein (mg)	Activity (U/ml)	Total activity (U)	Specific activity (U/mg)	Purific-ation factor	Activity yield (%)
Cell-free supern., 0.45 µM filtered	813	1.87	1522	0.71	580	0.38	1	100
Amm. sulf. ppt.: dialyzed and 0.45 µm filtered	17.0	2.27	38.6	6.83	116	3.01	7.89	20.0
Pooled 40 mM NaCl AEC fraction	181	0.052	9.41	0.27	48.6	5.17	13.6	8.39
10 kDa conc. pooled 40 mM NaCl AEC fraction	3.56	0.25	0.87	8.29	29.5	33.8	88.9	5.09

An SDS-PAGE gel was run to assess the purity of β-mannanase (Figure 3.3). The pooled β-mannanase containing fractions of the AEC and SEC steps were concentrated using 10

kDa PES Microsep™ Advance centrifugal filtration devices prior to SDS-PAGE. The crude supernatant displayed various bands with MWs of about 100 kDa or less. The 85% ammonium sulfate precipitate had a greater proportion of lower MW proteins. The pooled β-mannanase containing fractions of the AEC step also showed a change in the relative concentration of proteins, with a large increase in the relative abundance of proteins with a relative MW of 62 kDa and 40 kDa. The 40 kDa band is most possibly a β-mannanase, as this mass corresponds to the theoretical molecular masses calculated. The pooled β-mannanase containing fractions of the SEC step showed a single prominent band with a MW of 37 kDa and 2 very faint bands with molecular masses of around 65 kDa. The prominent band could be a β-mannanase. The protein load was low as there was not a lot of sample remaining after SEC.

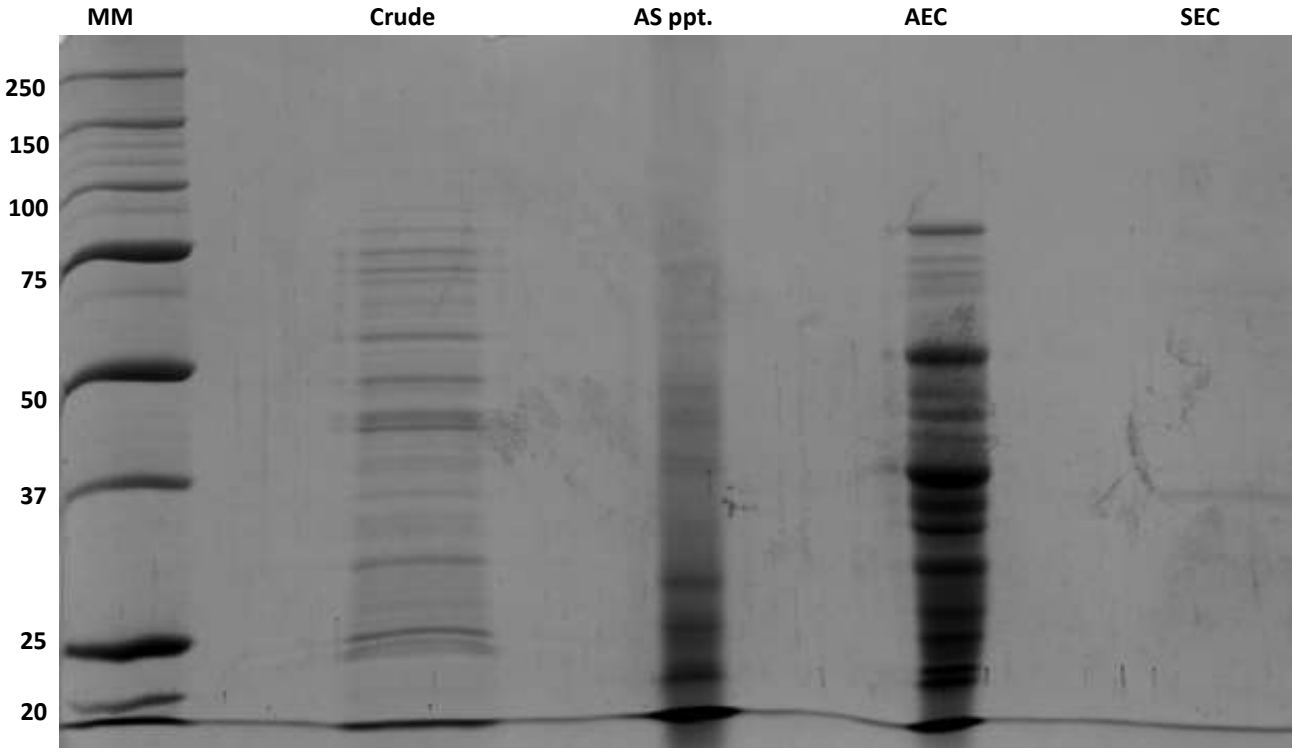

Figure 3.3. A 12% SDS-PAGE gel displaying purification of *B. paralicheniformis* SVD1 β-mannanase. Each lane was loaded with 20 µg of protein. Lane MM: Molecular weight markers (Bio-Rad Precision Plus Protein™ unstained protein standards); Lane Crude: cell-free supernatant; Lane AS ppt.: 85% ammonium sulfate precipitate; Lane AEC: pooled anion exchange chromatography elution fractions with β-mannanase activity; Lane SEC: pooled size exclusion chromatography fractions with β-mannanase activity.

3.4.4. Partial purification procedure

The SEC step of purification was not successful and therefore it was decided to just partially purify the β-mannanase given time constraints. Purification was repeated until after the AEC step. To further reduce any protease activity, an EDTA-free protease inhibitor cocktail (Roche) was added to the final partially purified AEC fraction. Glycerol was also added to 20% (v/v) to improve storage stability. Another SDS-PAGE gel was run and zymogram analysis was performed to determine the relative MW of the β-mannanase. The SDS-PAGE protocol was altered; boiling of the sample with sample buffer was performed for only 45 seconds, SDS-PAGE with 5 minutes of boiling gave a very similar protein profile. This was done so that the samples that were stained with Coomassie Brilliant Blue were boiled for the same amount of time as the samples that were stained with Congo Red. The protein profile of the concentrated AEC fraction (Figure 3.4) was very similar to the previous protein profile that was obtained (Figure 3.3). There were prominent proteins with molecular masses of 38 kDa, 52 kDa and 80 kDa and at lower MWs around 30 kDa. The konjac glucomannan zymogram showed a single activity band with a molecular mass of 41 kDa. The locust bean gum zymogram showed a single activity band with a molecular mass of 40 kDa. These masses corresponded to the theoretical molecular mass of the β-mannanases. Given that the zymogram of the crude concentrated mannanase displayed two activity bands at at 29.6 kDa and 33 kDa (Chapter 2 – Figure 2.7) with no protease inhibitors added, protease activity was probably the reason that the crude concentrated β-mannanase displayed smaller than expected sizes. The mannanases were probably catalytically active truncated products of protease hydrolysis. Given that the serine protease inhibitor PMSF was added during purification and that the β-mannanase MW was similar to its theoretical size, serine protease activity was probably responsible for the truncation of the crude concentrated β-mannanase (Chapter 2). It was not possible to determine if GH5, GH26 or both classes of β-mannanases, were present as their theoretical molecular masses were too similar to be resolved on SDS-PAGE (37.9 kDa and 42.1 kDa). Further studies would need to be performed to assess which β-mannanase classes are present.

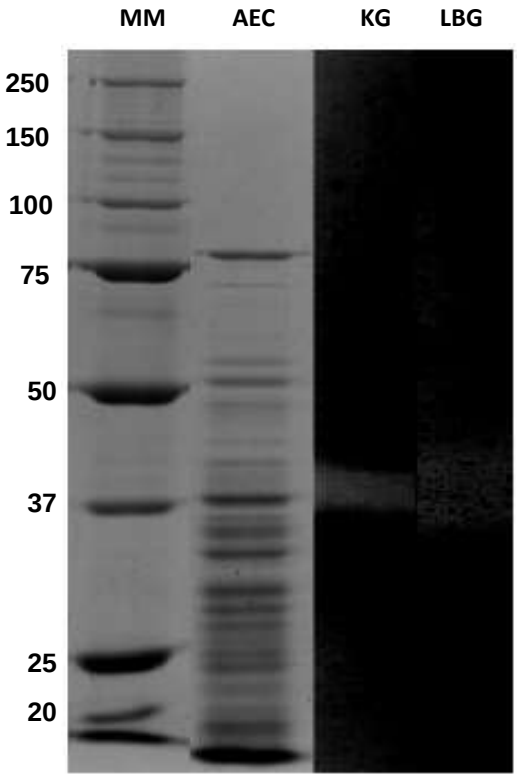

Figure 3.4. A 12% SDS-PAGE and zymogram gel displaying the partially pure *B. paralicheniformis* SVD1 β-mannanase. Each lane was loaded with 10 µg of protein. The zymogram lanes were loaded with 2 µg of protein. Lane MM: Molecular weight markers (Bio-Rad Precision Plus Protein™ unstained protein standards); Lane AEC: anion exchange chromatography concentrate; Lane KG: konjac glucomannan zymogram (6 h hydrolysis incubation); Lane LBG: locust bean gum zymogram (6 h hydrolysis incubation).

Native PAGE and native zymography were performed to assess if different β-mannanases or isomers of the β-mannanases were present (Figure 3.5). All of the proteins were expected to be negatively charged in the native PAGE buffers used (pH 6.8 stacking gel, pH 8.8 separating gel) as the partially purified mannanase contained proteins that bound to an AEC column at pH 6.58. The AEC concentrate showed a number of protein bands. The proteins that possibly displayed activity were the five protein bands (two of which were distinct) that migrated the least in the native gel. The two activity bands in the konjac glucomannan and locust bean gum native zymograms were too broad to determine which specific protein bands had activity. This indicated that there were at least two different β-mannanases or two charge isomers. Further studies would need to be performed to assess if they are different

β-mannanases or isomers. The low extent of migration may be due to a relatively low negative charge or binding of the β-mannanases to the mannan incorporated in the gels. The broadness of the bands could be reduced by decreasing the reaction time for hydrolysis.

Figure 3.5. A 12% native PAGE and native zymogram gel displaying the partially pure *B. paralicheniformis* SVD1 β-mannanase. The native PAGE lane was loaded with 10 µg of protein. The zymogram lanes were loaded with 1 µg of protein. Lane AEC: anion exchange chromatography concentrate; Lane KG: konjac glucomannan zymogram (3 h incubation); Lane LBG: locust bean gum zymogram (3 h hydrolysis incubation).

3.4.5. Time study

In order to determine if the locust bean gum substrate used to determine β-mannanase activity was limiting during the 1 h hydrolysis reaction time for the partially purified β-mannanase, the amount of reducing sugars released over time (3 h) was determined (Figure 3.6). The substrate hydrolysis rate increased linearly up to around 60 min and then the substrate started to become a limiting factor to the hydrolysis rate. Therefore, the substrate

was not limiting to the reaction rate in the standard enzyme activity assay (1 h hydrolysis) that was used (Section 3.3.8.).

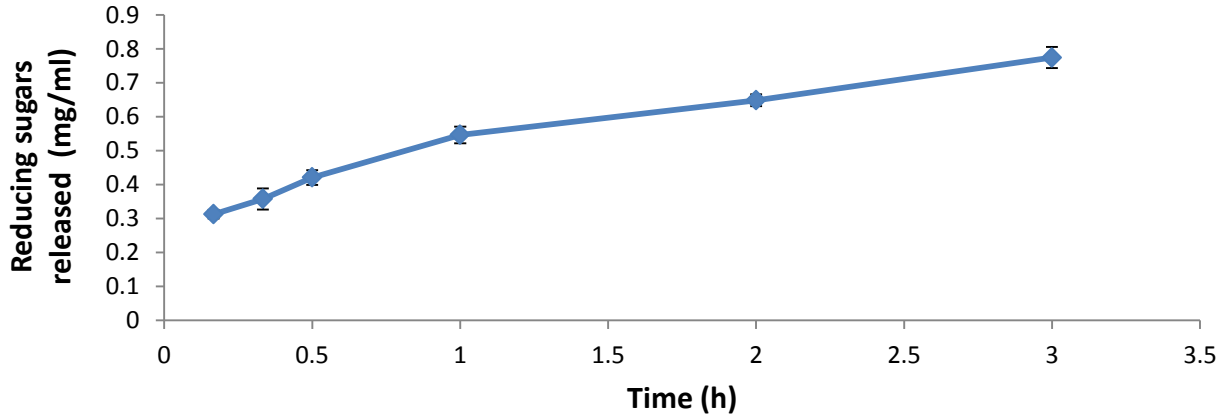

Figure 3.6. Partially purified β-mannanase activity on locust bean gum over 3 h. Values are represented as means ± standard deviations, n = 3.

3.4.6. Temperature optimum and stability

The temperature optimum and stability was assessed in order to determine the appropriate assay conditions for further studies. The temperature optimum of the partially purified β-mannanase was 55°C (Figure 3.7. A). Between 50°C and 55°C activity was greater than 80% of the maximum. The standard assay was employed at 50°C (Section 3.3.8.). The β-mannanase denatured rapidly at a temperature of 70°C or higher. The β-mannanase retained above 90% of its activity after 24 h of incubation at 37°C and retained above 80% of its activity after 24 h of incubation at 50°C (Figure 3.7. B). As 50 °C was used in the standard 1 h assay (Section 3.3.8.), the β-mannanase/s were stable during the standard assay, > 94% of activity was retained after 1 h. The temperature stability at 37°C showed an increase in activity between 30 min and 12 h of incubation, which then decreased (Figure 3.7. B). The increase in activity over time was not expected. This increase also occurred using the crude, concentrated enzyme (Figure 2.4). The cause of this increase may have been incomplete substrate dissolution, which increased during the incubation period. The crude concentrated β-mannanase displayed higher temperature stability (Figure 2.4) than the partially purified β-mannanase. The differences in temperature optima and stability between the crude concentrated and partially purified β-mannanase may have been due different concentrations and ratios of enzyme solution components such as proteins.

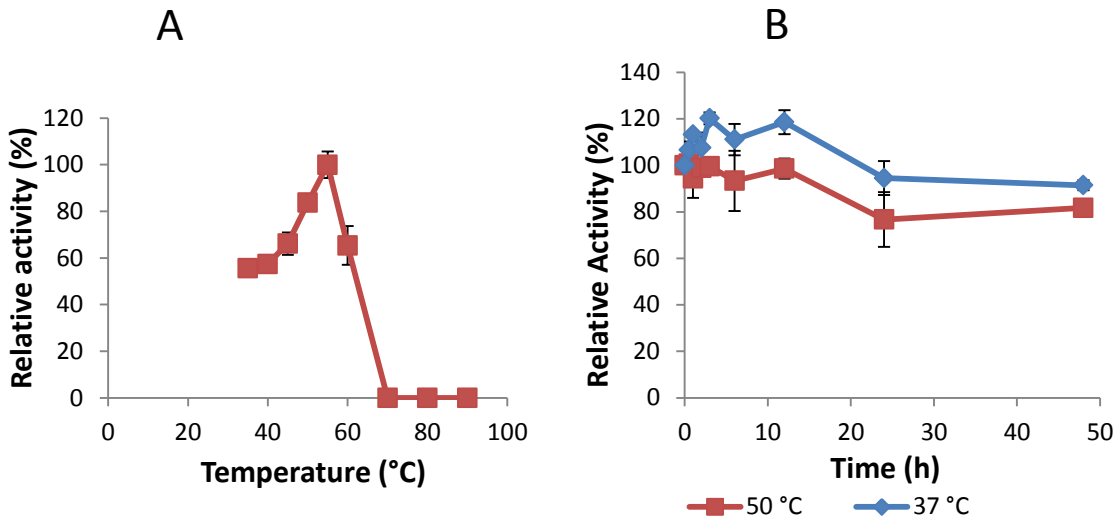

Figure 3.7. A: Temperature optimum of partially purified β-mannanase activity. B: Temperature stability of partially purified β-mannanase activity over 24 h at 37 °C and 50 °C. Values are represented as mean values ± standard deviations, n = 3.

3.4.7. pH optimum

To further assess the optimal assay conditions for the partially purified β-mannanase, the pH optimum was determined. The pH optimum was pH 6.0 (Figure 3.8). There was also a peak in activity at pH 9.0. Between pH 5.0 and pH 9.0, activity was greater than 80% of the maximum at pH 6.0. The standard assay employed a pH of 7.0, which showed 86% relative activity compared to the temperature optima. The partially purified β-mannanase displayed two pH optima like the crude concentrated β-mannanase (Figure 2.5), but the pH optima increased by 1 – 2 pH units. One reason for this may have been the difference in hydrolysis assay times, 30 min for the crude concentrated β-mannanase and 1 h for the partially purified β-mannanase. The β-mannanase may be more stable at a basic pH, which would explain why the pH optima for the 1 h assay were higher than those pH optima for the 30 min assay.

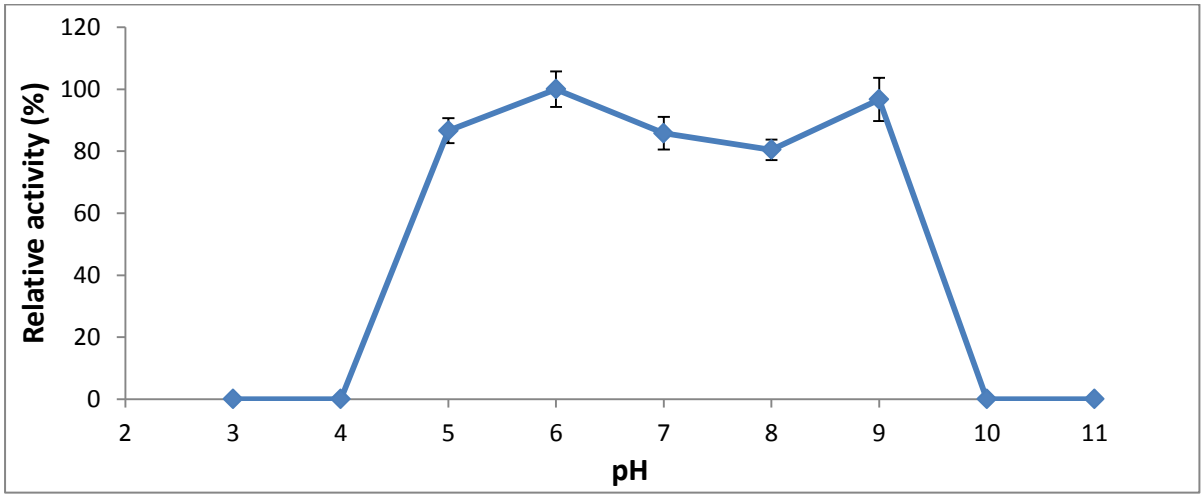

Figure 3.8. pH optimum of the partially purified β-mannanase activity. Values are represented as means ± standard deviations, n = 3.

3.4.8. Substrate specificity

Substrate specificity was determined to assess which glycosyl hydrolase activities were present (Table 3.2). Activity was the highest on soluble mannan substrates and galactose branching inhibited hydrolysis. This was also found with the crude concentrated β-mannanase (Figure 2.6). The highest specific activity was on konjac glucomannan (Table 3.2). Unlike the crude concentrated β-mannanase, activity was not detected on guar gum galactomannan and no cellulase or galactosidase activity was detected. Activity on the *p*NP substrate *p*NP α–L-arabinofuranoside indicated the presence of α-L-arabinofuranosidase activity. The hydrolysis of the mannan substrates by the partially purified β-mannanase (as with the crude concentrated β-mannanase) was mostly due to hydrolysis of internal β-1,4-glycosidic bonds by β-mannanase/s.

Table 3.2. Glycosyl hydrolase activities of the partially purified β-mannanase on defined substrates. Values are represented as the means, n = 3.

Substrate	Activity (U.mg^{-1} protein)
Konjac glucomannan	28.46 ± 1.97
Locust bean gum	17.44 ± 0.78
Ivory nut mannan	10.87 ± 0.39
Guar gum	nd
Carboxymethyl cellulose	nd
Avicel®	nd
Arabinogalactan	nd
Beechwood xylan	nd
Wheat arabinoxylan	nd
Xyloglucan	nd
Pectin from Apple	nd
4-Nitrophenyl α-L-arabinofuranoside	0.10 ± 0.029
4-Nitrophenyl β-D-mannopyranoside	nd
4-Nitrophenyl α-D-mannopyranoside	nd
4-Nitrophenyl β-D-galactopyranoside	nd
4-Nitrophenyl α-D-galactopyranoside	nd
4-Nitrophenyl β-D-glucopyranoside	nd
4-Nitrophenyl α-D-glucopyranoside	nd
4-Nitrophenyl β-D-cellobioside	nd
4-Nitrophenyl β-D-xylopyranoside	nd
4-Nitrophenyl β-D-glucuronide	nd
4-Nitrophenyl β-D-fucopyranoside	nd

* nd = not detected

3.4.9. Synergy between the partially purified β-mannanase and an α-galactosidase

Synergy between the partially purified β-mannanase of *B. paralicheniformis* SVD1 and a commercial GH27 α-galactosidase from *C. tetragonolobus* was assessed on locust bean gum (Figure 3.9). This was done to determine if the α-galactosidase could improve mannan hydrolysis. Hydrolysis for all the different combinations tended to increase over time. The only statistically significant (p-value < 0.05) increases in reducing sugar release, compared to M100, occurred with the M75G25 combination after 6 h of hydrolysis and the M50G50 combination after 24 h. The highest extent of hydrolysis occurred with the M50G50 combination after 24 h. There was a 1.39 fold increase in reducing sugar release and the DS was 4.64. For all the different enzyme combinations, the DS tended to increase over time. The increase in DS for the M75G25 and M50G50 combinations was greater than the

increase observed for the M25G75 combination. Hydrolysis of locust bean gum by the GH27 α-galactosidase alone was the lowest (as expected).

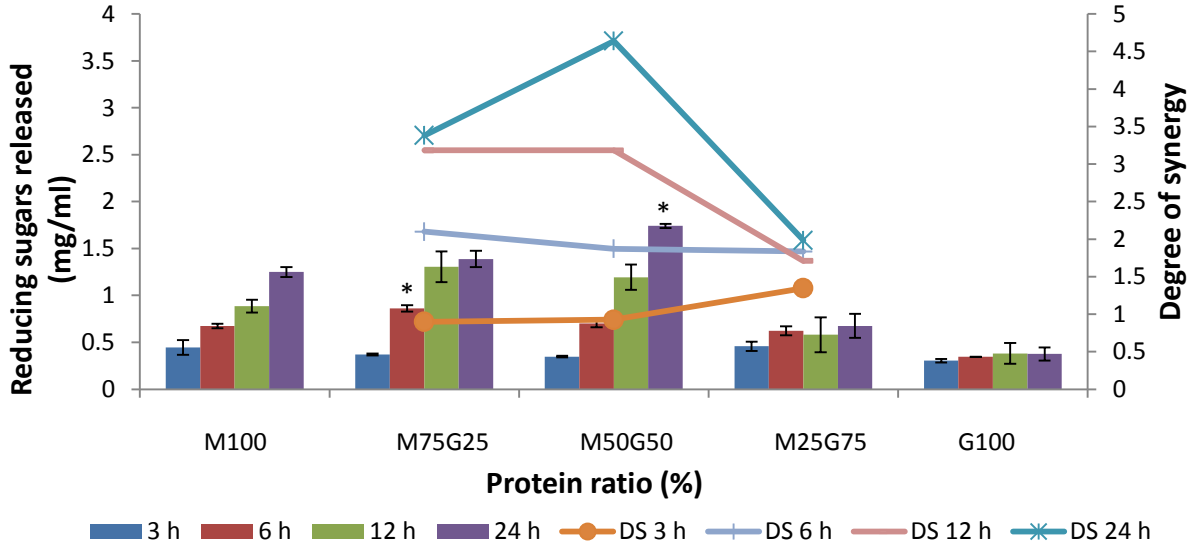

Figure 3.9. Reducing sugars released by and the degree of synergy between various combinations of the partially purified *B. paralicheniformis* SVD1 β- mannanase and the GH27 α-galactosidase from *Cyamopsis tetragonolobus* seeds obtained on 0.5% (w/v) locust bean gum. ANOVA was used to assess synergistic improvement of hydrolysis with respect to reducing sugar release by the enzyme combinations compared to 100% β-mannanase protein loading. key: *(p-value < 0.05). Values are represented as mean values ± standard deviations, n = 2.

Products formed from the hydrolysis of locust bean gum over 24 h by the partially purified *B. paralicheniformis* SVD1 β-mannanase and a commercial GH27 α-galactosidase from *C. tetragonolobus* seeds was determined qualitatively using TLC (Figure 3.10). This was done in order to assess the synergistic production of MOS for potential use as a prebiotic as well as for use in biomass saccharification for biofuel production. The β-mannanase alone (M100) produced an increase in MOS production over time as was expected given that reducing sugar release increased over time (Figure 3.9). Most of the resolved MOS products displayed R_f values between the R_f values of mannose and mannohexaose. The dominant products had the same R_f values as mannotetraose and mannose/ galactose. The hydrolysis profile was similar to what was found with the crude concentrated β-mannanase in Chapter 2 (Figure 2.8). However, there was a higher galactose/ mannose release. One reason for the difference may be that the partially purified β-mannanase had more α-galactosidase activity. The substrate specificity assays did not detect α-galactosidase activity (Table 3.2). However

the substrate specificity assays used a 30 min hydrolysis time, the synergy assays used a hydrolysis time of 3h – 24 h (Figure 3.9). The substrate specificity assays may have detected α-galactosidase activity if the assay hydrolysis time was increased. The hydrolysis profile of the M75G25 combination was similar to partially purified β-mannanase alone (M100). However, the M75G25 combination had a higher degree of hydrolysis based on the intensity of the spots. The M50G50 and M25G75 combinations showed a similar profile to the other β-mannanase combinations except the hydrolysis rates and extent was lower. The α-galactosidase alone showed very little hydrolysis; it appears as if only α-galactose release could be observed (as was expected). The hydrolysis rate was probably lower because there are fewer bonds available for hydrolysis than for the β-mannanases. These results (Figure 3.10) agree with the previous results (Figure 3.9), except that the M50G50 combination was expected to have the highest degree of hydrolysis. The reason for the hydrolysis being less than expected may have been due to TLC sample loading errors. As a large volume of each sample (20 µl) was manually loaded onto the TLC plates, pipetting errors may have occcured. The large sample volume and manual loading also led to uneven application of the samples. This resulted in smearing and uneven migration of the hydrolysis products, which made interpretation difficult. Resolution could be improved by using TLC plates with silica concentrating zones that allow for quick and easy sample application and high resolution.

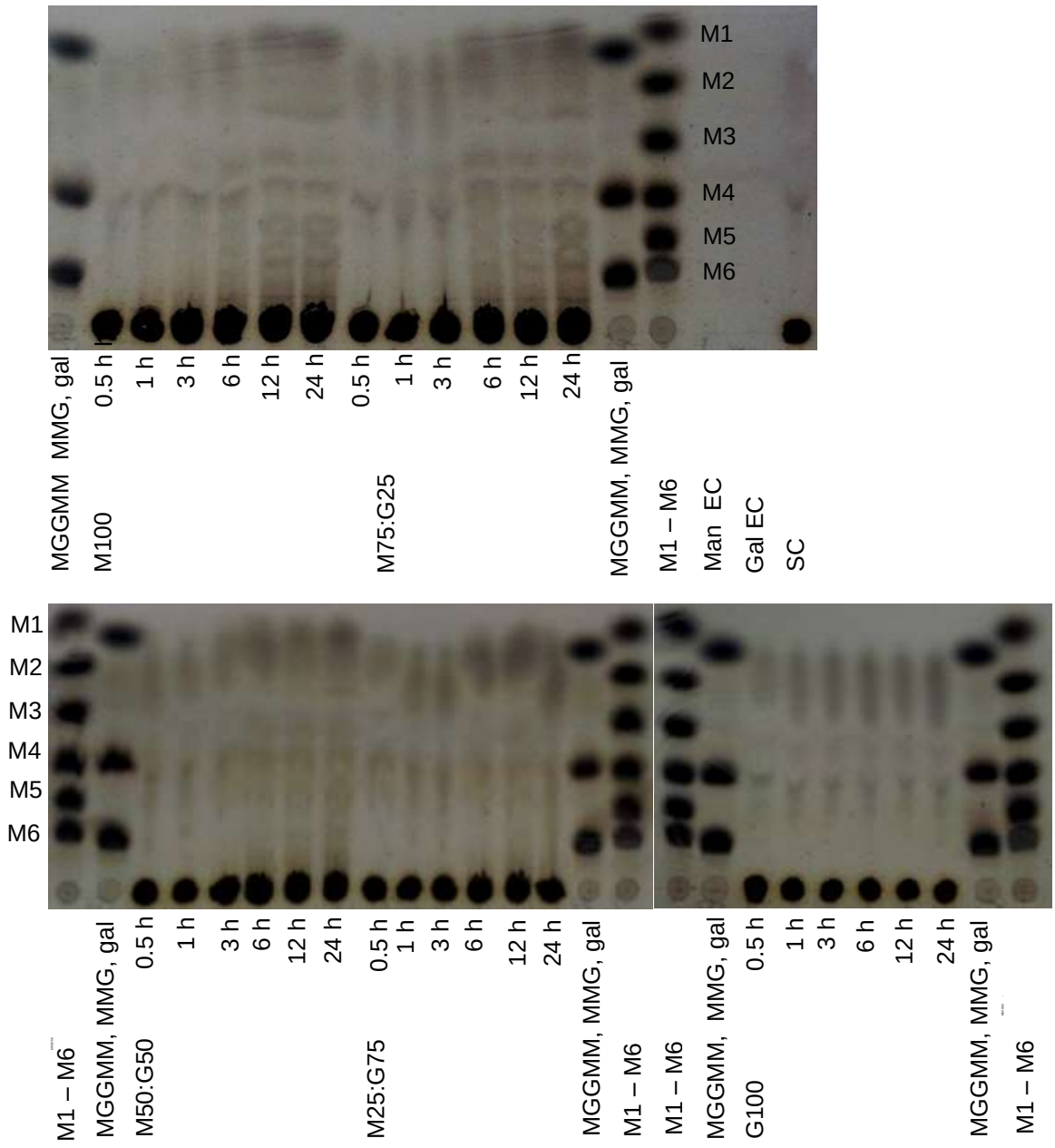

Figure 3.10. Thin layer chromatography of the products formed by hydrolysis of locust bean gum over 24 h by various combinations of the partially purified β-mannanase of *B. paralicheniformis* SVD1 and a commercial GH27 α-galactosidase from *Cyamopsis tetragonolobus* seeds. M1 – M6 = mannose to mannohexose. Gal = galactose. MMG = mannotriose with a galactose substituent on the reducing end. MGGMM = mannopentose with two galactose substituents. Man EC = β-mannanase enzyme control. Gal EC = α-galactosidase enzyme control. SC = substrate control. 0.5 h – 24 h represents the hydrolysis reaction times.

3.5. Discussion

β-mannanase purification from *B. paralicheniformis* SVD1 was attempted in order to characterize the individual activities of the β-mannanases. *B. paralicheniformis* SVD1 was cultured and the cell-free supernatant was concentrated. The concentrate was purified using AEC and SEC. β-mannanase production in the cell-free LBG broth was 0.710 $U.ml^{-1}$. This was low compared to other studies as discussed in chapter 2. Concentration using centrifugal filtration devices was not very successful. β-mannanase was partially retained on the membranes and the activity yields were low. Given that the activity yield was high (∼100%) when 3 kDa cellulose membrane centrifugal filtration devices were used (Chapter 2), β-mannanase was probably partially retained on larger MWCO membranes due to its size and shape. For future studies, concentration should be performed using 3 kDa centrifugal filtration devices. Acetone precipitation was assessed for concentration of the β-mannanase using different methods; various combinations of precipitation time and acetone to protein solution ratio were used. There was a high concentration of background reducing sugars - this seemed to affect β-mannanase binding to the AEC column as the β-mannanase eluted earlier than expected using the NaCl gradient (data not shown). The acetone precipitation protocol may have also been less successful than expected due to β-mannanase denaturation. Acetone precipitation often denatures proteins, which is why ammonium sulfate precipitation is recommended for protein concentration over acetone precipitation when there is a need to retain protein activity (Sheehan, 2009).

Ammonium sulfate precipitation was used as an alternative to acetone precipitation and centrifugal filtration, as this method allows for good separation of protein from carbohydrates. The yield using 85% ammonium sulfate saturation was low. Various other studies that concentrated and purified β-mannanases from *Bacillus* spp. obtained much higher activity yields (Li et al. 2006; Chauhan et al., 2014). Metal ion inhibition may have been one of the causes for the low activity yield in this study. Ammonium sulfate contains small amounts of heavy metal ions that can inhibit enzymes, including β-mannanases (Ghosh et al., 2013). It is recommended that the chelating agent EDTA be added when carrying out ammonium sulfate precipitation to minimize metal ion inhibition (Bollag et al., 1996) However, EDTA can also inhibit β-mannanases as some metal ions such as Ca^{2+} can increase β-mannanase thermostability (Ghosh et al., 2013; Kumagai et al., 2013). Yan et al. (2008) solved the structure of the GH26 β-mannanase of *B. subtilis*. They provided evidence of a metal binding motif, His1-His23-Glu336. that increased protein rigidity once bound to a metal. This motif

was also present in the *B. paralicheniformis* SVD1 GH26 β-mannanase. The GH26 β-mannanase of *B. subtilis* had 80.95% amino acid sequence similarity (Query coverage = 100%) to the *B. paralicheniformis* SVD1 GH26 β-mannanase. A homology model was made using SWISS-MODEL to assess the 3D structure of the *B. paralicheniformis* SVD1 GH26 β-mannanase. The GH26 β-mannanase of *B. subtilis* was used as a template (Data not shown). The predicted structure looked identical to the template, including the metal binding motif (GMQE = 0.95, QMEAN = -0.72), Therefore, EDTA may effect *B. paralicheniformis* SVD1 GH26 β-mannanase thermostability. This should be taken into consideration in future studies.

AEC, using a Toyopearl® DEAE-650M resin, was used to purify the β-mannanase. Activity yield after AEC was between 42%, using 40 mM NaCl for elution, and 77%, using 100 mM NaCl for elution. This activity yield is similar to the 64% yield of β-mannanase activity from *B. licheniformis* NK-27 obtained by Zhang et al. (2000). Use of 40 mM NaCl for elution had lower activity yield but led to a total higher purification fold after concentration of the pooled fractions (88.9 vs. 55.4). The total fold purification of 33.1 achieved by Zhang et al. (2000) was lower than what was achieved in our study, yet they obtained a specific activity of 4341 $U.mg^{-1}$ which was far higher than the highest measured specific activity that was achieved in this study (33.8 $U.mg^{-1}$). The specific activity of the cell-free broth in the study by Zhang et al. (2000) was 3.9 x higher than the specific activity of the partially purified AEC fraction from this study. One reason for the higher activity measured by Zhang et al. (2000) was that the DNS assay that they used to measure β-mannanase activity had a higher reaction temperature and a shorter reaction time (60°C, 10 min) than what was used in this study (50°C, 30 min). They also used the Bradford assay for protein concentration determination, which was found to be less sensitive than the BCA assay (data not shown). A problem with the study by Zhang et al. (2000) was that they did not report the purity of the β-mannanase using a method such as SDS-PAGE, which made it difficult to assess the level of purity that they achieved. Ge et al. (2016) purified β-mannanase from *B. licheniformis* HDYM-04. They confirmed purity by sequencing the excised single band obtained by SDS-PAGE using LC-MS/MS. Their activity yield was also much higher than what was achieved in this study. A problem with comparing the activity determination method used by Ge et al. (2016) and this study is that they did not provide the experimental details of the hydrolysis reaction that was used to measure β-mannanase activity. They did not indicate the substrate used, its concentration as well as the hydrolysis reaction time. Songsiriritthigul et al. (2010) found that

recombinantly expressed and purified GH26 β-mannanase had a specific activity of 1672 $U.mg^{-1}$. Their LBG substrate preparation method was different to the method used in this study. The substrate preparation method used by the other studies that purified β-mannanase was not reported. The difference in substrate preparation methods could have also played a role in the difference in reported β-mannanase activity. There were differences in the growth media and *B. licheniformis* strains used by the different studies. For the final purification step SEC on Sephadex® G-75 resin was used. It was not successful as the activity yield was very low. The use of higher resolution columns and an automated chromatography system would probably improve the fold purification and activity yield of IEC and SEC.

SDS-PAGE was performed to visually assess the success of the purification protocol. Even though high fold purification values were achieved (55.4 - 88.9) for AEC, SDS-PAGE gels revealed multiple protein bands in the partially purified β-mannanase. There was an increase in the relative abundance of a few proteins. One of the bands with a relative MW of 38 kDa corresponded to the locust bean gum and konjac glucomannan zymogram bands at around 40 kDa. Determination of which β-mannanases were present was not possible as their theoretical molecular masses are too similar for SDS-PAGE to resolve (Walker, 2010a). The MW of the β-mannanase was higher than before (Chapter 2), probably because the added PMSF inhibited serine protease activity. In order to identify the β-mannanases, the bands corresponding to the zymogram activity band would need to be excised and identified using a method such as tryptic peptide mapping using LC-MS/MS as done by (Ge et al., 2016). Native PAGE was also performed to assess if there were different isomers or β-mannanases in the partially purified β-mannanase. There were two broad activity bands detected in the native zymogram that corresponded to two abundant bands in the Coomassie Brilliant Blue stained native zymogram. Given that the mannan substrate was incorporated into the gels prior to polymerization, the β-mannanase or β-mannanases in their native states may have bound to the substrate during electrophoresis, leading to the broad activity bands. To avoid potential binding of β-mannanase to mannan, a future study could perform the native PAGE without incorporating the mannan substrate into the gel. The zymogram can be performed using the overlay method where an electrophoresed gel is sandwiched between two glass plates with a gel containing the mannan substrate as described by Van Dyk (2009). If multiple activity bands occur using the overlay method, they could be identified by LC-MS/MS to determine if they are isomers or different β-mannanases (GH5 and GH26).

Overall, the purification protocols used in this study could be improved substantially. The protocols used were tedious, yielded low activity and were not successful in purifying the β-mannanase to electrophoretic homogeneity. A better alternative to the protocols used would be to clone and heterologously express one or both of the β-mannanases. The β-mannanase gene sequences are known (Sakka et al., 2012). A company such as Genscript® could quickly and relatively cheaply construct expression plasmids, which would make the process quicker and easier. Recombinant expression has successfully been used for the production and purification of *B. licheniformis* β-mannanases (Kanjanavas et al., 2009; Songsiriritthigul et al., 2010). One potential problem with recombinant expression is that any post translational modifications that are important for activity or stability would not occur in the recombinant β-mannanase. So the recombinant β-mannanases activity or biochemical properties may differ from that of the native β-mannanase (Cain et al., 2014).

The partially purified β-mannanase of *B.* para*licheniformis* SVD1 was characterized and its synergistic hydrolysis with an α-galactosidase on locust bean gum was determined. The characteristics were similar to the characteristics of the crude enzyme (Chapter 2). The temperature optimum (55°C) was in the range reported for *B. licheniformis* β-mannanases in literature which was between 40°C and 60°C (Zhang et al., 2000; Kanjanavas et al., 2009; Van Dyk, 2009; Ge et al., 2016). The differences could be attributable due to the differences between β-mannanases of the different strains, differences in the purity of the enzyme preparations as well as different assay conditions. Some of the studies hydrolysis assay times were very short (5 – 10 min), so the effect of temperature denaturation would be less than for longer hydrolysis times, such as in this study, probably leading to higher estimated temperature optima. The temperature optimum was also similar to the temperature optimum of the crude, concentrated β-mannanase (Chapter 2). The β-mannanase was thermostable at 50°C. This is advantageous in an industrial setting as high temperatures increase reaction rates, decrease contamination risk, decrease substrate viscosity and increase the solubility of many substrates (Egorova and Antranikian; 2008). The pH optima displayed two peaks at pH 6.0 and pH 9.0, indicating the presence of two mannanases. The crude concentrated mannanase (Chapter 2) also displayed two pH optima peaks (at pH 5.0 and pH 7.0). This β-mannanase, which has its highest activity around a neutral pH, is probably best suited to prebiotic MOS production or biofuel production where neutral pH reaction conditions are used (Yamabhai et al., 2014). It would not be suitable for use in the paper and pulp industry or for use in detergents, where high

pH tolerance is required (Chauhan et al., 2012). Zymogram analysis revealed that the partially purified β-mannanase had a relative MW of 41 kDa, which was expected, based on the theoretical MW of the β-mannanases. Given that there was one zymogram activity band and two pH optima, there could have been two β-mannanases present with similar molecular masses.

Substrate specificity was assessed to determine what other enzyme activities were present. The partially purified β-mannanase displayed a small amount of α-L-arabinofuranosidase activity. This indicated that the β-mannanase fraction contained mostly β-mannanase activity. Activity was highest on soluble, low branched substrates, especially konjac glucomannan, as was found with the crude concentrated β-mannanase (Chapter 2). Given that the β-mannanase was quite pure in terms of glycosyl hydrolase activities present, further purification may not be necessary for most industrial uses as further purification would add to the process costs (Van Dyk & Pletschke, 2012). The required purity would depend on their use. For example, if the industrial product were MOS for human consumption then high purity would most likely be required (Jain et al., 2015). If the β-mannanase were sufficiently purified, it could potentially be used to produce MOS for human consumption. The reduced activity on branched mannan substrates indicates the need for debranching α-galactosidases for efficient hydrolysis. Simultaneous synergy over time between the partially purified β-mannanase and a commercial GH27 α-galactosidase from *Cyamopsis tetragonolobus* was assessed in terms of reducing sugars released and MOS production. The DS increased over time. This follows one type of pattern of synergy over time (Malgas et al., 2017a). Jung et al. (2008) proposed that this pattern of synergy occurs because an enzyme hydrolyzes a substrate component that shields another substrate component from hydrolysis. Over time more of the shielded substrate is exposed, leading to higher synergy. Significant synergy (p-value < 0.05) occurred with the M75G25 combination after 6 h and the M50G50 combination after 24 h. The increased synergy was possibly due to the α-galactosidase removing galactose residues, which exposed more of the mannan backbone for hydrolysis (Malgas et al., 2015[b]). Von Freiesleben et al. (2016) reported that various β-mannanases reached less than half of the maximum degree of hydrolysis of locust bean gum and guar gum due to galactose branching that decreased mannan accessibility. This shows the importance of α-galactosidases, not only for maximal monosaccharide release, but also for maximal oligosaccharide production.

The synergistic increase in reducing sugar release was between 1.28 fold (M75G25) and 1.39 fold (M50G50). Various studies have observed synergy between β-mannanases and α-galactosidases on galactomannan substrates (Malgas et al., 2015[b]). Malgas (2015[c]) found that simultaneous synergy between *Clostridium cellulovorans* GH5 Man5A and GH27 α-galactosidase from *Cyamopsis tetragonolobus* seeds (same α-galactosidase used in this study) increased reducing sugar release 1.59 fold when used in a M75G25 ratio. Synergy between *Aspergillus niger* GH26 Man26A and GH27 α-galactosidase from *C. tetragonolobus* seeds increased reducing sugar release 1.14 fold when used in a M75G25 ratio. Malgas (2015) found that the increase in hydrolysis was mostly due to the α-galactosidase removing galactose residues that would have sterically hindered mannan hydrolysis. To determine if this was true for this study, galactose release could be measured using monosaccharide assay kits or HPLC. The study by Malgas (2015) is not directly comparable to this study as the hydrolysis conditions were different and all the proteins used in their study were pure. The benefit of assessing synergy over time was indicated by the results; synergy is dependent on assay time. The DS tended to increase over the 24 h assay period. To further develop these synergy studies, sequential vs. simultaneous synergy could also be assessed. An in-depth study of β-mannanase characteristics, such as active site mannan accommodation would provide a better understanding of the hydrolysis profile (von Freiesleben et al., 2016), which could aid in the choice of reaction conditions and enzymes for optimal synergy. However, this would require a pure β-mannanase.If purified β-mannanase was obtained, β-mannanase synergy with β-mannanases from other GH families could also be assessed. Couturier et al. (2013) found that the activity of *Podospora anserina* GH5 and GH26 mannanases are complementary; therefore they probably synergistically hydrolyze mannan.

TLC results of the synergy between the partially purified *B. paralicheniformis* SVD1 β-mannanase and the α-galactosidase of *C. tetragonolobus* seeds agree with the hydrolysis assay where the amount reducing sugars released was measured. The M50G50 TLC results were an exception; the activity was lower than expected. The M75G25 combination showed synergistic production of MOS. Further studies could quantitatively assess MOS production, using a method such as HPLC, to get a better understanding of the synergistic interaction. Also longer TLC plates would allow for better resolution of oligosaccharides with a DP above 6. For this study a GH27 α-galactosidase was selected, as Malgas et al. (2015[c]) found that a GH27 α-galactosidase displayed better synergy with β-mannanases

(than a GH36 α-galactosidase) on galactomannan. However, it is not enough to simply choose complementary GH families as discussed in Section 1.3.2.4. Different α-galactosidases could be assessed for synergy and *in silico* analysis of their structure-function relationship could help explain synergy. Literature studies clearly show the importance of in-depth biochemical characterization, including structural analysis, for understanding the phenomena of synergy. These characterization studies could lead to a better understanding of enzyme synergy and consequently more efficient industrial utilization of lignocellulose degrading enzymes.

3.6. Conclusion

In general, the purification procedure was not very successful as the β-mannanase activity was only partially purified. The best concentration procedure employed 85% ammonium sulfate precipitation, although the activity yield obtained was only 20.0%. AEC was the most successful purification step employed as it provided good activity yields and fold purification, comparable to other studies that purified β-mannanases from *B. licheniformis*. SEC was not successful as the yields were low. The optimized purification procedure only partially purified the β-mannanase and omitted the SEC step. The partially purified β-mannanase was found to be ~40 kDa in size, as expected, using zymography. Native PAGE indicated the presence of two or more different isoforms or β-mannanases. However, further studies would need to be performed to determine if one or more β-mannanases were present. The biochemical characteristics of the partially purified β-mannanase were similar to the crude β-mannanase (Chapter 2) and various *B. licheniformis* β-mannanases. Differences observed were probably due to the use of different strains and assays. The differences between the crude concentrated β-mannanase and the partially purified β-mannanase may have also been due to proteolytic hydrolysis of the crude concentrated β-mannanase, as could be seen with zymography analysis. The β-mannanase displayed synergy with the GH27 α-galactosidase of *C. tetragonolobus* seeds. The DS depended not only on the ratio of β-mannanase to α-galactosidase, but also on time. TLC analysis showed that the synergistic improvement in reducing sugar release also increased small DP MOS production. This initial characterization study can be used as a basis for further studies. The results from this study were subsequently used to assess the synergistic hydrolysis of SCG, an abundant industrial waste product. This is discussed in the following chapter; Chapter 4.

Chapter 4 – Synergism between partially purified *Bacillus paralicheniformis* SVD1 β-mannanase and CTec2 for the hydrolysis of spent coffee grounds

4.1. Introduction

Coffee is the most traded commodity after petroleum; over 8 million tons were produced and consumed worldwide between October 2015 and September 2016 (Murthy & Naidu, 2012, International Coffee Organization (ICO; www.ico.org)). A major by-product of coffee production is SCG, which are the solids that remain after hot water extraction of solubles from coffee beans (Mussatto et al., 2011). Around 65% (w/w) of coffee beans are unextractable and remain as SCG after processing (Murthy & Naidu, 2012). SCG has various uses such as compost for growing edible mushrooms. However, there are many higher value potential uses that are being explored such as use for biofuel and prebiotic oligosaccharide production due to its high polysaccharide and lipid content (Murthy & Naidu, 2012). Dried SCG consists of around 45.3% (w/w) polysaccharides, 13.6% (w/w) protein, 9.3% - 15.4% (w/w) lipids, 1.5% - 19% (w/w) polyphenolics, 16% melanoidins as well other components such as amino acids and minerals (Campos-Vega et al., 2015). The dominant polysaccharides are mannan, cellulose and arabinogalactan. Coffee mannan has a low degree of α-1,6-linked D-galactose substitution and also has some arabinose and acetyl groups (Simões et al., 2013). The composition varies substantially depending on factors such as growing conditions, coffee roasting conditions and the extraction process (Mussatto et al., 2011; Campos-Vega et al., 2015).

The polysaccharides can be hydrolyzed via thermal, chemical or enzymatic routes. The use of enzymes has the advantage of the absence of production of undesirable side products (Aachary & Prapulla, 2011). There have been studies on the use of enzymes to produce monosaccharides - for biofuel production and prebiotic oligosaccharides from SCG (Kwon et al., 2013; Chiyanzu et al., 2014). There have also been studies on the use of enzymes to hydrolyze SCG to increase the soluble solids yield of instant coffee (Jooste et al., 2013; Chiyanzu et al., 2015). The Japanese company Aginomoto Co. Inc. produces MOS derived from coffee mannan that is commercially used as a prebiotic food additive.

Lignocellulosic biomass is recalcitrant to enzymatic hydrolysis and usually requires pretreatment to remove or modify lignin that inhibits hydrolytic enzyme activity as well as to open up the lignocellulose structure (Chundawat et al., 2011). The SCG were pretreated in order to improve enzymatic hydrolysis. NaOH pretreatment was selected because it has been shown to be an effective pretreatment method that does not solubilize most of the hemicelluloses (Sills & Gossett, 2011; Chen et al., 2013). This is important for SCG pretreatment, as a large portion of the polysaccharides are hemicelluloses. NaOH pretreatment decreases cellulose crystallinity, DP and causes biomass swelling (Agbor et al., 2011). It also improves hydrolysis by solubilisation or modification of lignin. NaOH hydrolyzes ester bonds between lignin and carbohydrates (Grohmann et al., 1989; Alvira et al., 2010). These effects increase the available holocellulose surface area for enzymatic hydrolysis. The effects largely depend on the process conditions such as concentration, temperature, time, pressure and biomass properties (Zhao et al., 2008; Chen et al., 2013). The process used in this study was a high concentration, low pressure and mild temperature method. Under these conditions improved hydrolysis is mostly due to opening up of the cellulose structure (Gümüşkaya & Usta, 2006; Zhao et al., 2008). Unconsumed NaOH can be recycled under these conditions, which decreases the cost of pretreatment (Sills & Gossett, 2011). The aim of this study was to assess the synergistic hydrolysis of untreated and NaOH pretreated SCG by *B. paralicheniformis* SVD1 β-mannanase and the commercial cellulase preparation Cellic® CTec2 (Novozymes). The synergistic interactions between these enzymes on SCG have not been assessed. These enzymes could potentially be used to produce industrially useful monosaccharides and oligosaccharides.

4.2. Objectives

- To pretreat spent coffee grounds.
- To characterize the untreated and pretreated SCG in order to assess which factors may affect hydrolysis and which holocellulases are most important for SCG hydrolysis.
- To assess synergy between the partially purified *B. paralicheniformis* SVD1 β-mannanase and a commercial cellulase preparation Cellic CTec2 (Novozymes) on SCG.

4.3. Materials and Methods

4.3.1. Pretreatment of spent coffee grounds

SCG were supplied by National Brands Limited (Isando, South Africa). The SCG was pressed to remove water. The resulting cake (45% dry matter) was dried at 43°C for 48 h – 120 h until there was no change in mass and was then stored in air-tight containers. Dried SCG was ground with a pestle and mortar and then passed through a 0.5 mm mesh, the SCG particles that passed through the 0.5 mm mesh were used for further studies. For NaOH pretreatment, 1.25 g NaOH was added to 5 g of SCG in 100 ml of diH_2O. This solution was then placed in an oven at 70°C for 4 h; the solution was stirred occasionally. The SCG was then filtered with a cheese cloth and washed with 3 l of 70°C diH_2O to neutralize the pH; this was confirmed with pH test strips. These mild pH and temperature conditions were chosen in order to minimize hemicellulose loss, particularly mannan that is abundant in the SCG. The pretreated SCG was air dried in a sealed fumehood with an exhaust fan until there was no change in mass. For the untreated sample, 5 g of SCG was washed with 3 l of room temperature diH_2O - the wash pH was checked with pH test strips to make sure the pH was equal to the pH of diH_2O. The untreated SCG sample was then dried in the same way as the NaOH pretreated SCG sample.

4.3.2. Spent coffee grounds characterization

4.3.2.1. Scanning electron microscopy

To assess the effect of NaOH pretreatment on SCG morphology, scanning electron microscopy (SEM) was conducted. Prior to SEM analysis, the untreated and NaOH pretreated SCG samples were placed on metal stubs, dried using a critical point-drying process and then coated with a thin layer of gold prior to SEM analysis (Cross, 2001).

4.3.2.2. Composition

The untreated and NaOH pretreated SCG were characterized using a modified sulphuric acid method (Sluiter et al., 2010; National Renewable Energy Laboratory-NREL). Samples of untreated and NaOH pretreated SCG (300 mg) were placed in glass test tubes and hydrolyzed by the addition of 3 ml of 72% (v/v) sulphuric acid. The samples were incubated at 30°C for 1 h with frequent mixing using glass rods. The samples were then transferred into Schott bottles and the concentration of sulphuric acid was diluted to 3% (v/v) by adding

74 ml of diH_2O. To complete hydrolysis, the samples were autoclaved for 1 h. The samples were then filtered to remove the acid insoluble fraction from the sugar solution. The insoluble fraction was dried in an oven at 50°C until there was no change in mass. It was then weighed to determine the insoluble content. A portion of the acid soluble fraction was neutralized with $CaCO_3$ prior to sugar and phenolic determination. The soluble phenolics present in the soluble hydrolyzate was determined using a modified Folin-Ciocalteu method for phenolics (Folin & Ciocalteau, 1927). Soluble hydrolyzate (190 µl) was mixed with 20 µl Folin reagent in eppendorf tubes. These were left to stand at room temperature for 1 min before the addition of 50 µl of 2 M Na_2CO_3. The tubes were covered with tinfoil and incubated at 40°C in an AccuBlock digital dry bath heater (Labnet) for 30 min. The solutions were placed in a 96-well microtitre plate and the absorbance at 765 nm was then read using a Powerwave X microplate reader (BioTek Instruments) and KC Junior software. The soluble phenolic concentration was determined using a gallic acid standard curve (Appendix 4 - Figure A.9). The content of glucose, mannose, galactose and arabinose was determined using Megazyme sugar kits. The D-Mannose/D-Fructose/D-Glucose Assay kit and L-Arabinose/D-Galactose Assay Kit were used according to the supplier's instructions. Reducing sugar content was determined using the DNS method as described in Section 2.3.4.2. Measurements were performed in duplicate.

4.3.3. Synergy between β-mannanase and CTec2 on untreated and NaOH pretreated spent coffee grounds

The hydrolysis of SCG by the partially purified *B. paralicheniformis* SVD1 β-mannanase (Chapter 3) alone, and in combination with the commercial cellulase preparation Cellic® CTec2 (Novozymes), was assessed using the DNS assay for reducing sugar determination as described in section 2.3.4.2. The hydrolysis by a pure GH26 β-mannanase from *Bacillus* sp. (Megazyme) was used as an additional positive control. The specific activity of the positive control β-mannanase on locust bean gum was determined as in Section 3.3.8. Protein concentration was determined using the BCA assay (Section 3.3.8.). The hydrolysis reaction conditions used were based on a study by Chiyanzu et al. (2014). Dried SCG (untreated and NaOH pretreated) were ground with a mortar and pestle, and then passed through a 0.5 mm mesh to reduce particle size. The substrates were pre-wetted for 5 h at 50°C, 150 rpm, using pH 7.0 potassium phosphate buffer containing 0.02% (w/v) NaN_3.

SCG, at a final concentration of 4% (w/v), was hydrolyzed by incubation with enzyme (5 mg protein / g SCG) at 50°C, 150 rpm for 48 h. Bovine serum albumin was added to a final concentration of 0.5 mg/ml in the reaction mixture to minimize non-productive adsorption of the enzymes to the SCG. The reactions were terminated by boiling for 5 min, followed by centrifugation at 16 060 *x g* for 5 min to pellet insoluble SCG. The supernatant was assessed for reducing sugars using the DNS assay. The enzymes were added alone or in binary combinations with CTec2. The DS was calculated by dividing the actual activity of the combination of enzymes by the theoretical sum of the individual enzyme activities (Van Dyk and Pletschke, 2012). The assays were performed in duplicate. The assays were performed in duplicate. One way analysis of variance (ANOVA), using the Data analysis feature in Microsoft Excel 2010, was used to compare the activity of the different enzyme combinations. The enzyme combinations were assessed for significant ($p < 0.05$) differences in reducing sugar release compared to that released by 100% Cellic® CTec2.

4.4. Results

4.4.1. Pretreatment of spent coffee grounds

The SCG were NaOH pretreated in an attempt to improve enzymatic hydrolysis by increasing polysaccharide accessibility and removing some lignin as well as breaking the lignin - carbohydrate bonds. The dried samples showed a difference in colour and shape (Figure 4.1). The untreated SCG was brown and the NaOH pretreated SCG was dark brown and contained flake shaped granules. The NaOH pretreated SCG was more coarse than the untreated SCG. It was noted that the wash of the untreated SCG was clear. The wash after NaOH pretreatment was very dark and formed an upper layer above a clearer layer. The upper layer may have contained extracted lipids as well as solubilized phenolics and brown colored compounds. The mass of the samples after pretreatment and drying were 4.537 g (untreated) and 3.489 g (NaOH pretreated). The untreated SCG experienced a small loss of mass after washing and drying (9.26 % (w/w)); this was probably mostly due to the very fine SCG that passed through the cheese cloth during washing. The relatively large decrease in mass of the NaOH pretreated SCG (30 % (w/w)) was expected as alkaline pretreatments solubilize lignin.

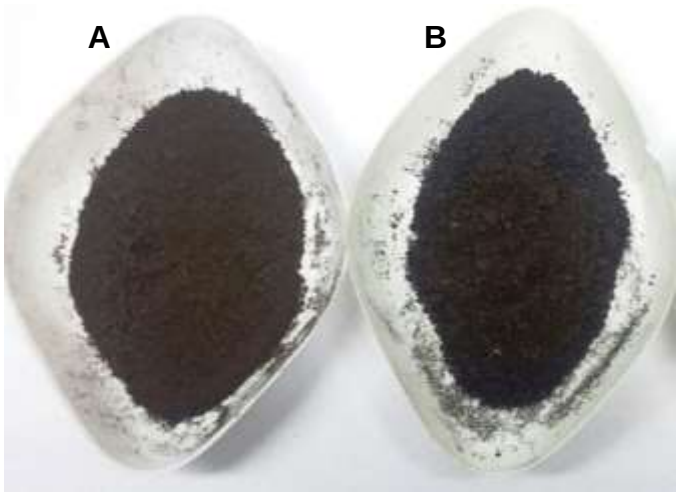

Figure 4.1. Observable differences between: (A) untreated spent coffee grounds (SCG) and (B) NaOH pretreated SCG.

4.4.2. Spent coffee grounds characterization

4.4.2.1. Scanning electron microscopy

The surface morphology of untreated SCG and NaOH pretreated SCG was assessed using SEM to assist in the understanding of morphological factors that may affect enzymatic hydrolysis (Figure 4.2). Most of the NaOH pretreated SCG particles displayed a more rough and porous surface than the untreated SCG particles. NaOH is known to cause biomass swelling. The swelling increases available surface area, which increases enzymatic hydrolysis efficiency.

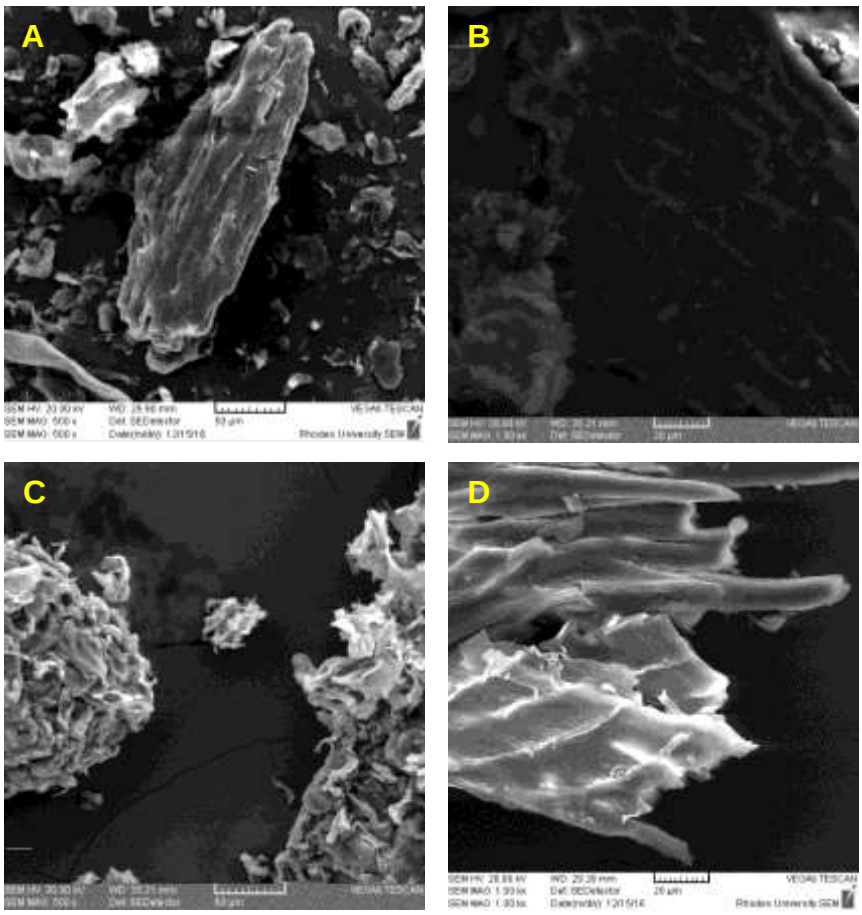

Figure 4.2. SEM images of untreated and pretreated spent coffee grounds. (A): Untreated SCG at a magnification of 50 x. (B): Untreated SCG at a magnification of 1000 x. (C): NaOH pretreated SCG at a magnification of 50 x. (D): NaOH pretreated SCG at a magnification of 1000 x.

4.4.2.2. Composition

The sugar, insolubles and soluble phenolic percentage composition of untreated and pretreated SCG was determined (Table 4.1). The main sugars were mannose and glucose and the sugar content increased after NaOH pretreatment. The percentage composition of glucose and mannose were the same in the untreated SCG (16.1%). The glucose percentage composition (20.4%) was higher than the mannose percentage composition (18.5%) in the NaOH pretreated SCG. This means that more mannose was lost during NaOH pretreatment than glucose. The more crystalline and recalcitrant nature of cellulose, compared to mannan, is probably the cause for less glucose being lost. The percentage composition of soluble phenolics also increased. The NaOH pretreated SCG contained less

insolubles compared to the untreated SCG; this was expected as NaOH solubilizes insoluble lignin, which is removed after the washing step of NaOH pretreatment.

Table 4.1. Untreated and pretreated spent coffee grounds chemical composition. Values are represented as mean values ± standard deviations, n = 2.

	Untreated SCG (%)	NaOH pretreated SCG (%)
Total reducing sugars[a]	47.3 ± 0.6	53.7 ± 0.3
Glucose[b]	16.1 ± 0.9	20.4 ± 0.5
Mannose[b]	16.1 ± 1.6	18.5 ± 1.2
Galactose / Arabinose[b]	0.324 ± 0.017	0.341 ± 0.008
Soluble phenolics[c]	0.461 ± 0.007	0.487 ± 0.033
Insolubles[d]	64	52.7
Total mass accounted for	97	92

[a-] DNS method, [b-] Megazyme sugar kits, [c-] Folin-Ciocalteu method ,[D-] Weighing balance

4.4.3. Synergy between the β-mannanases and CTec2 on untreated and NaOH pretreated spent coffee grounds

The ability of the partially purified *B. paralicheniformis* SVD1 mannanase to hydrolyze SCG alone and in synergy with the commercial cellulase preparation Cellic CTec2® (Novozymes) was assessed (Figure 4.3). This was performed to assess their ability to hydrolyze this waste substrate, which could be exploited commercially. A cellulase mixture was selected as cellulose was one of the most abundant polymers in the SCG (Table 4.1). The partially purifed *B. paralicheniformis* SVD1 β-mannanase had detectable but not quantifiable activity on NaOH pretreated SCG under the assay conditions used. The partially purifed *B. paralicheniformis* SVD1 β-mannanase had not detectable activity on un-treated SCG under the assay conditions used. CTec2 alone displayed the highest activity - about 40% (untreated SCG) and 36% (NaOH pretreated SCG) of the total reducing sugars in the substrate (Table 4.1) were released. Even though hydrolysis by the combinations was lower than hydrolysis by the cellulase cocktail alone, there was synergy (in terms of DS) between

some of the enzyme combinations. The DS was above 1.0 for all of the combinations on NaOH pretreated SCG. The highest DS (2.12) occured with the M75C25 combination on NaOH pretreated SCG. The DS on untreated SCG was above 1.0 for the M75C25 combination, but below 1.0 for the other combinations, indicating competition for hydrolysis sites. This could be due to β-mannanase activity present in CTec2, the competition was reduced at lower CTec2 loadings. The higher synergy on NaOH pretreated SCG may have been due to greater enzyme accessibility on NaOH pretreated SCG, which would decrease competition. The synergy increased with an increase in the protein loading of partially purified β-mannanase. Mannan hydrolysis may have improved cellulase activity by removing mannan that encapsulated cellulose and cellulose hydrolysis may have exposed more mannan, leading to increased mannan hydrolysis. Quantification of the monosaccharides released would be required to better understand the synergy.

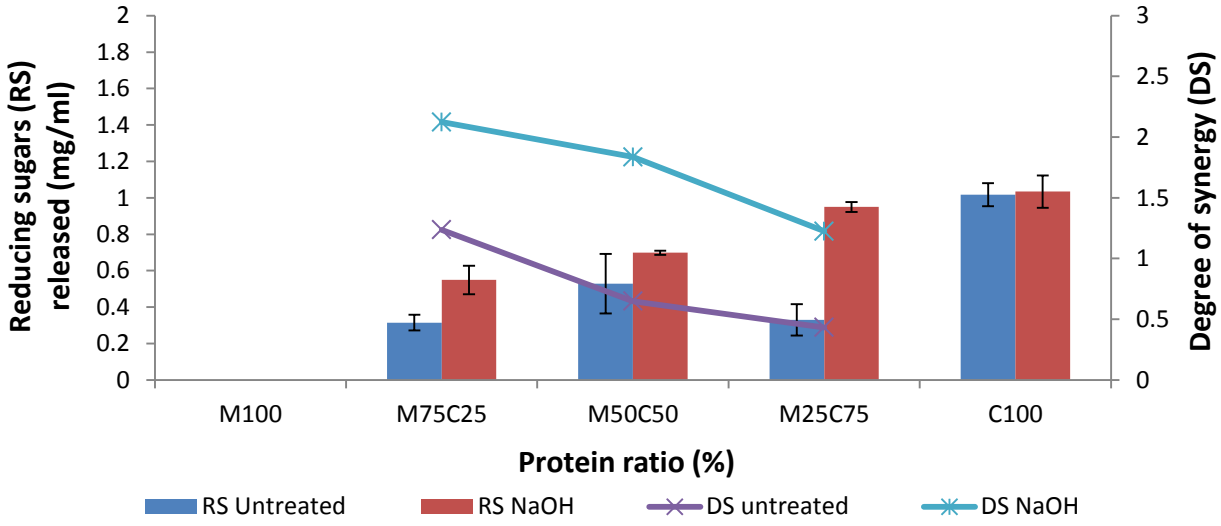

Figure 4.3. Reducing sugars released by and degree of synergy between various combinations of partially purified *B. paralicheniformis* SVD1 β- mannanase and a commercial cellulase preparation Cellic® CTec2 (Novozymes) obtained on 4% (w/v) spent coffee grounds by various combinations of the enzymes. The protein load was 5 mg protein.g^{-1} SCG. Values are represented as mean values ± standard deviations, n = 2.

As a positive control, the activity of a pure GH26 β-mannanase, that was purchased from Megazyme, on SCG, was determined. Its synergy with CTec2 was also assessed (Figure 4.4). CTec2 alone displayed the highest activity; the purchased β-mannanase had

quantifiable activity that was highest on the pretreated SCG. The DS was above 1 for all of the combinations. The highest DS (1.78) occured with the M75C25 combination on NaOH pretreated SCG. The reducing sugar yield for the enzyme combinations was higher than for CTec2 alone except for the M75C25 and M50C50 combinations on untreated SCG. The highest reducing sugar (RS) release (1.56 mg/ml) occurred using the M25C75 combination on NaOH pretreated SCG. About 54% of the total reducing sugars in the substrate (Table 4.1) was released. SEM images of the substrate after hydrolysis using this enzyme combination were taken but the effect of hydrolysis on the SCG surface morphology could not be seen (data not shown). The only enzyme combination that showed a significant (p-value < 0.05) improvement in hydrolysis was the M25C75 combination on untreated SCG. The other combinations that increased RS release possibly did not have a significant improvement due to the high variabililty of the measurements and the low number of replicates (n = 2). The wide range of particle sizes, as seen in the SEM images (Figure 4.1) may have contributed to this. Overall, the NaOH pretreatment improved synergy and reducing sugar yield for both β-mannanases alone and most of the enzyme combinations. This was not the case for CTec2 alone. The control purified GH26 β-mannanase performed better than the partially purified *B. paralicheniformis* SVD1 β-mannanase. This was probably due to the difference in specific activity. The partially purified *B. paralicheniformis* SVD1 β-mannanase displayed 17.44 $U.mg^{-1}$ on LBG using the standard assay (Chapter 3) - the control purified GH26 mannanase had 2.5 x higher specific activity on LBG (43.4 $U.mg^{-1}$).

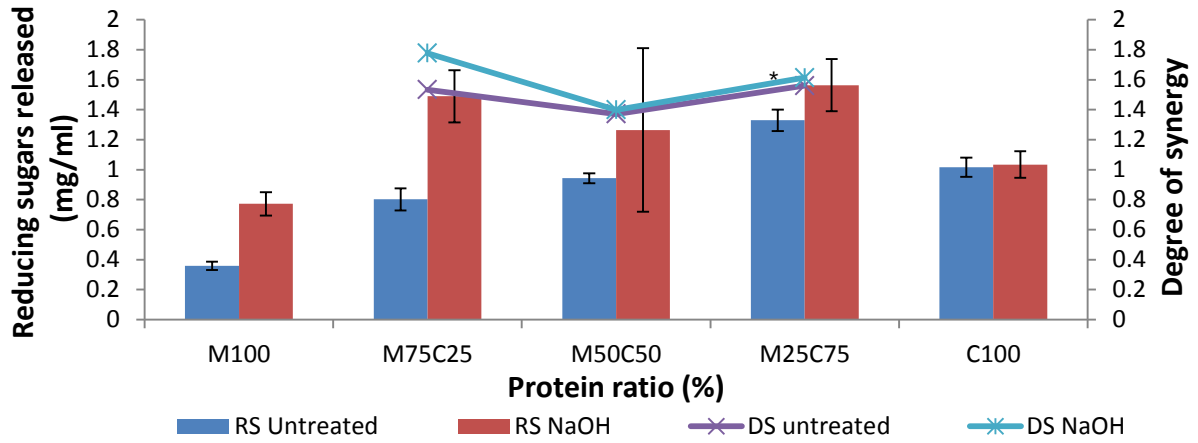

Figure 4.4. Reducing sugars released by and degree of synergy between various combinations of *Bacillus* sp. GH26 β-mannanase and a commercial cellulase preparation Cellic® CTec2 (Novozymes) obtained on 4% (w/v) spent coffee ground (SCG) by various combinations of the enzymes. The protein load was 5 mg protein.g^{-1} SCG. ANOVA was used to assess synergistic improvement of hydrolysis with respect to reducing sugar release by the enzyme combinations compared to 100% β-mannanase protein loading. key: * (p-value < 0.05). Values are represented as mean values ± standard deviations, n = 2.

4.5. Discussion

The SCG were pretreated in order to improve enzymatic hydrolysis. The 30% (w/w) decrease in mass of the SCG after NaOH pretreatment was probably mostly due to removal of acid insoluble phenolics and lipids that are abundant in SCG (Campos-Vega et al., 2015). Lipids constitute 16.7% - 17.2% (w/w) of SCG (Grohmann et al., 1989; Vicente et al., 2004; Campos-Vega et al., 2015). The separated lipids could be used for biodiesel production, which would improve the process economics for the production of value-added products. However, the pretreatment process would need to be altered to minimize soap formation (Vicente et al., 2004). NaOH pretreatment resulted in the swelling of the SCG particles and increased porosity, which was expected (Goshadrou et al., 2011). The NaOH pretreatment also decreased the insoluble solids percentage composition by 11.3%. This would be beneficial to enzymatic sugar release as lignin inhibits holocellulolytic enzyme activity (Duarte et al., 2012). Cellulose in the SCG experienced the lowest percentage loss as it was the most crystalline. Mannan can also have a crystalline structure, which is probably why

less was removed than arabinose/galactose (Van Zyl et al., 2010). Oosterveld et al. (2003) found that cellulose in roasted coffee is less heat and NaOH extractable than mannan in roasted coffee. The arabinose/galactose in the SCG would have occurred as part of arabinogalactan as well as galactomannan. Most of the arabinogalactan would have been lost during the production of the instant coffee, as roasting and hot water extraction solubilizes a large part of the arabinogalactan (Van Zyl et al., 2010). Branching on the mannan in the SCG would be reduced by NaOH pretreatment (Agbor et al., 2011); this would aid β-mannanase hydrolysis by improving accessibility. The *B. lichenifomis* SVD1 β-mannanase activity was shown to be inhibited by galactose substituents (Chapter 2 and Chapter 3). The most abundant sugars in the SCG were mannose and glucose, these are often the most abundant sugars in SCG (Mussatto et al., 2011). The content of glucose and mannose in the untreated SCG was 16.1% (w/w) each. This is similar to that content found by Chiyanzu et al. (2014) - their study sourced SCG from the same company we used and reported that the SCG glucan content was 24.17% (w/w) and its mannan content 24.67% (w/v). Another study that sourced SCG from the same company we used reported that the glucose content was higher than the mannose content (Jooste et al., 2013). The composition of SCG varies substantially depending on factors such as the coffee bean variety and extraction conditions (Mussatto et al., 2011; Campos-Vega et al., 2015).

Synergy between the partially purified *B. paralicheniformis* SVD1 β-mannanase and the commercial cellulase preparation Cellic® CTec2 was assessed on SCG. The control β-mannanase displayed higher activity (due to a higher specific activity) on SCG than the *B. paralicheniformis* SVD1 β-mannanase. Using an enzyme loading based on activity, as opposed to protein mass, may have been a better basis for comparison. However, the *B. paralicheniformis* SVD1 β-mannanase did not show quantifiable activity. Improvement of the purification procedure, as discussed in Chapter 3, would increase the specific activity and consequently improve SCG hydrolysis. Enzyme-substrate binding studies, including the evalutation of surfactants to decrease non-productive lignin binding, and alternative pretreatment methods could also be evaluted for the improvement of SCG hydrolysis (Agbor et al., 2011; Van Dyk & Pletschke, 2012; Donohoe & Resch, 2015). Previous studies reported no synergy between β-mannanases and cellulases on SCG in terms of an increase in soluble solids (Jooste et al., 2013; Chiyanzu et al., 2015) and MOS production (Chiyanzu et al., 2014). Jooste et al. (2013) found an additive effect in soluble solids yield between β-

mannanase and pectinase, as well as between β-mannanase and xylanase. Contrary to the findings of Jooste et al. (2013) and Chiyanzu et al. (2015), synergy between β-mannanases and cellulases was found. However, only the control β-mannanase, a pure *Bacillus* sp. GH26 mannanase, showed synergy and increased reducing sugar yield when used in combination with CTec2 (M75C25 and M25C75). The only combination that showed a statistically significant increase in reducing sugar release (p-value < 0.05) was the M25C75 combination on untreated SCG. The lack of significant increase with the other combinations that showed an increase in reducing sugars was possibly due to the low number of replicates ($n = 2$) and the high variablility of the measurements which was most likely caused by the wide range of SCG particle sizes. The SCG particle size could be decreased and made more uniform in size by better grinding and filtering. The SCG pretreatment did not affect cellulase hydrolysis on its own - this may have been because the pretreatment did not affect the SCG structure in such a way that cellulose hydrolysis was improved. Another reason for this observation may be that cellobiose could have accumulated. This would have inhibited cellobiohydrolases in the CTec2 cellulase cocktail (Bhattacharya et al., 2015). CTec2 is a *Trichoderma reesei* celllulase preparation. The problem with the use of *Trichoderma* species for cellulase production is that they have a low level of β-glucosidase activity (Nieves et al., 1998). A β-glucosidase could have been added to prevent product inhibition (Malgas, 2015).

In coffee beans, arabinogalactan is one of the main polysaccharide components. All or some of this arabinogalactan is covalently bound to protein forming arabinogalactan-protein (AGP) (Redgwell et al., 2002; Sutherland et al., 2004; Redgwell and Fischer, 2006; Campos-Vega et al., 2015). A immuno-histochemical study of green coffee bean cell walls showed that arabinogalactan proteins are distributed throughout the cell wall (Sutherland et al., 2004; Kasai et al., 2006). Although roasting and hot water extraction during instant coffee production removes most of the arabinogalactan (Oosterveld et al., 2003; Jooste et al., 2013), some of the AGP may remain in the SCG. SCG consists of around 13.6% (w/w) protein (Campos-Vega et al., 2015), some which may be covalently bound to polysaccharides during the coffee bean roasting process (Nunes & Coimbra, 2001). Proteases could be used to hydrolyze these proteins in SCG, which could open up the substrate and consequently improve holocellulose hydrolysis. Histochemical studies would be useful to assess the distribution of protein and AGP in untreated and pretreated SCG.

There is an AGP-specific monoclonal antibody (LM2) and a reagent that specifically detects AGP, the Yariv reagent (Yariv et al., 1962; Smallwood et al., 1996; Sutherland et al., 2004).

4.6. Conclusion

The results showed that NaOH pretreatment improved β-mannanase hydrolysis of SCG by increasing substrate accessibility. The partially purified *B. paralicheniformis* SVD1 β-mannanase displayed synergy with CTec2, in terms of DS, on NaOH pretreated SCG. On untreated SCG only the M75C25 combination showed synergy. NaOH pretreatment increased DS and reducing sugar (RS) release. The control purified β-mannanase displayed synergy on untreated and NaOH pretreated SCG in terms of DS and increased RS yield. However, the highest DS reached was not as high as that DS obtained when using the partially purified *B. paralicheniformis* SVD1 β-mannanase. Only the M25C75 combination on untreated SCG showed a significant improvement in RS release. The lack of significant improvement in hydrolysis by the other combinations was possibly due to the high variation in the measured RS release, variation in SCG particle size and the small sample size used. This study, which was only an initial study to assess hydrolysis, is the first report to show β-mannanase and cellulase synergy on SCG. The next chapter (Chapter 5) provides a general discussion about the work conducted in this study, as well as recommendations for follow-up studies.

Chapter 5 – General discussion and future recommendations

5.1. General discussion

β-mannanases have potential industrial applications in the hydrolysis of mannan in lignocellulosic biomass. They can be used for the production of prebiotic MOS and biofuels. In the hemicellulose of softwoods, mannans are the major component (Moreira & Filho, 2008). They are also abundant in the endosperm walls of seeds such as coffee bean and locust bean, as well as in the vacuoles of vegetative tissues of various plants (Yamabhai et al., 2014). LBG and konjac are cultivated for use as gelling agents in the food industry; they are readily available and relatively cheap (Van Zyl et al., 2010; Chauhan et al., 2012). LBG was used as the standard substrate in this study for biochemical characterization due to it being readily available and relatively cheap. For optimal hydrolysis, as well as synergy of β-mannanases with other enzymes, it is important to know the biochemical characteristics of the enzymes in order to choose compatible enzymes and suitable hydrolysis conditions. In this study, the β-mannanase activity of *B. paralicheniformis* SVD1 was biochemically characterized in order to assess its potential industrial uses. The β-mannanases of *B. paralicheniformis* SVD1 have not been fully biochemically characterized.

All but one of the objectives of this study were achieved. Purification of the β-mannanase/s was not attained as β-mannanase activity was only partially purified. β-mannanase production by *B. paralicheniformis* SVD1 was successfully induced using LBG broth. The specific activity of the β-mannanase, concentrated with a 3 kDa centrifugal filtration device, was 8.00 $U.mg^{-1}$. This was 39.6 x higher than the β-mannanase specific activity reported by Van Dyk (2009) when *B. paralicheniformis* SVD1 β-mannanase activity was concentrated, using a 10 kDa membrane filtration device, from a LBG broth culture. This difference may be due to variations in growth conditions, as well as the difference in LBG concentration used for the hydrolysis assay (0.25% (w/v) vs. 0.5% (w/v)). Van Dyk (2009) detected protease activity in the broth, protease activity was also detected in this study. Zymogram analysis, at pH 5.0, revealed that the crude concentrated β-mannanase consisted of two β-mannanases with relative MWs of 29.6 kDa and 33 kDa, respectively. Van Dyk (2009) found, using zymography, three different β-mannanases in a birchwood xylan culture. The theoretical molecular masses, based on gene sequences (Sakka et al., 2012) of the *B. paralicheniformis* SVD1 β-mannanases, were 42.1 kDa for the GH5 β-mannanase and 37.9 kDa for the GH26 β-mannanase. The detected protease activity could explain the smaller

than expected MWs of the β-mannanase-active bands. The zymogram (at pH 7.0) of the partially purified β-mannanase in this study showed a β-mannanase-active band with a MWs of 40-41 kDa. A serine protease inhibitor, PMSF, was added during the purification. This indicated that the β-mannanase/s in the crude concentrate were hydrolyzed by serine protease activity of *B. paralicheniformis* SVD1. Ferrero et al. (1996) found that *B. licheniformis* MIR 29 produced a thermostable serine protease. The proteolytic cleavage may have functional significance; proteolysis has been found to be an important post translational modification in bacteria (Cain et al., 2014). Takasuka et al. (2014) reported that proteolytic processing of the β-mannanase from a *Streptomyces* sp. altered its substrate binding properties through truncation that resulted in modification of the 3D structure of two loops adjacent to the active site channel. The functional significance of this may be that the different enzyme variants may act together to hydrolyze mannan.

The purification procedure was not very successful, as the β-mannanase was only partially purified and the activity yield was low. The only successful step was AEC as the activity yield and fold purification obtained was relatively high. SEC and the concentration methods used for the purification procedures were not very successful due to the low activity yield obtained (≤ 20%). However, SDS-PAGE analysis showed that there were only a few protein contaminants in the SEC fraction. However, the yield was too low to allow for extensive biochemical characterization. A higher degree of purification would be necessary to determine the true characteristics of the β-mannanases. Even though zymogram analysis revealed that the partially purified β-mannanase displayed a single β-mannanase active band, the theoretical molecular masses of the GH5 and GH26 mannanase were too similar for SDS-PAGE to resolve. The amino acid sequences of the active bands would need to be determined to assess which β-mannanases were present. Native PAGE zymograms suggested that at least two different isoforms or β-mannanases were present.

The biochemical characteristics of the crude and partially purified β-mannanases were similar to what has been reported for other *B. licheniformis* β-mannanases. Differences were probably due to strain and assay variation. The crude and partially purified β-mannanases had temperature optima around 50°C, were stable at 50°C for at least 24 h and had predominaintly β-mannanase activity. These are suitable characteristics for the industrial production of biofuels and MOS. Industrial hydrolysis of lignocellulose is typically conducted for 24 h – 72 h (Liu et al., 2013; Malgas et al., 2017b). High reaction temperatures increase reaction rates and substrate solubility and decrease substrate viscosity and microbial contamination (Egorova and Antranikian; 2008). The crude *B. paralicheniformis* SVD1 β-

mannanase may suitable as an enzyme cocktail supplement, for biofuel production, or for animal feed MOS production. Purified *B. paralicheniformis* SVD1 β-mannanase could be used for MOS production suitable for human consumption. The *B. paralicheniformis* SVD1 β-mannanases showed 95 - 96% protein sequence similarity to the *B. licheniformis* DSM13^T (=ATCC14580^T) β-mannanases (Sakka et al., 2012). These sequence differences could affect biochemical characteristics. The substrate specificity assays and the qualitative determination of MOS production over time using TLC showed that the β-mannanase activity was highest on soluble, low branched mannan substrates, especially glucomannan. Songsiriritthigul et al. (2010) found the same substrate specificity with a recombinant GH26 β-mannanase from *B. licheniformis* DSM13^T (=ATCC14580^T). Galactose branching on mannan decreased activity and the galacto-MOS investigated were not hydrolyzed. This shows the importance of α-galactosidase for galactomannan hydrolysis. Galactose branching sterically hinders mannan hydrolysis (Van Dyk & Pletschke, 2012). The partially purified β-mannanase and a *Cyamopsis tetragonolobus* GH27 α-galactosidase synergistically hydrolyzed locust bean gum. The M50G50 combination displayed the highest extent of hydrolysis - after 24 h, there was a 1.39 fold increase in reducing sugar release and the DS was 4.64. This increase in reducing sugar release is similar to that reported by Malgas et al. (2015^c). The TLC results indicated that synergy increased the release of small MOS. These low DP MOS could be used as prebiotics (Jain et al., 2015; Srivastava & Kapoor, 2017).

The synergy between the partially purified β-mannanase and a commercial cellulase mixture Cellic® CTec2 was assessed on untreated and NaOH pretreated SCG. SCG is a major by-product of coffee production that has a high polysaccharide content, including mannan, and various industrial uses, including potential production of prebiotic MOS (Mussatto et al., 2011). In this study, glucose and mannose were the most abundant monosaccharides in acid hydrolysed SCG, which implied that cellulose and mannan were the most abundant polysaccharides. The NaOH pretreatment improved β-mannanase hydrolysis of SCG. It opened up and resulted in the swelling of the SCG particles and removed some of the insoluble solids. The control purified β-mannanase had a higher activity than the partially purified *B. paralicheniformis* SVD1 β-mannanase. This was probably because the control β-mannanase had a 2.5 x higher specific activity - due to its higher purity. The partially purified *B. paralicheniformis* SVD1 β-mannanase only displayed detectable activity on NaOH pretreated SCG, but displayed synergy with CTec2, in terms of DS, on untreated and NaOH pretreated SCG. The purified β-mannanase control displayed synergy on untreated and NaOH pretreated SCG in terms of DS and increased reducing sugars yield. However, the

highest DS reached was not as high as that DS obtained when using the partially purified *B. paralicheniformis* SVD1 β-mannanase. However, only the M25C75 combination on untreated SCG showed a significant improvement in reducing sugar release. The lack of significant improvement in hydrolysis by the other combinations was possibly due to the high variation in the measured RS release due to the wide range of SCG particle sizes as seen with SEM as well as the small sample size.

As mannan covers and intertwines with cellulose fibrils (Banerjee et al., 2010; Malgas et el., 2017), there were probably two possible causes for cellulase – mannanase synergy. Firstly, hydrolysis of mannan would expose more cellulose to cellulase activity. Secondly, hydrolysis of cellulose would expose more mannan to mannanase hydrolysis (Malgas et al., 2017a). Measurement of monosaccharide and oligosaccharide release during synergy would have allowed for a better understanding of the synergistic relationship.

In conclusion, this study demonstrated the production and partial purification of β-mannanase from *B. paralicheniformis* SVD1. The partially purified β-mannanase showed synergy with an α-galactosidase on locust bean gum and synergy with a commercial cellulase mixture on SCG. This is the first report of mannanase-cellulase synergy on SCG. SCG is a major coffee waste product that has potential for the production of prebiotic MOS. The results obtained in this study are only an initial assessment of the biochemical properties of *B. paralicheniformis* SVD1 β-mannanases and their synergy with other enzymes. The results obtained can be used to inform future studies.

5.2. Future recommendations

As β-mannanase production was relatively low compared to other studies, the growth conditions for β-mannanase production could be optimized in terms of media composition, growth temperature, media pH and aeration (Zhang et al., 2000; Feng et al., 2003; Ge et al., 2016). SCG could also be assessed as a carbon source in the media. *Bacillus paralicheniformis* SVD1 may be induced to release an efficient synergistic cocktail of lignocellulytic enzymes optimized for SCG hydrolysis (Madigan, et al., 2003). For effective purification of the β-mannanase activity, pre-packed AEC and SEC columns could be used. These have much higher resolution than the manually packed columns that were used in this study. An alternative purification procedure would be to clone and heterologously express one or both of the β-mannanases in *Escherichia coli*, given that the β-mannanase gene

sequences are known (Sakka et al., 2012). A company such as Genscript® could quickly and relatively cheaply construct expression plasmids.

In terms of biochemical characterization, metal ion inhibition and activation could be determined. The metal ions Ba^{2+}, K^{+}, Co^{2+} and Mg^{2+} were shown to improve activity of a β-mannanase from *B. licheniformis* HDYM-04 (Ge et al., 2016). Inhibition by lignin, phenolics and organic acids that occur in plant biomass and that are released or produced during pretreatment could also be assessed. These substances inhibit holocellulose hydrolysis (Jönsson et al., 2013). Product inhibition could also be determined (Van Dyk & Pletschke, 2012). Substrate binding studies would be useful to determine if non-productive adsorption occurs, as well as the effect of surfactants or enzyme synergy to decrease non-productive adsorption (Van Dyk & Pletschke, 2012). Binding studies may be particularly important for assessing hydrolysis of SCG, which is very insoluble and has a high insoluble solid content. For future synergy studies, measurement of monosaccharides released using techniques such as monosaccharide quantification kits or HLPC would be informative. This would allow determination of whether synergy is due to increased hydrolysis of mannan, cellulose, galactose branching, or if it is due to increased hydrolysis of multiple saccharide bonds. Synergy on more mannan substrates could also be assessed. This would allow for a better understanding of the effect of different structures on synergy such as the extent and distribution of galactose branching. Structurally different GH27 and GH36 α-galactosidases could be assessed for synergy with β-mannanase, as studies have shown that the GH family, as well as structure, affects synergy (Wang et al., 2015; Malgas et al., 2015[c]; Reddy et al., 2016). MOS production was qualitatively assessed using TLC. Quantitative assessment of MOS, using techniques such as HPLC or TLC followed by mass spectrometry, could be performed. Knowing which MOS are produced would allow for a better assessment and understanding of the prebiotic potential of the β-mannanase. It would also be useful for the selection of enzymes for total biomass hydrolysis for biofuel production. To assess the prebiotic potential of the MOS, the MOS's prebiotic properties would need to be determined - for example, its metabolism by gut microorganisms (Bindels et al., 2015).

Future studies with a molecular biology focus could explore the effect of CBM's on substrate binding and activity. The effect of attaching different CBM's, with different substrate binding specificities, on binding and activity could be assessed as was performed by Zhang et al. (2014). Efficient hydrolysis of SCG probably requires a CBM as SCG is very insoluble. The *B. paralicheniformis* SVD1 β-mannanases do not have CBM's (Sakka et al., 2012).

Alternative methods for SCG pretreatment could also be evaluated. Recently, Balch et al. (2017) found that switchgrass carbohydrate solubilization by *Clostridium thermocellum was* higher when milling was used as a co-treatment during hydrolysis and fermentation than when the substrate was hydrothermally pretreated. This method could help reduce the particle size of SCG and is also beneficial, as pretreatment by-products from thermo-chemical pretreatment methods (such as phenolics and organic acids that inhibit enzyme activity and fermentation) would not be produced (Jönsson et al., 2013). Bioinformatics studies such as structural analysis and substrate and inhibitor docking studies would help in understanding biochemical characteristics, such as substrate specificity, inhibition, as well as synergy. It could also inform genetic engineering studies for the improvement of β-mannanase activity. The study by von Freiesleben et al. (2016) is a good example of how *in silico* substrate docking studies can improve our understanding of substrate specificity.

References

Aachary, A.A. & Prapulla, S.G. 2011. Xylooligosaccharides (XOS) as an emerging prebiotic: microbial synthesis, utilization, structural characterization, bioactive properties, and applications. *Comprehensive Reviews in Food Science and Food Safety*, 10: 2–16.

Ademark, P., Larsson, M., Tjerneld, F. & Stålbrand, H. 2001. Multiple α-galactosidases from *Aspergillus niger*: purification, characterization and substrate specificities. *Enzyme and Microbial Technology*, 29: 441–448.

Agbor, V.B., Cicek, N., Sparling, R., Berlin, A. & Levin, D.B. 2011. Biomass pretreatment: fundamentals toward application. *Biotechnology Advances*, 29: 675–685.

Akcan, N., 2011a. High Level Production of Extracellular α-Amylase from *Bacillus licheniformis* ATCC 12759 in Submerged Fermentation. *Romanian Biotechnological Letters*, 16(6): 6833-6840.

Akcan, N., 2011b. High level production of extracellular β-galactosidase from *Bacillus licheniformis* ATCC 12759 in submerged fermentation. *African Journal of Microbiology Research*, 5(26): 4615-4621.

Akcan, N., 2012. Production of extracellular protease in submerged fermentation by *Bacillus licheniformis* ATCC 12759. *African Journal of Microbiology Research*, 11(7): 1729-1735.

Allagheny, N., Obanu, Z.A., Campbell-Platt, G. & Owens, J.D. 1996. Control of ammonia formation during *Bacillus subtilis* fermentation of legumes. *International Journal of Food Microbiology*, 29: 321–333.

Altschul, S.F., Gish, W., Miller, W., Myers, E.W. & Lipman, D.J. 1990. Basic local alignment search tool. *Journal of Molecular Biology,* 215: 403-410.

Alvira, P., Tomás-Pejó, E., Ballesteros, M. & Negro, M.J. 2010. Pretreatment technologies for an efficient bioethanol production process based on enzymatic hydrolysis: a review. *Bioresource Technology*, 101(13): 4851–4861.

Anon. 2009. Tech Tip #49: Acetone Precipitation of Proteins. Thermo Fisher Scientific - Pierce Biotechnology.

Anon. 2010. Thermo Scientific Pierce Protein Assay Technical Handbook. Version 2. Thermo Fisher Scientific.

Anon. 2011. Technical bulletin: Bradford Reagent (B6916). Sigma-Aldrich.

Anon. 2016a. Ion Exchange Chromatography: Principles and Methods..GE Healthcare Bio-Sciences AB.

Anon. 2016b. Size Exclusion Chromatography: Principles and Methods. 18th edn. GE Healthcare Bio-Sciences AB.

Anson, M.L. 1938. The estimation of pepsin, trypsin, papain, and cathepsin with hemoglobin. *Journal of General Physiology*, 22(1): 79-89.

Araki, T. & Kitamikado, M. 1988. Exo-1, 4-β-mannanase from *Aeromonas hydrophila*. *Methods in Enzymology*, (160): 583–589.

Balch, M.L., Holwerda, E.K., Davis, M., Sykes, R., Happs, R.M., Kumar, R., Wyman, C.E. & Lynd, L.R. 2017. Lignocellulose fermentation and residual solids characterization for senescent switchgrass fermentation by *Clostridium thermocellum* in the presence and absence of continuous *in-situ* ball-milling. *Energy & Environmental Science*, 10: 1252–1261.

Banerjee, G., Scott-Craig, J. S. and Walton, J. D. 2010. Improving enzymes for biomass conversion: a basic research perspective*. Bioenergy Research*. 3: 82–92.

Beynon, R.J. & Oliver, S. 2004. Avoidance of Proteolysis in Extracts. *In: Protein Purification Protocols*, 2nd edn. P. Cutler, ed. Humana Press Inc., New Jersey, U.S.A., 483 pp.

Bhattacharya, A.S., Bhattacharya, A. & Pletschke, B.I. 2015. Synergism of fungal and bacterial cellulases and hemicellulases: a novel perspective for enhanced bio-ethanol production. *Biotechnology Letters*, 37(6): 1117–1129.

Bindels, L.B., Delzenne, N.M., Cani, P.D. & Walter, J. 2015. Towards a more comprehensive concept for prebiotics. *Nature Reviews: Gastroenterology & Hepatology*, Advance Online Publication.

Bollag, D.M., Rozycki, M.D. & Edelstein, S.J. 1996. *Protein methods*, 2nd edn. Wiley-Liss, New York, U.S.A., 432 pp.

Bose, K. & Das, D. 1996. Thermostable alpha-amylase production using *Bacillus licheniformis* NRRL B14368. *Indian Journal of Experimental Biology*, 34(12): 1279-1282.

Bourne, Y. & Henrissat, B. 2001. Glycoside hydrolases and glycosyltransferases: families and functional modules. *Current Opinion in Structural Biology*, 11(5): 593–600.

Bradford, M.M. 1976. A rapid and sensitive method for the quantitation of microgram quantities of protein utilizing the principle of protein dye binding. *Analytical Biochemistry*, 72(1-2): 248–254.

Cain, J.A., Solis, N. & Cordwell, S.J. 2014. Beyond gene expression: the impact of protein post-translational modifications in bacteria. *Journal of Proteomics*, 97: 265–286.

Campos-Vega, R., Loarca-Piña, G., Vergara-Castañeda, H. & Oomah, B.D. 2015. Spent coffee grounds: A review on current research and future prospects. *Trends in Food Science & Technology*, 45(1): 24–36.

Carroll, B. & Van Dyk, J.W. 1952. The Activity of α-Amylase as determined by adsorption indicators. *Science*, 116 (3007): 168–169.

Cartmell, A., Topakas, E., Ducros, V.M.-A., Suits, M.D.L., Davies, G.J. & Gilbert, H.J. 2008. The *Cellvibrio japonicus* mannanase CjMan26C displays a unique exo-mode of action that is conferred by subtle changes to the distal region of the active site. *The Journal of Biological Chemistry*, 283: 34403–34413.

Chauhan, P.S., Puri, N., Sharma, P. & Gupta, N. 2012. Mannanases: microbial sources, production, properties and potential biotechnological applications. *Applied Microbiology and Biotechnology*, 93: 1817–1830.

Chauhan, P.S., George, N., Sondhi, S., Puri, N. & Gupta, N. 2014. An overview of purification strategies for microbial mannanases. *International Journal of Pharma and Bio Sciences*, 5(1): 176–192.

Chen, Y., Stevens, M. A, Zhu, Y., Holmes, J. & Xu, H. 2013. Understanding of alkaline pretreatment parameters for corn stover enzymatic saccharification. *Biotechnology for Biofuels*, 6(1): 8.

Chiyanzu, I., Brienzo, M., García-Aparicio, M.P. & Görgens, J.F. 2014. Application of endo-β-1,4,D-mannanase and cellulase for the release of mannooligosaccharides from steam-pretreated spent coffee ground. *Applied Biochemistry and Biotechnology*, 172: 3538–57.

Chiyanzu, I., Brienzo, M., García-Aparicio, M., Agudelo, R. & Görgens, J. 2015. Spent coffee ground mass solubilisation by steam explosion and enzymatic hydrolysis. *Journal of Chemical Technology & Biotechnology*, 90: 449–458.

Choudhury, B., Chauhan, S., Singh, S.N. & Ghosh, P. 2006. Production of xylanase of *Bacillus coagulans* and its bleaching potential. *World Journal of Microbiology and Biotechnology*, 22(3): 283–288.

Chundawat, S.P.S., Beckham, G.T., Himmel, M.E. & Dale, B.E. 2011. Deconstruction of lignocellulosic biomass to fuels and chemicals. *Annual Review of Chemical and Biomolecular Engineering*, 2(1): 121–145.

Clarke, J.H., Davidson, K., Rixon, J.E., Halstead, J.R., Fransen, M.P., Gilbert, H.J. & Hazlewood, G.P. 2000. A comparison of enzyme-aided bleaching of softwood paper pulp using combinations of xylanase, mannanase and α-galactosidase. *Applied Microbiology and Biotechnology*, 53: 661–667.

Conti, J., Holtberg, P., Diefenderfer, J., Larose, A., Turnure, J. & Westfall, L. 2016. *International Energy Outlook 2016*. U.S. Energy Information Administration. DOE/EIA-0484(2016).

Couturier, M., Roussel, A., Rosengren, A., Leone, P., Stålbrand, H. & Berrin, J.-G. 2013. Structural and biochemical analyses of glycoside hydrolase families 5 and 26 β-(1,4)-mannanases from *Podospora anserina* reveal differences upon manno-oligosaccharide catalysis. *The Journal of Biological Chemistry*, 288: 14624–14635.

Cross, R. 2001. The Preparation of Biological Material for Electron Microscopy Part 3: The Preparation of Material for Scanning Electron Microscopy (SEM). Grahamstown: Rhodes University Press, South Africa.

Dale, B.E., Anderson, J.E., Brown, R.C., Csonka, S., Dale, V.H., Herwick, G., Jackson, R.D., Jordan, N., Ka, S., Kline, K.L., Lynd, L.R., Malmstrom, C., Ong, R.G., Richard, T.L., Taylor, C. & Wang, M.Q. 2014. Take a closer look: biofuels can support environmental, economic and social goals. *Environmental Science and Technology*, 48: 7200–7203.

Davies, G. & Henrissat, B. 1995. Structures and mechanisms of glycosyl hydrolases. *Structure*, 3(9): 853–859.

Deutscher, M.P. 2009. Maintaining Protein Stability. *Methods in Enzymology,* 463: 121–127.

Dhawan, S. & Kaur, J. 2007. Microbial mannanases: an overview of production and applications. *Critical Reviews in Biotechnology*, 27(4): 197–216.

Donohoe, B.S. & Resch, M.G. 2015. Mechanisms employed by cellulase systems to gain access through the complex architecture of lignocellulosic substrates. *Current Opinion in Chemical Biology*, 29: 100–107.

Doonan, S. 2004. Bulk Purification by Fractional Precipitation. *In: Protein Purification Protocols*, 2nd edn. P. Cutler, ed,.Humana Press Inc., New York City, U.S.A., 117–124 pp.

Duarte, G.C., Moreira, L.R.S., Jaramillo, P.M.D. & Filho, E.X.F. 2012. Biomass-derived inhibitors of holocellulases. *BioEnergy Research*, 5(3): 768–777.

Dunlop, C.A., Kwon, S-W., Rooney, A.P., Kim, S-J. 2015. *Bacillus paralicheniformis* sp. *nov*., isolated from fermented soybean paste. *International Journal of Systematic and Evolutionary Microbiology.* 65: 3487-3492.

Egorova, K., Antranikian, G. 2006. Industrial relevance of thermophillic Archaea. *Current Opinion in Microbiology*, 8(6): 649-655.

Fenel, F., Leisola, M., Jänis, J. & Turunen, O. 2004. A *de novo* designed N-terminal disulphide bridge stabilizes the *Trichoderma reesei* endo-1,4-β-xylanase II. *Journal of Biotechnology*, 108(2): 137–143.

Feng, Y., He, Z., Ong, S.L., Hu, J., Zhang, Z. & Ng, W.J. 2003. Optimization of agitation, aeration, and temperature conditions for maximum β-mannanase production. *Enzyme and Microbial Technology*, 32(2): 282–289.

Ferenczi, S., Szegi, K., Winkler, Z., Barna, T. & Kovács, K.J. 2016. Oligomannan prebiotic attenuates immunological, clinical and behavioral symptoms in mouse model of inflammatory bowel disease. *Scientific Reports*, 6: 34132.

Ferrero, M.A., Castro, G.R., Abate, C.M., Baigori, M.D. & Siñeriz, F. 1996. Thermostable alkaline proteases of *Bacillus licheniformis* MIR 29: Isolation, production and characterization. *Applied Microbiology and Biotechnology*, 45: 327–332.

Folin, O. & Ciocalteau, V. 1927. On tyrosine and tryptophane determinations in proteins. *Journal of Biological Chemistry*, 73: 627–648.

Fulton, L.M., Lynd, L.R., Körner, A., Greene, N. & Tonachel, L.R. 2015. The need for biofuels as part of a low carbon energy future. *Biofuels, Bioproducts and Biorefining*, 9(5): 476–483.

Gasteiger, E., Hoogland, C., Gattiker, A., Duvaud, S., Wilkins, M.R., Appel, R.D. & Bairoch, A. 2005. Protein Identification and Analysis Tools on the ExPASy Server. In J. M. Walker, ed. *The Proteomics Protocols Handbook*. Totowa, NJ: Humana Press, pp. 571–607.

Ge, J.P., Du, R.P., Zhao, D., Song, G., Jin, M. & Ping, W.X. 2016. Bio-chemical characterization of a β-mannanase from *Bacillus licheniformis* HDYM-04 isolated from flax water-retting liquid and its decolorization ability of dyes. *Royal Society of Chemistry Advances*, 6(28): 23612–23621.

Ghosh, A., Luís, A.S., Brás, J.L.A., Fontes, C.M.G.A. & Goyal, A. 2013. Thermostable recombinant β-(1→4)-mannanase from *C. thermocellum*: biochemical characterization and manno-oligosaccharides production. *Journal of Agricultural and Food Chemistry*, 61(50): 12333–12344.

Goshadrou, A., Karimi, K. & Taherzadeh, M.J. 2011. Bioethanol production from sweet sorghum bagasse by *Mucor hiemalis*. *Industrial Crops and Products*, 34(1): 1219–1225.

Gourlay, K., Hu, J., Arantes, V., Penttilä, M. & Saddler, J.N. 2015. The use of carbohydrate binding modules (CBMs) to monitor changes in fragmentation and cellulose fiber surface morphology during cellulase and swollenin induced deconstruction of lignocellulosic substrates. *Journal of Biological Chemistry*, 290: 2938–2945.

Grohmann, K., Mitchell, D.J., Himmel, M.E., Dale, B.E. & Schroeder, H.A. 1989. The role of ester groups in resistance of plant cell wall polysaccharides to enzymatic hydrolysis. *Applied Biochemistry and Biotechnology*, 20: 45–61.

Gümüşkaya, E. & Usta, M. 2006. Dependence of chemical and crystalline structure of alkali sulfite pulp on cooking temperature and time. *Carbohydrate Polymers*, 65(4): 461–468.

Hahn-Hägerdal, B., Karhumaa, K., Larsson, C.U., Gorwa-Grauslund, M., Görgens, J. & Van Zyl, W.H. 2005. Role of cultivation media in the development of yeast strains for large scale industrial use. *Microbial Cell Factories*, 4: 31.

Harris, P. V, Xu, F., Kreel, N.E., Kang, C. & Fukuyama, S. 2014. New enzyme insights drive advances in commercial ethanol production. *Current Opinion in Chemical Biology*, 19: 162–170.

Hasunuma, T., Okazaki, F., Okai, N., Hara, K.Y., Ishii, J. & Kondo, A. 2013. A review of enzymes and microbes for lignocellulosic biorefinery and the possibility of their application to consolidated bioprocessing technology. *Bioresource Technology*, 135: 513–522.

Henrissat, B. 1991. A classification of glycosyl hydrolases based on amino acid sequence similarities. *Biochemical Journal*, 280(2): 309-316.

Henrissat, B., Callebaut, I., Lehn, P., Mornon, J. & Davies, G. 1995. Conserved catalytic machinery and the prediction of a common fold for several familes of glycosyl hydrolases. *Proceedings of the National Academy of Sciences of the United States of America*, 92: 7090–7094.

Hogg, D., Pell, G., Dupree, P., Goubet, F., Martín-Orúe, S.M., Armand, S. & Gilbert, H.J. 2003. The modular architecture of *Cellvibrio japonicus* mannanases in glycoside hydrolase families 5 and 26 points to differences in their role in mannan degradation. *Biochemical Journal*, 371(3), 1027–1043.

Hu, J., Arantes, V., Pribowo, A. & Saddler, J.N. 2013. The synergistic action of accessory enzymes enhances the hydrolytic potential of a ‘cellulase mixture’ but is highly substrate specific. *Biotechnology for Biofuels*, 6(1): 112.

Hu, J., Chandra, R., Arantes, V., Gourlay, K., Van Dyk, J.S. & Saddler, J.N. 2015. The synergistic action of accessory enzymes enhances the hydrolytic potential of a cellulase enzymes at high solid loadings. *Bioresource Technology*, 186: 149-153.

Igarashi, K., Koivula, A., Wada, M., Kimura, S., Okamoto, T., Ando, T. & Samejima, M. 2011. Traffic jams reduce hydrolytic efficiency of cellulase on cellulose surface. *Science*, 333(6047): 1279–1282.

Jain, I., Kumar, V. & Satyanarayana, T. 2015. Xylooligosaccharides: an economical prebiotic from agroresidues and their health benefits. *Indian Journal of Experimental Biology*, 53(3): 131–142.

Jian, H.L., Zhu, L.W., Zhang, W.M., Sun, D.F. & Jiang, J.X. 2013. Enzymatic production and characterization of manno-oligosaccharides from *Gleditsia sinensis* galactomannan gum. *International Journal of Biological Macromolecules*, 55: 282–288.

Jönsson, L.J., Alriksson, B. & Nilvebrant, N. 2013. Bioconversion of lignocellulose: inhibitors and detoxification. *Biotechnology for Biofuels*, 6(1): 16.

Jooste, T., García-Aparicio, M.P., Brienzo, M., Van Zyl, W.H. & Görgens, J.F. 2013. Enzymatic hydrolysis of spent coffee ground. *Applied Biochemistry and Biotechnology*, 169: 2248–2262.

Jørgensen, H., Sanadi, A.R., Felby, C., Lange, N.E.K., Fischer, M. & Ernst, S. 2010. Production of ethanol and feed by high dry matter hydrolysis and fermentation of palm kernel press cake. *Applied Biochemistry and Biotechnology*, 161: 318–332.

Jung, H., Yoon, H.G., Park, W., Choi, C., Wilson, D.B., Shin, D.H. & Kim, Y.J. 2008. Effect of sodium hydroxide treatment of bacterial cellulose on cellulase activity. *Cellulose*, 15(3): 465–471.

Kalambur, S.B. 2012. Modification of Biodegradable Polymers through Reactive Extrusion-II*. In: Starch-Based Polymeric Materials and Nanocomposites: Chemistry, Processing, and Applications*. J. Ahmed, B. K. Tiwari, S. H. Imam, & M. A. Rao (eds). Taylor & Francis Group CRC, Boca Raton, U.S.A., 395 pp.

Kanjanavas, F., Khawsak, P., Pakpitcharoen, A., Areekit, S., Sriyaphai, T., Pothivejkul, K., Santiwatanakul, S., Matsui, K., Kajiwara, T. & Chansiri, K. 2009. Over-expression and characterization of the alkalophilic, organic solvent-tolerant, and thermotolerant endo-1,4-ß-mannanase from *Bacillus licheniformis* isolate THCM 3.1. *ScienceAsia*, 35(1): 17–23.

Karlen, D.L., Beeler, L.W., Ong, R.G. & Dale, B.E. 2015. Balancing energy, conservation, and soil health requirements for plant biomass. *Journal of Soil and Water Conservation*, 70(5): 279–287.

Kasai, N., Konishi, A., Iwai, K. & Maeda, G. 2006. Efficient digestion and structural characteristics of cell walls of coffee beans. *Journal of Agricultural and Food Chemistry*, 54: 6336–6342.

Kumagai, Y., Kawakami, K., Uraji, K. & Hatanaka, T. 2013. Binding of bivalent ions to actinomycete mannanase is accompanied by conformational change and is a key factor in its thermal stability. *Biochimica et Biophysica Acta - Proteins and Proteomics*, 1834(1): 301-307.

Kumar, R., Wyman, C.E. 2014. Strong Cellulase Inhibition by Mannan Polysaccharides in Cellulose Conversion to Sugars. *Biotechnology* and Bioengineering, 111(7): 1341-1353.

Kwon, E.E., Yi, H. & Jeon, Y.J. 2013. Sequential co-production of biodiesel and bioethanol with spent coffee grounds. *Bioresource Technology*, 136: 475–480.

Laemmli, U.K. 1970. Cleavage of structural proteins during the assembly of the head of bacteriophage T4. *Nature*, 227(5259): 680–685.

Leung, D., Abbenante, G. & Fairlie, D.P. 2000. Protease inhibitors: current status and future prospects. *Journal of Medicinal Chemistry*, 43(3): 305–341.

Li, Y.N., Meng, K., Wang, Y.R. & Yao, B. 2006. A β-mannanase from *Bacillus subtilis* B36: purification, properties, sequencing, gene cloning and expression in *Escherichia coli*. *Zeitschrift für Naturforschung. C,* 61(11-12): 840–846.

Liepman, A.H., Nairn, C.J., Willats, W.G.T., Sørensen, I., Roberts, A.W. & Keegstra, K. 2007. Functional genomic analysis supports conservation of function among cellulose synthase-like A gene family members and suggests diverse roles of mannans in plants. *Plant Physiology*, 143(4): 1881–1893.

Liska, A.J., Yang, H., Milner, M., Goddard, S., Blanco-Canqui, H., Pelton, M.P., Fang, X.X., Zhu, H. & Suyker, A.E. 2014. Biofuels from crop residue can reduce soil carbon and increase CO^2 emissions. *Nature Climate Change*, 4: 398–401.

Liu, G., Qin, Y., Li, Z. & Qu, Y. 2013. Development of highly efficient, low-cost lignocellulolytic enzyme systems in the post-genomic era. *Biotechnology Advances*, 31(6): 962–975.

Lombard, V., Golaconda Ramulu, H., Drula, E., Coutinho, P.M., Henrissat, B. 2014. The Carbohydrate-active enzymes database (CAZy) in 2013. *Nucleic Acids Reseach*, 42: D490–D495.

Lynd, L.R., Weimer, P.J., Van Zyl, W.H. & Pretorius, I.S. 2002. Microbial cellulose utilization: fundamentals and biotechnology. *Microbiology and Molecular Biology Reviews,* 66(3): 506–577.

Lynd, L.R., Sow, M., Chimphango, A.F., Cortez, L.A., Brito Cruz, C.H., Elmissiry, M., Laser, M., Mayaki, I. a, Moraes, M.A., Nogueira, L.A., Wolfaardt, G.M., Woods, J. & Van Zyl, W.H. 2015. Bioenergy and African transformation. *Biotechnology for Biofuels*, 8(1): 1–18.

Madigan, M.T., Martinko, J.M. & Parker, J. 2003. *Brock Biology of Microorganisms*, 10th edn. Pearson Education Inc., New Jersey, U.S.A., 1019 pp.

Malgas, S. 2015. *The effect of GH family affiliations of mannanolytic enzymes on their synergistic associations during the hydrolysis of mannan-containing substrates*. MSc. thesis. Rhodes University, South Africa.

Malgas, S., Van Dyk, J.S., Abboo, S. & Pletschke, B.I. 2015a. The inhibitory effects of various substrate pre-treatment by-products and wash liquors on mannanolytic enzymes. *Journal of Molecular Catalysis B: Enzymatic*, 123: 132–140.

Malgas, S., Van Dyk, J.S. & Pletschke, B.I. 2015b. A review of the enzymatic hydrolysis of mannans and synergistic interactions between β-mannanase, β -mannosidase and α-galactosidase. *World Journal of Microbiology and Biotechnology*, 31(8): 1167-1175.

Malgas, S., Van Dyk, S.J. & Pletschke, B.I. 2015c. β-mannanase (Man26A) and α-galactosidase (Aga27A) synergism - a key factor for the hydrolysis of galactomannan substrates. *Enzyme and Microbial Technology*, 70: 1–8.

Malgas, S., Thoresen, M., Van Dyk, J.S. & Pletschke, B.I. 2017a. Time dependence of enzyme synergism during the degradation of model and natural lignocellulosic substrates. *Enzyme and Microbial Technology*, 103: 1–11.

Malgas, S., Chandra, R., Van Dyk, J.S., Saddler, J.N. & Pletschke, B.I. 2017b. Formulation of an optimized synergistic enzyme cocktail, HoloMix, for effective degradation of various pre-treated hardwoods. Bioresource Technology, 245: 52-65.

Mayende, L. 2006. *Isolation of a Clostridium beijerinckii sLM01 cellulosome and the effect of sulphide on anaerobic digestion*. MSc. thesis. Rhodes University, South Africa.

Merino, S.T. & Cherry, J. 2007. Progress and challenges in enzyme development for biomass utilization. *Advances in Biochemical Engineering &* Biotechnology, 108: 95-120.

Miller, G.L. 1959. Use of dinitrosalicylic acid reagent for determination of reducing sugar. *Analytical Chemistry*, 31(3): 426–428.

Moreira, L.R.S. & Filho, E.X.F. 2008. An overview of mannan structure and mannan-degrading enzyme systems. *Applied Microbiology and Biotechnology*, 79: 165–178.

Mosbach, K. 1971. Enzymes Bound to Artificial Matrixes. *Scientific American*, 224(3): 26-33.

Muñoz-Gutiérrez, I., Rodríguez-Alegría, M.E., Munguía, A.L. Kinetic behaviour and specificity of b-fructosidases in the hydrolysis of plant and microbial fructans. *Process Biochemistry*, 44: 891-898.

Murthy, P.S. & Naidu, M.M. 2012. Sustainable management of coffee industry by-products and value addition — a review. *Resources, Conservation & Recycling*, 66: 45–58.

Mussatto, S.I., Machado, E.M.S., Martins, S. & Teixeira, J.A. 2011. Production, composition, and application of coffee and its industrial residues. *Food and Bioprocess Technology*, 4(5): 661–672.

Nieves, R.A., Ehrman, C.I., Adney, W.S., Elander, R.T. & Himmel, M.E. 1998. Technical communication : survey and analysis of commercial cellulase preparations suitable for biomass conversion to ethanol. *World Journal of Microbiology and Biotechnology*, 14: 301–304.

Novozymes®. 2017. Frequently asked questions. Enzymes for biocatalysts. [ONLINE] Available at: https://www.novozymes.com/en/advance-your-business/pharma/pharma-biocatalysts. [Accessed 27 March 2018].

Nunes, F.M. & Coimbra, M.A. 2001. Chemical characterization of the high molecular weight material extracted with hot water from green and roasted arabica coffee. *Journal of Agricultural and Food Chemistry*, 49: 1773–1782.

Olsson, L. & Saddler, J.N. 2013. Biorefineries, using lignocellulosic feedstocks, will have a key role in the future bioeconomy. *Biofuels, Bioproducts and Biorefining*, 6: 475–477.

Oosterveld, A., Voragen, A.G.J. & Schols, H.A. 2003. Effect of roasting on the carbohydrate composition of *Coffea arabica* beans. *Carbohydrate Polymers*, 54(2): 183–192.

Paloheimo, M., Haarman, T., Mäkinen, S., Vehmaanperä, J. 2016. Production of industrial enzymes by Trichoderma reesei. *In: Gene Expression Systems in Fungi: Advancements and Applications.* M. Schmoll C. Dattenböck, eds. Springer International, Heidelberg, 498 pp.

Payne, C.M., Knott, B.C., Mayes, H.B., Hansson, H., Himmel, M.E., Sandgren, M., Ståhlberg, J. & Beckham, G.T. 2015. Fungal cellulases. *Chemical Reviews*, 115(3): 1308–1448.

Qing, Q., Li, H., Kumar, R. & Wyman, C.E. 2013. Xylooligosaccharides Production, Quantification, and Characterization in Context of Lignocellulosic Biomass Pretreatment. *In: Aqueous Pretreatment of Plant Biomass for Biological and Chemical Conversion to Fuels and Chemicals.* C.E. Wyman ed, John Wiley & Sons Inc., Chichester, U.K., 538 pp.

Rachinger, M., Volland, S., Meinhardt, F., Daniel, R., Liesegang, H. 2013. First Insights into the Completely Annotated Genome Sequence of *Bacillus Licheniformis* Strain 9945A. *Genome Announcements*, 1(4): e00525-13.

Ragauskas, A.J., Beckham, G.T., Biddy, M.J., Chandra, R., Chen, F., Davis, M.F., Davison, B.H., Dixon, R.A., Gilna, P., Keller, M., Langan, P., Naskar, A.K., Saddler, J.N., Tschaplinski, T.J., Tuskan, G.A., Wyman, C.E. 2014. Lignin valorization : improving lignin processing in the biorefinery. *Science,* 344(6185).

Redgwell, R., Fischer, M. 2006. Coffee carbohydrates. *Brazilian Journal of Plant Physiology*, 18(1): 165-174.

Redgwell, R.J., Trovato, V., Curti, D. & Fischer, M. 2002. Effect of roasting on degradation and structural features of polysaccharides in Arabica coffee beans. *Carbohydrate Research*, 337(5): 421–431.

Reddy, S.K., Bågenholm, V., Pudlo, N.A., Bouraoui, H., Koropatkin, N.M., Martens, E.C. & Stålbrand, H. 2016. A β-mannan utilization locus in *Bacteroides ovatus* involves a GH36 α-galactosidase active on galactomannans. *FEBS Letters*, 590: 2106–2118.

Resch, M.G., Donohoe, B.S., Baker, J.O., Decker, S.R., Bayer, E. a, Beckham, G.T. & Himmel, M.E. 2013. Fungal cellulases and complexed cellulosomal enzymes exhibit synergistic mechanisms in cellulose deconstruction. *Energy & Environmental Science*, 6(6): 1858–1867.

Rey, M.W., Ramaiya, P., Nelson, B.A., Brody-Karpin, S.D., Zaretsky, E.J., Tang, M., Lopez de Leon, A., Xiang, H., Gusti, V., Clausen, I.G., Olsen, P.B., Rasmussen, M.D., Andersen, J.T., Jørgensen, P.L., Larsen, T.S., Sorokin, A., Bolotin, A., Lapidus, A., Galleron, N., Ehrlich, S.D. & Berka, R.M. 2004. Complete genome sequence of the industrial bacterium *Bacillus licheniformis* and comparisons with closely related *Bacillus* species. *Genome biology*, 5(10): R77.

Roberfroid, M.B. 2008. General Introduction: Prebiotics in Nutrition*. In*: *Handbook of Prebiotics*. G. R. Gibson & M. B. Roberfroid, eds. Taylor & Francis Group, Boca Raton, U.S.A.,487 pp.

Sadaie, Y., Nakadate, H., Fukui, R., Yee, L.M. & Asai, K. 2008. Research letter: Glucomannan utilization operon of *Bacillus subtilis*. *FEMS Microbiology Letters*, 279: 103–109.

Sakka, M., Tachino, S., Katsuzaki, H., Van Dyk, J.S., Pletschke, B.I., Kimura, T. & Sakka, K. 2012. Characterization of Xyn30A and Axh43A of *Bacillus licheniformis* SVD1 identified by its genomic analysis. *Enzyme and Microbial Technology*, 51(4): 193–199.

Sarkar, P.K., Cook, P.E. & Owens, J.D. 1993. *Bacillus* fermentation of soybeans. *World Journal of Microbiology & Biotechnology*, 9(3): 295–299.

Schurmann, H. & Steffensen, J.F. 1992. Lethal oxygen levels at different temperatures and the preferred temperature during hypoxia of the Atlantic cod, Gadus morhua L. *Journal of Fish*

Biology, 41(6): 927–934.

Sheehan, D. 2009. Hydrodynamic Methods. *In: Physical Biochemistry: Principles and Methods*, 2nd edn. Wiley-Blackwell, West Sussex, U.K., 285 pp.

Sills, D.L. & Gossett, J.M. 2011. Assessment of commercial hemicellulases for saccharification of alkaline pretreated perennial biomass. *Bioresource Technology*, 102(2): 1389–1398.

Simões, J., Nunes, F.M., Domingues, M.R. & Coimbra, M.A. 2013. Extractability and structure of spent coffee ground polysaccharides by roasting pre-treatments. *Carbohydrate Polymers*, 97(1): 81–89.

Sluiter, J.B., Ruiz, R.O., Scarlata, C.J., Sluiter, A.D. & Templon, D.W. 2010. Compositional analysis of lignocellulosic feedstocks 1: review and description of methods. *Journal of Agricultural and Food Chemistry*, 58(16): 9043–9053.

Smallwood, M., Yates, E.A., Willats, W.G.T., Martin, H. & Knox, J.P. 1996. Immunochemical comparison of membrane-associated and secreted arabinogalactan-proteins in rice and carrot. *Planta*, 198: 452–459.

Songsiriritthigul, C., Buranabanyat, B., Haltrich, D. & Yamabhai, M. 2010. Efficient recombinant expression and secretion of a thermostable GH26 mannan endo-1,4-beta-mannosidase from *Bacillus licheniformis* in *Escherichia coli*. *Microbial Cell Factories*, 9: 20.

Sorek, N., Yeats, T.H., Szemenyei, H., Youngs, H. & Somerville, C.R. 2014. The implications of lignocellulosic biomass chemical composition for the production of advanced biofuels. *BioScience*, 64(3): 192–201.

Srivastava, P.K. & Kapoor, M. 2017. Production, properties, and applications of endo-β-mannanases. *Biotechnology Advances*, 35(1): 1–19.

Stülke, J. & Hillen, W. 2000. Regulation of carbon catabolism in *Bacillus* species. *Annual Reviews of Microbiology*, 54: 849–880.

Subramaniyan, S., Sandhia, G.S. & Prema, P. 2001. Control of xylanase production without protease activity in *Bacillus* sp. by selection of nitrogen source. *Biotechnology Letters*, 23(5): 369–371.

Sutherland, P.W., Hallett, I.C., MacRae, E., Fischer, M. & Redgwell, R.J. 2004. Cytochemistry and immunolocalisation of polysaccharides and proteoglycans in the endosperm of green Arabica coffee beans. *Protoplasma*, 223: 203–211.

Szakacs, G., Tengerdy, R.P. & Nagy, V.2006. Cellulases. In: *Enzyme Technology*. A. Pandey, C. Webb, C.R. Soccol & C. Larroche, eds. Asiatech Publishers, Inc., New York, New Delhi., 747

pp.

Tailford, L.E., Ducros, V.M.-A., Flint, J.E., Roberts, S.M., Morland, C., Zechel, D.L., Smith, N., Bjornvad, M.E., Borchert, T. V., Wilson, K.S., Davies, G.J. & Gilbert, H.J. 2009. Understanding how diverse β-mannanases recognize heterogeneous substrates. *Biochemistry*, 48(29): 7009–7018.

Takasuka, T.E., Acheson, J.F., Bianchetti, C.M., Prom, B.M., Bergeman, L.F., Book, A.J., Currie, C.R. & Fox, B.G. 2014. Biochemical properties and atomic resolution structure of a proteolytically processed β-mannanase from cellulolytic *Streptomyces* sp. SirexAA-E. *PLoS ONE*, 9(4): e94166.

Teather, R.M. & Wood, P.J. 1982. Use of Congo red - polysaccharide interactions in enumeration and characterization of cellulolytic bacteria from the bovine rumen. *Applied and Environmental Microbiology*, 43(4): 777–780.

Tsukagoshi, H., Nakamura, A., Ishida, T., Otagiri, M., Moriya, S., Samejima, M., Igarashi, K., Kitamoto, K. & Arioka, M. 2014. The GH26 β-mannanase RsMan26H from a symbiotic protist of the termite *Reticulitermes speratus* is an endo-processive mannobiohydrolase: heterologous expression and characterization. *Biochemical and Biophysical Research Communications*, 452(3): 520-525.

Van Dyk, J.S. 2009. *Characterization of the cellulolytic and hemicellulolytic system of Bacillus licheniformis SVD1 and the isolation and characterization of a multienzyme complex*. PhD thesis. Rhodes University.

Van Dyk, J.S., Sakka, M., Sakka, K. & Pletschke, B.I. 2009. The cellulolytic and hemi-cellulolytic system of *Bacillus licheniformis* SVD1 and the evidence for production of a large multi-enzyme complex. *Enzyme and Microbial Technology*, 45(5): 372–378.

Van Dyk, J.S., Sakka, M., Sakka, K. & Pletschke, B.I. 2010. Identification of endoglucanases, xylanases, pectinases and mannanases in the multi-enzyme complex of *Bacillus licheniformis* SVD1. *Enzyme and Microbial Technology*, 47(3): 112–118.

Van Dyk, J.S. & Pletschke, B.I. 2012. A review of lignocellulose bioconversion using enzymatic hydrolysis and synergistic cooperation between enzymes - factors affecting enzymes, conversion and synergy. *Biotechnology Advances*, 30(6): 1458–1480.

Van Dyk, J.S., Kee, N.L., Frost, C.L. & Pletschke, B.I. 2012. Extracellular polysaccharide production in *Bacillus licheniformis* SVD1 and its immunomodulatory effect. *BioResources*, 7(4): 4976–4993.

Van Zyl, W.H., Rose, S.H., Trollope, K. & Görgens, J.F. 2010. Fungal β-mannanases: mannan

hydrolysis, heterologous production and biotechnological applications. *Process Biochemistry*, 45(8): 1203–1213.

Veith, B., Herzberg, C., Steckel, S., Feesche, J., Maurer, K.H., Ehrenreich, P., Bäumer, S., Henne, A., Liesegang, H., Merkl, R., Ehrenreich, A. & Gottschalk, G. 2004. The complete genome sequence of *Bacillus licheniformis* DSM13, an organism with great industrial potential. *Journal of Molecular Microbiology and Biotechnology*, 7(4): 204–211.

Vicente, G., Martínez, M. & Aracil, J. 2004. Integrated biodiesel production: a comparison of different homogeneous catalysts systems. *Bioresource Technology*, 92(3): 297–305.

Voigt, B., Le, T.H., Jürgen, B., Albrecht, D., Ehrenreich, A., Veith, B., Evers, S., Maurer, K.H., Hecker, M. & Schweder, T. 2007. The glucose and nitrogen starvation response of *Bacillus licheniformis*. *Proteomics*, 7(3): 413–423.

von Freiesleben, P., Spodsberg, N., Blicher, T.H., Anderson, L., Jørgensen, H., Stålbrand, H., Meyer, A.S. & Krogh, K.B.R.M. 2016. An *Aspergillus nidulans* GH26 endo-β-mannanase with a novel degradation pattern on highly substituted galactomannans. *Enzyme and Microbial Technology*, 83: 68–77.

Walker, J. 2010a. Electrophoretic Techniques. *In: Principles and Techniques of Biochemistry and Molecular Biology*, 7th edn. K. Wilson & J. Walker, eds. Cambridge University Press, New York, U.S.A., 410 pp.

Walker, J. 2010b. Protein Structure, Purification, Characterization and Function Analysis. *In: Principles and Techniques of Biochemistry and Molecular Biology*, 7th edn. K. Wilson & J. Walker, eds. Cambridge University Press, New York, U.S.A., 744 pp.

Walsh, G. 2002. Protein Purificaition and Characterization. *In: Proteins: Biochemistry and Biotechnology*. John Wiley and Sons Ltd., West Sussex, U.K., 549 pp.

Walton, G.E., Rastall, R.A., Rastall, R.A., Martini, M.C., Williams, C.E., Jeffries, R.L. & Gibson, G.R. 2010. A double-blind, placebo controlled human study investigating the effects of coffee derived manno-oligosaccharides on the faecal microbiota of a healthy adult population. *International Journal of Probiotics and Prebiotics*, 5(2): 75–83.

Wang, H., Ma, R., Shi, P., Huang, H., Yang, P., Wang, Y., Fan, Y. & Yao, B. 2015. Insights into the substrate specificity and synergy with mannanase of family 27 α-galactosidases from *Neosartorya fischeri* P1. *Applied Microbiology and Biotechnology*, 99: 1261–1272.

Wang, M., Li, Z., Fang, X., Wang, X., Wang, L. & Qu, Y. 2012. Cellulolytic enzyme production and

enzymatic hydrolysis for second-generation bioethanol production. *Advances in Biochemical Engineering/Biotechnology*, 128: 1–24.

Wenbo, Y., Shumin, T. & Qing, S. 1995. Properties of β-mannanase from *Bacillus Licheniformis*. *Microbiology*, 6.

Withers, S.G. 2001. Mechanisms of glycosyl transferases and hydrolases. *Carbohydrate Polymers*, 44: 325–337.

Yamabhai, M., Sak-ubol, S., Srila, W. & Haltrich, D. 2014. Mannan biotechnology : from biofuels to health. *Critical Reviews in Biotechnology*, Online Publication: 1–11.

Yan, X.X., An, X.M., Gui, L.L. & Liang, D.C. 2008. From structure to function: insights into the catalytic substrate specificity and thermostability displayed by *Bacillus subtilis* mannanase BCman. *Journal of Molecular Biology*, 379(3): 535–544.

Yang, B., Dai, Z., Ding, S. & Wyman, C.E. 2011. Enzymatic hydrolysis of cellulosic biomass. *Biofuels*, 2(4): 421–450.

Yariv, J., Rapport, M.M. & Graf, L. 1962. The interaction of glycosides and saccharides with antibody to the corresponding phenylazo glycosides. *Biochemical Journal*, 85: 383–388.

Youngs, H. & Somerville, C. 2012. Development of feedstocks for cellulosic biofuels. *F1000 Biology Reports*, 4: 1–11.

Zhao, Y., Wang, Y., Zhu, J.Y., Ragauskas, A. & Deng, Y. 2008. Enhanced enzymatic hydrolysis of spruce by alkaline pretreatment at low temperature. *Biotechnology and Bioengineering*, 99(6): 1320–1328.

Zhang, X., Rogowski, A., Zhao, L., Hahn, M.G., Avci, U., Knox, J.P. & Gilbert, H.J. 2014. Understanding how the complex molecular architecture of mannan-degrading hydrolases contributes to plant cell wall degradation. *Journal of Biological Chemistry*, 289: 2002–2012.

Zhang, Y.H.P. & Lynd, L.R. 2004. Toward an aggregated understanding of enzymatic hydrolysis of cellulose: noncomplexed cellulase systems. *Biotechnology and Bioengineering*, 88(7): 797–824.

Zhang, J., He, Z. & Hu, K. 2000. Purification and characterization of β-mannanase from *Bacillus licheniformis* for industrial use. *Biotechnology Letters*, 22(17): 1375–1378.

Appendices

Appendix 1 – Reagents and materials used

Table A.1. Reagents and materials used.

(+)-Arabinogalactan	Sigma (10830)
1-propanol	Sigma-Aldrich (402893)
2-propanol	Sigma-Aldrich (278475)
3,5-Dinitrosalicyclic acid	Sigma (D0550)
4-Nitrophenyl α-D-galactopyranoside	Sigma (N0877)
4-Nitrophenyl α-D-glucopyranoside	Sigma (N1377)
4-Nitrophenyl α-D-mannopyranoside	Sigma (N2127)
4-Nitrophenyl α-L-arabinofuranoside	Sigma (N3641)
4-Nitrophenyl β-D-cellobioside	Sigma (N5759)
4-Nitrophenyl β-D-fucopyranoside	Sigma (N3378)
4-Nitrophenyl β-D-galactopyranoside	Sigma (N1252)
4-Nitrophenyl β-D-glucopyranoside	Sigma (N7006)
4-Nitrophenyl β-D-glucuronide	Sigma (N1627)
4-Nitrophenyl β-D-mannopyranoside	Sigma (N2168)
4-Nitrophenyl β-D-xylopyranoside	Sigma (N2132)
6^1-α-D-Galactosyl-mannotriose	Megazyme
6^3, 6^4-α-D-galactosyl-mannopentaose	Megazyme
Acetic acid	Sigma(A6283)
Acetone	Merck-Millipore (8.22251)
Acetonitrile	Merck-Millipore (1.00030)
Acrylamide	Sigma (A8887)
Ammonium persulfate	Sigma (A3678)
Ammonium sulfate	Merck (SAAR1124020EM)
Avicel® PH-101	Fluka (11365)
Bacteriological agar	Biolab-Merck (HG000BX1)
BCA protein assay kit	Sigma (BCA1 -1KT)
Beechwood xylan	Megazyme
BIS-TRIS	Fluka (14880)
Bovine serum albumin	Sigma (A4503)

Bradford reagent	Sigma (B6916)
Bromophenol blue	Sigma (B-8026)
Calcium acetate	Merck (2052)
Calcium carbonate	SAARCHEM (28311)
Calcium chloride	Sigma-Aldrich (449709)
Carboxymethylcellulose sodium salt	Sigma (5678)
Casein	UniLAB SAARCHEM (152813)
Cellic® CTec2	Novozymes
Citric Acid	Merck-Millipore (1.00244)
Citric acid monohydrate	Merck-Millipore (1.04169)
Congo Red	Sigma (C6767)
Coomassie Brilliant Blue R250	Merck-Millipore (1.12553)
D(+) galactose	Sigma (G-6404)
D-(+)-cellobiose	Sigma (C7252)
D-(+)-mannose	Sigma(M2069)
D-(+)-xylose	Sigma-Aldrich (X3877)
DEAE-650M anion exchange resin	Toyopearl®
Dextran Blue from *Leuconostoc* spp.	Biochemika (31393)
Dextran from *Leuconostoc* spp.	Sigma (31392)
D-mannose, D-fructose, D-glucose kit	Megazyme
EDTA free protease inhibitor cocktail	Roche (05056489001)
endo-1,4 β-mannanase (*Bacillus* sp.)	Megazyme
Ethanol	Merck. 1.00980)
Ethylenediaminetetraacetic acid disodium salt	Saarchem (2236020EM)
Folin-Ciocalteu reagent	Merck (1.09001)
Gallic acid	Sigma (G7384)
Glacial acetic acid	Merck-Millipore (1.00063)
Glucose (anhydrous)	Saarchem (2676020EM)
Glycerol	Merck (1.04092)
Glycine	Merck-Millipore (1.04169)
Guar galactomannan, medium viscosity	Megazyme
Hydrochloric acid	Merck (1.00319)
Hydrochloric acid 37%	(Merck-Millipore, 1.00317)
Iron sulfate	Sigma-Aldrich (215422)

Ivory nut mannan	Megazyme
Konjac glucomannan, native, low viscosity	Megazyme
L-(+)-Arabinose	Sigma (A3256)
L-arabinose, D-galactose kit	Megazyme
Locust bean gum	Sigma (G0753)
Magnesium chloride	Sigma-Aldrich (208337)
Magnesium sulfate	Saarchem (4123920EM)
mannobiose	Megazyme
mannohaxaose	Megazyme
mannopentaose	Megazyme
mannotetraose	Megazyme
Meat extract for microbiology	Sigma-Aldrich (70164)
Methanol	Merck-Millipore (8.22283)
Millex®-HPF 0.45µM PVDF filter	Merck-Millipore (SLHVM25NS)
N,N′-Methylenebisacrylamide	Sigma (M7279)
n-butanol	Sigma-Aldrich (360465)
Pectin from apple	Sigma (76282)
Pepsin	Merck (1.07185)
Peptone	Merck (1.02239)
PES centrifugal filtration devices	Pall (MAP001C)
Phenol	Merck-Millipore (1.00206)
Phenylmethylsulfonyl fluoride	Sigma (P7626)
p-Nitrophenol	Aldrich (42575-3)
Potassium phosphate dibasic	Merck (1.05104)
Potassium phosphate monobasic	Merck (1.04877)
Protein molecular weight markers - stained	NewEngland BioLabs (P7712)
Protein molecular weight markers - unstained	BioRad (161-0363)
Regenerated cellulose centrifugal filtration devices	Merck-Millipore (UFC900324)
Rochelle salt	Sigma - Aldrich (21755)
Sephadex® G-75	Sigma, G7550)
Silica Gel HPTLC plates	Merck (1.00390)
Sodium acetate	Sigma (S8750)
Sodium azide	Sigma-Aldrich (S2002)
Sodium carbonate	Merck-Millipore (1.06392)

Sodium chloride	Merck (SAAR5822320EM)
Sodium dodecyl sulfate	Merck (8.170314)
Sodium hydroxide	Merck (SAAR5823180EM)
Sodium metabisulfite	Sigma-Aldrich (255556)
Sulfuric acid	Merck-Millipore (1.01833)
Tetramethylethylenediamine	Sigma (T9281)
Trichloroacetic acid	Merck (1.000807)
Triton X-100	Merck (1.08603)
Trizma® base	Sigma (T1503)
Tryptone	Merck-Biolab (HG000BX4)
Wheat arabinoxylan	Megazyme
Xyloglucan from tamarind seed	Megazyme
Yeast extract	Merck-Biolab (HG000BX6)
α-galactosidase from *Cyamopsis tetragonolobus*	Megazyme
α-naphthol	Sigma-Aldrich (N1000)
β-mercaptoethanol	Sigma (M3148)

Appendix 2 – Sugar standard curves

Dinitrosalicylic (DNS) assay:

Sugar concentration was measured using a modified DNS method (Miller, 1959) using mannose, glucose, galactose or arabinose as the sugar standard. The DNS reagent (100 ml) was prepared follows: Sodium hydroxide (1 g) was dissolved in 50 ml of distilled water. Then 1 g DNS was dissolved in the solution. The following reagents were then dissolved: 20 g potassium sodium tartrate (Rochelle salts), 0.2 g phenol and 0.05 g sodium metabisulfite. Distilled water (50 ml) was then added and the bottle was covered with foil.

Sugar standard curves were generated using various concentrations of each sugar standard. A volume of each concentration of sugar standard used (150 µl) was added to 300 µl of DNS reagent and mixed. The mixture was then heated at 100^{o}C for 5 min in a AccuBlock digital dry bath heater (Labnet) and then cooled on ice for 5 min. An aliquot (250 µl) was then pipetted into a 96-well microtiter plate and the absorbance readings were then taken at 540 nm using a Powerwave X microplate reader (BioTek Instruments) and KC Junior software. The standard curve was generated in Microsoft Excel® 2010.

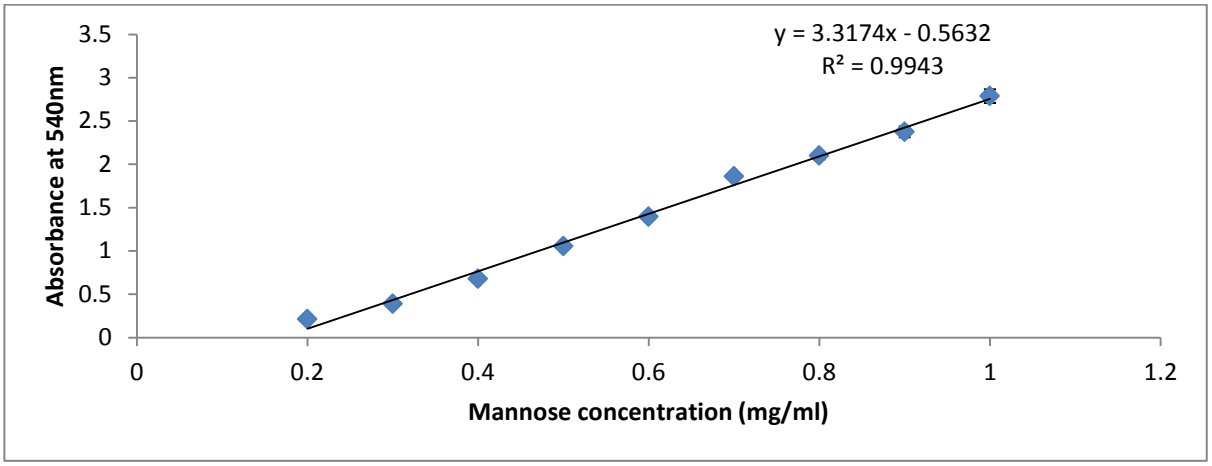

Figure A.1. Standard curve for DNS assay using mannose as a standard. Values are represented as means ± standard deviations, n=3.

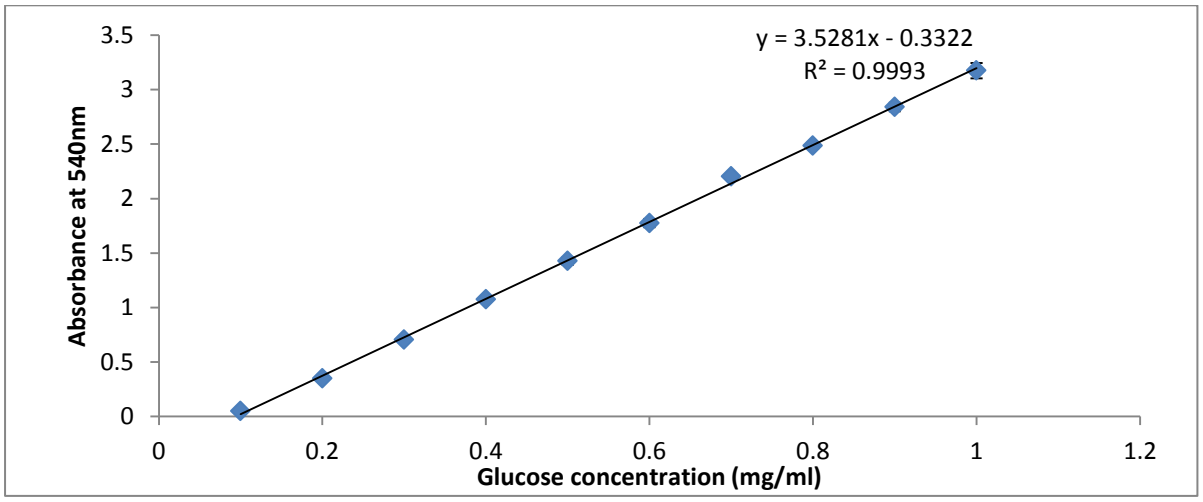

Figure A.2. Standard curve for DNS assay using glucose as a standard. Values are represented as means ± standard deviations, n=3.

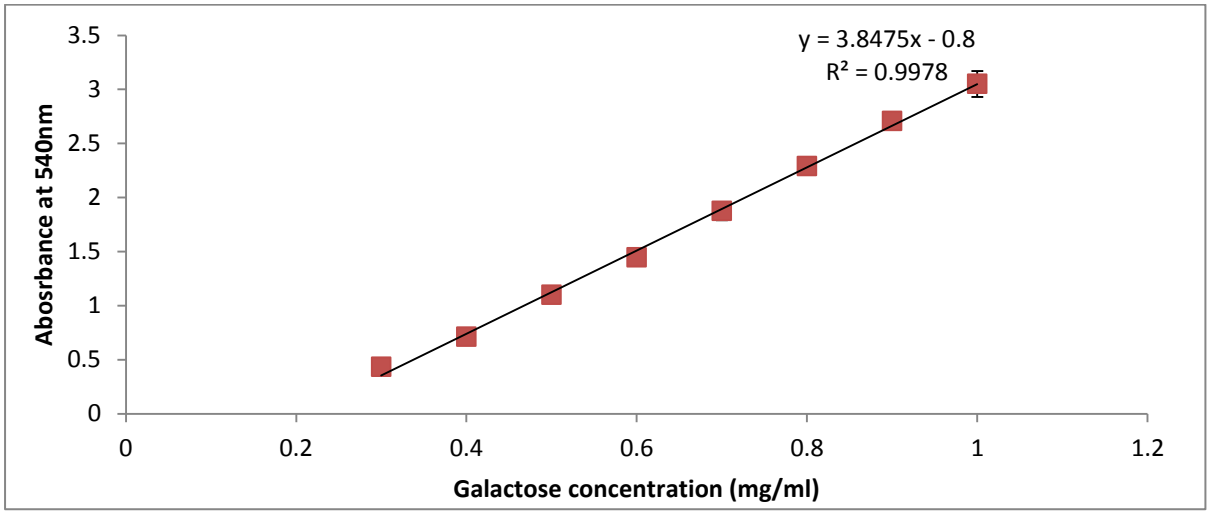

Figure A.3. Standard curve for DNS assay using galactose as a standard. Values are represented as means ± standard deviations, n=3.

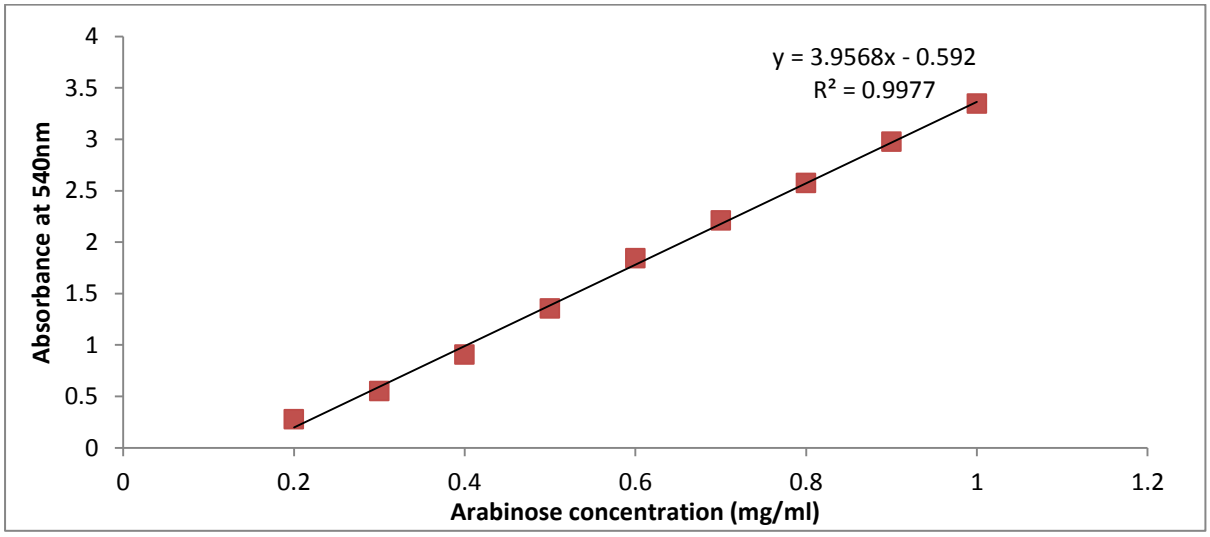

Figure A.4. Standard curve for DNS assay using arabinose as a standard. Values are represented as means ± standard deviations, n=3.

Appendix 3 – Protein standard curves

A modified Bradford's protein assay (Bradford, 1976; Anon., 2011) was used to determine protein concentration using Bradford's reagent (Sigma). BSA in 0.05 M pH 7.0 phosphate buffer was used as a protein standard. A low concentration range and a high concentration range standard curve was generated. The low concentration range standard curve used

BSA concentrations from 0.001 mg/ml to 0.0125 mg/ml. The high concentration range standard curve used BSA concentrations from 0.1 mg/ml to 0.6 mg/ml. For the low concentration range assay, 150 µl of Bradford's reagent was added to 150 µl of suitably diluted protein solution in a 96-well microtiter plate. For the high concentration range assay, 230µl of Bradford's reagent was added to 25 µl of suitably diluted protein solution in a 96-well microtiter plate. The plates were then gently mixed for 5 minutes at room temperature. Absorbance at 595 nm was then read with a Powerwave X microplate reader (Bio-Tek Instruments) using KC Junior software. Samples were gently shaken in the microplate reader for 10 seconds prior to absorbance readings being taken. Standard curves were generated using Microsoft Excel® 2010.

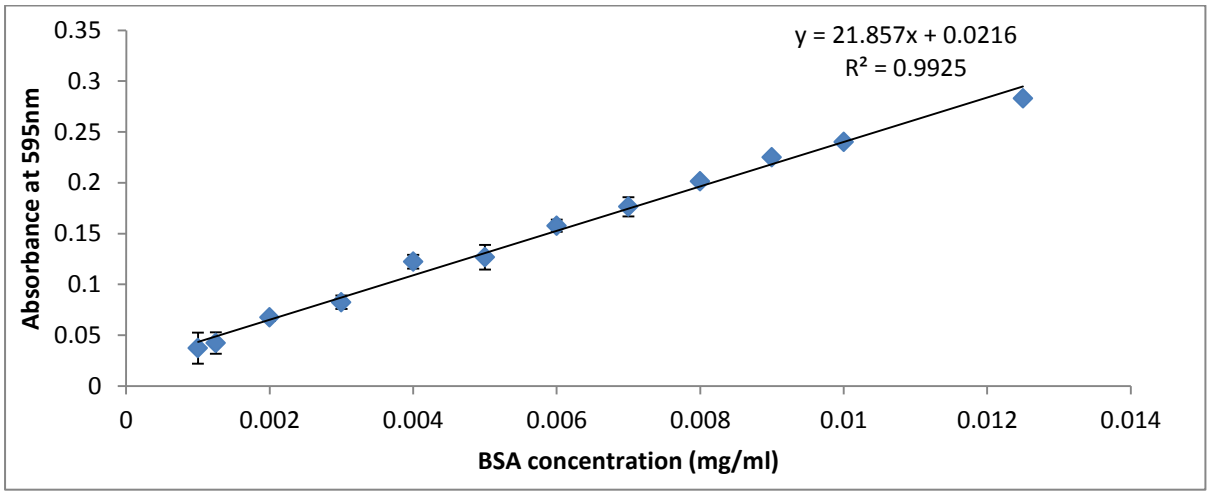

Figure A.5. Low protein concentration standard curve for the Bradford assay using bovine serum albumin as a standard. Values are represented as means ± standard deviations, n=3.

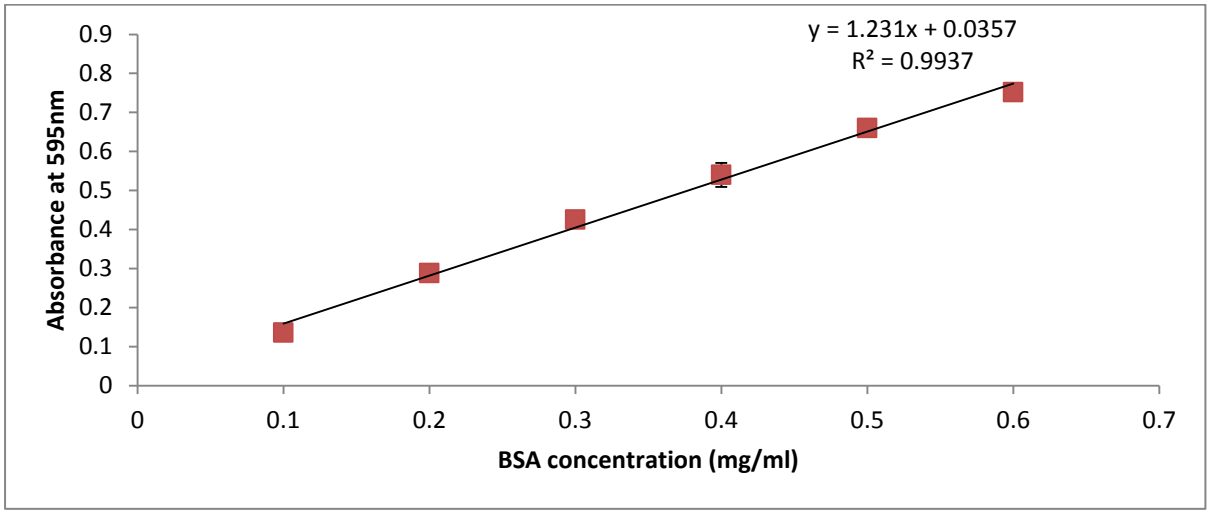

Figure A.6. High protein concentration standard curve for the Bradford assay using bovine serum albumin as a standard. Values are represented as means ± standard deviations, n=3.

A BCA assay was also used to determine protein concentration using a BCA assay kit (Sigma). BSA in diH_2O was used as a protein standard. The assays were conducted according to the manufacturer's instructions. The BCA working reagent was prepared by adding 50 parts of Reagent A to 1 part of Reagent B. Protein solution (25 µl) was added to 200 µl freshly prepared BCA working reagent in a 96-well microtiter plate. The plate was then covered with a lid and foil and incubated at 37°C for 30 min. Absorbance at 562 nm was then read with a Powerwave X microplate reader (Bio-Tek Instruments) using KC Junior software. Samples were gently shaken in the microplate reader for 10 seconds prior to absorbance readings being taken. Standard curves were generated using Microsoft Excel® 2010.

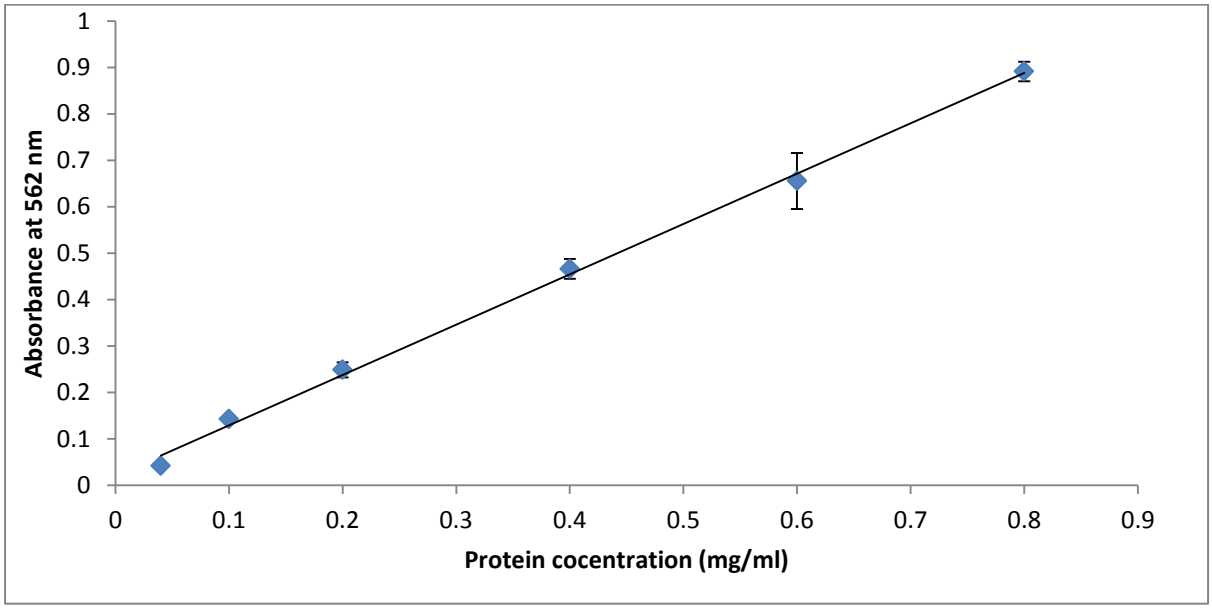

Figure A.7. Standard curve for BCA assay using bovine serum albumin as a standard. Values are represented as means ± standard deviations, n=3.

Appendix 4 – Phenolics standard curves

ρ-Nitrophenol assays:

A standard curve was generated using various concentrations of *ρ*NP. A volume of each concentration of *p*NP used (400 µl) was added to 400 µl of 2 M Na_2CO_3 and mixed. An aliquot (250 µl) was then pipetted into a 96-well microtiter plate and the absorbance readings were then taken at 405 nm using a Powerwave X microplate reader (BioTek Instruments) and KC Junior software. The standard curve was generated in Microsoft Excel® 2010.

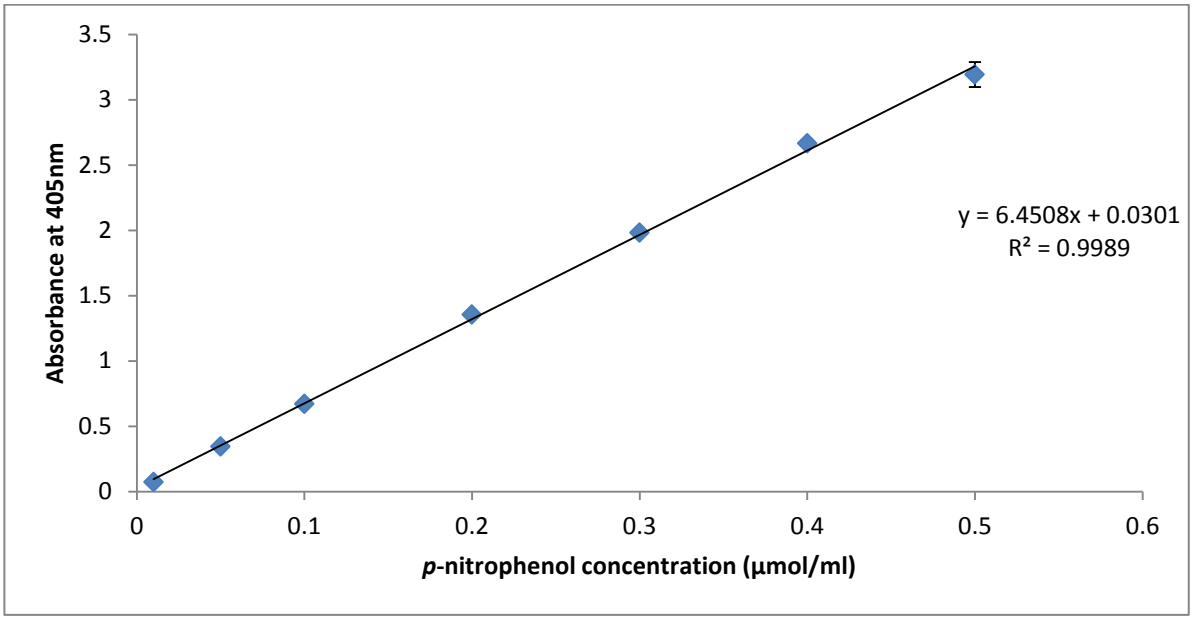

Figure A.8. Standard curve for *p*-nitrophenol quantification. Values are represented as means ± standard deviations, n=3.

Folin-Ciocalteu assay for soluble phenolics:

A standard curve was generated using various concentrations of gallic acid. Gallic acid solutions in diH_2O (190 µl) were mixed with 20 µl Folin reagent in eppendorf tubes. These were left to stand at room temperature for 1 min before the addition of 50 µl of 2 M Na_2CO_3. The tubes were then covered with tinfoil and incubated at 40°C in an AccuBlock digital dry bath heater (Labnet) for 30 min. The solutions were placed in a 96-well microtitre plate and the absorbance at 765 nm was then read using a Powerwave X microplate reader (BioTek Instruments) and KC Junior software.

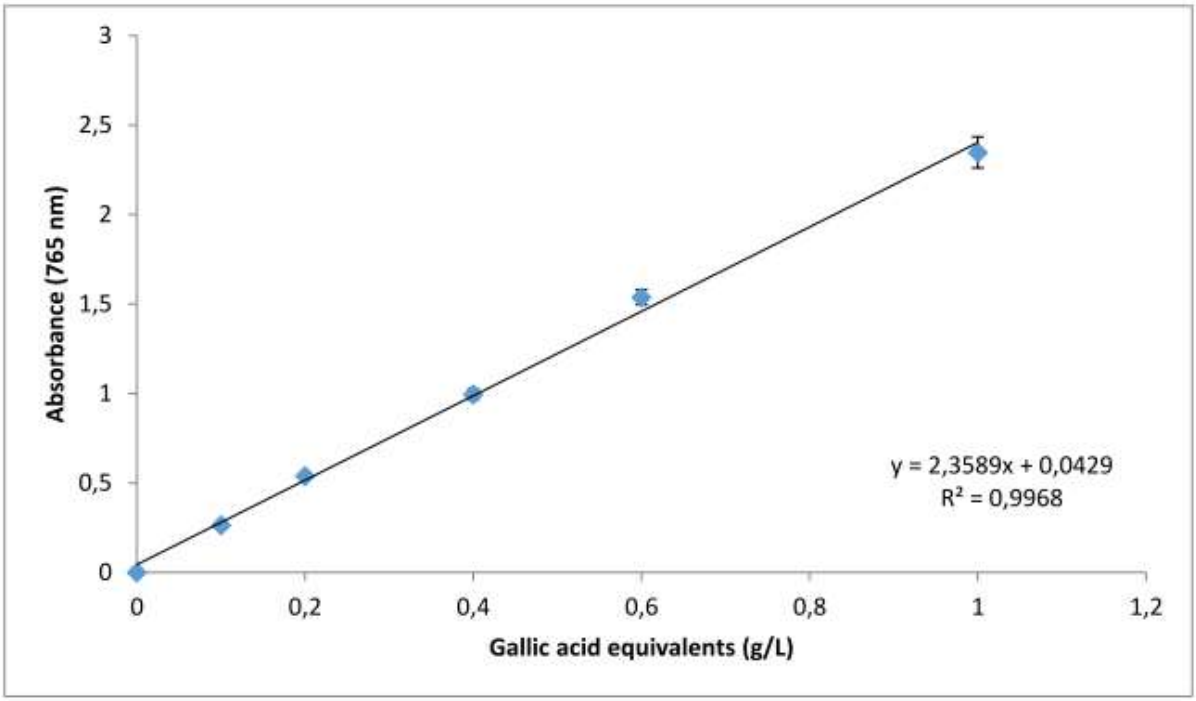

Figure A.9. Standard curve for soluble phenolics quantification using the Folin-Ciocalteu method. Gallic acid was used as a standard. Values are represented as means ± standard deviations, n=3.

.

Appendix 5 – 16S rRNA sequence BLAST results

Table A.2. Results of a BLAST search of the 16S rRNA sequence of *B. paralicheniformis* SVD1 (http://blast.ncbi.nlm.nih.gov/BlastAlign.cgi; See section 2.3.2).

Accession number	Description	Total score	Query Coverage	E value	Identities	Gaps	Strand
EU770587.1	*Bacillus licheniformis* strain SVD1 16S ribosomal RNA gene, partial sequence	2237	100%	0.0	1216/1219 (99.75%)	0/1219 (0%)	Plus/ Plus